2009

Provenance of the Miocene-Pliocene Muddy Creek Formation near Mesquite, Nevada

Steven Wayne Forrester
University of Nevada Las Vegas

PROVENANCE OF THE MIOCENE-PLIOCENE MUDDY CREEK FORMATION NEAR MESQUITE, NEVADA

by

Steven Wayne Forrester

Bachelor of Science
Washington State University
2007

A thesis submitted in partial fulfillment
of the requirements for the

Master of Science Degree in Geoscience
Department of Geoscience
College of Sciences

Graduate College
University of Nevada, Las Vegas
December 2009

UNLV
UNIVERSITY OF NEVADA LAS VEGAS

THE GRADUATE COLLEGE

We recommend that the thesis prepared under our supervision by

Steven Wayne Forrester

entitled

Provenance of the Miocene-Pliocene Muddy Creek Formation near Mesquite, Nevada

be accepted in partial fulfillment of the requirements for the degree of

Master of Science
Geoscience

Andrew Hanson, Committee Chair

Stephen Rowland, Committee Member

Wanda Taylor, Committee Member

Vernon Hodge, Graduate Faculty Representative

Ronald Smith, Ph. D., Vice President for Research and Graduate Studies
and Dean of the Graduate College

December 2009

ABSTRACT

Provenance of the Miocene-Pliocene Muddy Creek Formation near Mesquite, Nevada

by

Steven Wayne Forrester

Dr. Andrew Hanson, Examination Committee Chair
Associate Professor of Geology
University of Nevada, Las Vegas

The provenance, stratigraphy, and depositional history of the Miocene-Pliocene Muddy Creek Formation (MCF) in southern Nevada are poorly studied and poorly constrained. Previous studies of the MCF have concluded that the formation consists of lacustrine, eolian, and fluvial deposits. Currently the age of deposition is loosely constrained between 8.5 and 4.1 Ma. This study documents the evolution of one portion of the eastern extent of the MCF and determines its provenance and depositional history at Flat Top and Mormon Mesas in Nevada; and near Beaver Dam and Littlefield, Arizona.

This study intended to determine whether the MCF was deposited by a paleo-Colorado River that flowed through the Virgin River Gorge and into the Mesquite basin prior to ~5.5 Ma. Methods used in this study included petrographic analyses, detrital zircon analyses, facies analyses, paleocurrent indicators, and conglomerate clast counts. Detrital zircons from the MCF, a Pliocene unit near Littlefield, Arizona, and modern day Virgin River were compared to previously analyzed zircons from the Bidahochi Formation and known Colorado River zircons.

Results from the MCF in the Beaver Dam Wash and at Flat Top Mesa indicate paleotransport was to the south-southeast and south-southwest respectively and in an inset Pliocene unit near Littlefield, Arizona paleotransport was to the south-southwest. Based upon sedimentological data the MCF within the study area was deposited in a fluvial environment. Conglomerate clasts and sandstone petrography from the MCF at Mormon Mesa indicate mixed volcanic, metamorphic, and sedimentary sources for the sediment which is dissimilar to deposits at Flat Top Mesa and Beaver Dam Wash which were derived from a volcanic source. The provenance data indicate the MCF at Flat Top Mesa and Beaver Dam Wash were derived from the Caliente Caldera complex, while the deposits at Mormon Mesa were derived from both the Caliente Caldera complex and the Colorado Plateau, which was deposited by a paleo-Virgin River. Results from an inset Pliocene unit in the Beaver Dam Wash indicate this unit was derived from the Caliente Caldera complex. In contrast, results from an inset Pliocene unit near Littlefield, Arizona indicate it was derived from the Colorado Plateau and deposited by a paleo-Virgin River. Despite the MCF at Mormon Mesa having a partial Colorado Plateau provenance results are consistent with previous models that indicated that neither the younger units nor the portions of the MCF that were studied were deposited by a paleo-Colorado River.

TABLE OF CONTENTS

LIST OF FIGURES

ACKNOWLEDGEMENTS

First and foremost I would like to thank Dr. Andrew Hanson for all his support and guidance throughout this project. Dr. Hanson's interest in this project made it possible for me to really understand the Muddy Creek Formation throughout southern Nevada and possible to reach the end of the project. His guidance and insight helped to make this project a success.

I would like to thank Aubrey Shirk, Jonathan Sarich, Tom Muntean, and Dr. Andrew Hanson for their assistance in helping me with field work. I would also like to thank Dr. Andrew Hanson and Tom Muntean for their assistance with preparation of samples and conducting analyses. I need to thank Tom Muntean for all the discussions we had on the Muddy Creek Formation, which helped me really understand the Muddy Creek Formation and all sediment sources. I also want to thank Peter Druschke for the numerous discussions we have had on detrital zircons, it really helped me to understand possible zircon provenance. I would like to say thank you to Dr. Wanda Taylor, Dr. Vernon Hodge, and Dr. Stephen Rowland for their assistance and for serving on my committee.

This project was funded thanks to generous grants from the Geological Society of America (GSA), Nevada Petroleum Society (NPS), UNLV Geoscience Department, Rocky Mountain Section of the Society for Sedimentary Geology (RMS-SEPM) and thanks to funding from Dr. Andrew Hanson. Generous funding from sources made it possible for me to complete the project and achieve results.

I would also like to thank all my fellow graduate students in the UNLV Geoscience Department that helped me get through the past two years. Special thanks go to Aubrey,

Jonathan, Jeremy, Meg, Josh, Christi, Laura, James, Bobby, and Kelly for all the talking, laughing, and fun we shared. I would like to thank the UNLV Geoscience Department for allowing me to use the equipment and laboratory space in the department, so that I could complete this project.

CHAPTER 1

INTRODUCTION

The provenance, stratigraphy, and depositional history of the Miocene-Pliocene Muddy Creek Formation in southern Nevada are poorly studied and poorly constrained. The provenance of the Muddy Creek Formation has been hypothesized to be either the Colorado Plateau or Neogene volcanic sources in Nevada (Lucchitta, 1990; Pederson, 1998; Schmidt, 2000). The stratigraphy of the Muddy Creek Formation has been variably described as having been deposited in lacustrine, eolian, fluvial, and playa environments (Bohannon, 1984; Kowallis and Everett, 1986; Dicke, 1990; Billingsley, 1995; Pederson, 2001, 2008). The Muddy Creek Formation was deposited in an arid environment similar to the environment today, but with more periods of occasional rainfall (Bohannon, 1984; Kowallis and Everett, 1986). Researchers who study the Muddy Creek Formation have raised two questions that indicate how little is known about this formation: 1) What is the provenance of the Muddy Creek Formation? and 2) What is the stratigraphy of the Muddy Creek Formation?

Before the Muddy Creek Formation was deposited, southern Nevada was a tectonically active region. Prior to the initiation of the Basin and Range province during the Oligocene and Miocene; five orogenic events occurred along the western United States from the late Devonian through the early Eocene. The five orogenic events were the Antler Orogeny, the Sonoma Orogeny, the Nevadan Orogeny, the Laramide Orogeny, and the Sevier Orogeny (Schweickert et al., 1984; Dickinson, 2004). Extension and basin formation occurred throughout southern Nevada during the Oligocene and Miocene

before the Muddy Creek Formation was deposited (Eaton, 1982). Neogene extension and basin development created the Basin and Range province (Fig. 1) which is characterized by evenly spaced parallel mountain ranges and intervening desert basins (Stewart, 1978).

Southern Nevada is the location of the central Basin and Range province (Fig. 1), which is a sub-province of the Basin and Range province (Wernicke, 1992). The central Basin and Range province is a structurally complex province, with predominately east-west extension and many fault bounded basins, that initiated during the Oligocene and Miocene (Wernicke, 1981; Wernicke et al., 1985; Axen et al., 1990). The Neogene faults in this region are normal, strike-slip, and low-angle detachment faults. The basins that were created during Basin and Range extension have been filled with sediments that were deposited in fluvial, alluvial, and eolian environments. Sediments that accumulated in the newly formed basins were deposited by rivers that were formed by different processes.

Rivers typically form and propagate by one of five generally accepted processes; antecedence, superimposition, stream piracy, lake overflow, and headward erosion. Douglass et al. (2009) reviewed and summarized four river forming processes that cross transverse drainages; antecedence, superimposition, stream piracy, and lake overflow. Antecedence is when a pre-existing river drains across and erodes a channel into an uplifting bedrock structure. A present-day example of a river that propagates via antecedence is the Wind River in Wyoming. Superimposition occurs when a river flows across a covermass that buries a comparatively resistant bedrock structure. During superimposition the river erodes and transports the covermass as well as the uplifted bedrock structure once it erodes to that level. A modern-day example of a river that

propagates via superimposition is the Susquehanna River in Pennsylvania. Stream piracy or stream capture is when a river is diverted from its channel and flows down the channel of a neighboring river. Stream piracy occurs when the soon to be captured river erodes, infiltrates, or flows into a drainage basin with a steeper gradient. Rivers can also propagate downstream through a less common process known as lake overflow. Lake overflow occurs when water in one lake basin spills over the basins divide into another basin, which then fills up and spills over its banks into another basin, and continues to do so until it reaches base level. As a result a river is created which connects the basins (House et al., 2005). A present-day example of a river that propagates downstream via lake overflow is the Mojave River in California (Meek and Douglass, 2001). Rivers can also form by a fifth method which is headward erosion. Headward erosion is the downcutting through a substrate (i.e., rock or sediment) that results in propagation of the river up gradient (Popescu et al., 2004). Headward erosion occurs when water erodes rock at the headwaters in the opposite direction that the river flows, thus lengthening a stream. A present-day example of a river propagating upstream via headward erosion is the Shenandoah River (Trapp and Horn, 1997).

The present-day path of the Colorado River is well documented, but the path of the Colorado River, prior to its inception into the Grand Canyon is poorly understood (Pederson, 2008). Some researchers have hypothesized that the Muddy Creek Formation may have been derived from the Colorado Plateau and deposited by a paleo-Colorado River (Lucchitta, 1990; Schmidt, 2000). Previous research has shown that the composition of the Muddy Creek Formation varies throughout southern Nevada. This study documents the provenance of one portion of the eastern portion of the Muddy

Creek Formation in the Mesquite basin from location F at Flat Top Mesa, location A at Mormon Mesa, and location H in the Beaver Dam Wash (Fig. 2) in order to test the paleo-Colorado River hypothesis. This study also documents the provenance of a Pliocene unit inset into the Muddy Creek Formation from location G at Littlefield, Arizona and from location I in the Beaver Dam Wash (Fig. 2).

All previous research has concluded that the modern Colorado River began flowing through the Grand Wash Trough, which lies about 80 km south of the Mesquite basin, around 5.5 Ma (Young and Spamer, 2001, and references contained therein). During the Miocene a paleo-Colorado River is known to have flowed on the northern portion of the Colorado Plateau (Pederson, 2008), but there is no evidence of a river flowing westward off of the Colorado Plateau until the Colorado River flowed through its modern day drainage sometime after 5.5 Ma and before 4.0 Ma. Some researchers have concluded that a lake overflow process caused integration of the modern Colorado River into the Grand Canyon (Meek and Douglass, 2001; Spencer and Pearthree, 2001, 2005; Kimbrough et al., 2007). Although, a lake overflow process is responsible for the integration of the lower Colorado River, gradual headward erosion helped to lengthen the upper Colorado River (Spencer and Pearthree, 2001). Based upon the proximity of the Mesquite basin to the Colorado Plateau, a paleo-Colorado River could have flowed off the Colorado Plateau and into the Mesquite basin prior to 5.5 Ma (Lucchitta, 1990).

Previous researchers have worked on the Muddy Creek Formation and postulated different hypotheses about the provenance of the Muddy Creek Formation. There are two main hypotheses that have been proposed related to where the Muddy Creek Formation was derived from: 1) The Muddy Creek Formation was derived from the Colorado

Plateau and deposited by a paleo-Colorado River; and 2) The Muddy Creek Formation was derived from the Caliente Caldera complex and other local Neogene volcanic complexes in Nevada. Schmidt (2000) hypothesized that the Muddy Creek Formation was derived from the Colorado Plateau and deposited by a paleo-Colorado River based on conglomerate clasts contained within the Muddy Creek Formation that were similar in composition to strata on the Colorado Plateau. In contrast, Pederson (2001, 2008) hypothesized that the Muddy Creek Formation was not derived from the Colorado Plateau, but was derived from the Caliente Caldera complex and other Neogene volcanic complexes. Pederson (2001, 2008) studied outcrops of the Muddy Creek Formation throughout southern Nevada along an east-west transect (Fig. 3) and based on petrographic evidence concluded that the Muddy Creek Formation was derived from local Neogene volcanic sources; i.e. the Caliente Caldera complex and Kane Springs volcanic center. Although Pederson (2001, 2008) concluded that the Muddy Creek Formation was derived from volcanic sources, high quartz and low volcanic lithics for a subset of the data (Fig. 4) suggest that the Muddy Creek Formation was not derived from local volcanic sources, but are compatible with derivation from the Colorado Plateau. Two other provenance studies have been conducted on different portions of the Muddy Creek Formation, yielding different provenance sources for the Muddy Creek Formation. Scott (1988) studied the Muddy Creek Formation near Lake Mead and determined that the Muddy Creek Formation was derived from the River Mountains based on volcanic and plutonic clasts within interbedded conglomerates (Fig. 5). Dicke (1990) worked in the Meadow Valley Wash and determined that the Muddy Creek Formation was derived from the Moenkopi and Chinle Formations, as well as Neogene volcanic sources (Fig. 6).

Researchers have also studied the structural history of the Muddy Creek Formation. The Muddy Creek Formation is commonly thought to be post-tectonic Basin and Range basin fill, based on the relatively low dip angles that occur throughout much of the unit (Bohannon, 1984; Dicke, 1990; Anderson and Barnhard, 1993). Dicke (1990) determined that the Muddy Creek Formation is an undeformed sequence that shows no lateral or vertical movements indicative of a structurally active basin. However, recent work by Hanson et al. (2005) showed that the uppermost Pliocene(?) Muddy Creek Formation is syn-tectonic in the vicinity of Overton Arm in the Lake Mead area, which indicates how little is known regarding the Muddy Creek Formation.

Volcanic deposits within the Muddy Creek Formation have been dated and the age of the Muddy Creek Formation is loosely constrained. Absolute ages derived from tuffs and basalt flows within the Muddy Creek Formation indicate that the Muddy Creek Formation was deposited between 8.5 Ma and 4.1 Ma (Metcalf, 1982; Williams, 1996). Vertebrate bones found within the Muddy Creek Formation have been suggested to be either Miocene or Pliocene in age (Stock, 1921; Longwell, 1946; Kowallis and Everett, 1986).

The Miocene-Pliocene Muddy Creek Formation is exposed in elevational lows throughout southern Nevada as it is predominantly post-Basin and Range basin fill (Bohannon, 1984) (Fig. 7). The study area encompasses the eastern most extent of the Muddy Creek Formation approximately 75 to 90 miles northeast of Las Vegas, Nevada (Fig. 2). Excellent exposures of the Muddy Creek Formation were examined at location F at Flat Top Mesa, at location H in the Beaver Dam Wash, and at locations A-E at Mormon Mesa (Fig. 2). Exposures of a Pliocene unit inset into the Muddy Creek

Formation at location G at Littlefield, Arizona and at location I in the Beaver Dam Wash were also examined (Fig. 2). By testing whether a paleo-Colorado River deposited the Muddy Creek Formation, this project: 1) bears on how large cratonic rivers, like the Colorado River, integrate and make their way to the ocean; 2) illuminates the geomorphological evolution of the Colorado River over time; 3) shows the evolution of the Colorado Plateau drainage; and 4) increases our understanding of the nature and timing of tectonic events and basin fill during the Neogene in southern Nevada. This study intended to test the hypothesis that the Muddy Creek Formation was derived from the Colorado Plateau and deposited by a paleo-Colorado River into the Mesquite basin prior to ~5.5 Ma, as well as the alternative hypothesis that the Muddy Creek Formation was derived from the Caliente Caldera complex (Figs. 8a and 8b).

CHAPTER 2

PREVIOUS WORK

The Muddy Creek Formation was first identified, named, and described in the Muddy Mountains by Stock (1921) and later reexamined and more thoroughly described by Longwell (1946). Longwell (1946) studied the Muddy Creek Formation to determine if it was a possible pre-Grand Canyon Colorado River deposit. Longwell (1946) interpreted that if a Colorado River flowed west off of the Colorado Plateau it did not deposit the Muddy Creek Formation because he concluded that the Muddy Creek Formation was deposited in an arid environment. Longwell (1946) concluded that more studies on the Muddy Creek Formation were needed to determine its age in order to constrain whether the Muddy Creek Formation is Miocene or Pliocene in age. Although the Muddy Creek Formation was first identified and described during the 1920's and 1930's, it was not until the 1980's that new studies were undertaken to determine its provenance, depositional environment, and structural history.

Scott (1988) conducted a provenance study on the Muddy Creek Formation along the southwestern portion of Lake Mead and along the Arizona-Nevada border to the south. To determine the provenance of the Muddy Creek Formation, Scott (1988) determined the composition of clasts from interbedded conglomerates within the Muddy Creek Formation exposed along the western shore of Lake Mead east of the River Mountains. The conglomerates within the Muddy Creek Formation within the study area contained dacite, andesite, rhyolite, quartz monzonite, granite, and basalt clasts. Scott (1988) interpreted that the Muddy Creek Formation was deposited during the waning stages of

extension in Lake Mead. To determine where the predominantly volcanic and plutonic clasts in the Muddy Creek Formation were derived from, Scott (1988) investigated various source locations around Lake Mead in southern Nevada including the River Mountains, McCullough Mountains, Eldorado Mountains, and Saddle Island (Fig. 5). Based upon clast compositions and paleocurrent analyses, Scott (1988) determined the portion of the Muddy Creek Formation within the study area was derived from the River Mountains.

Dicke (1990) completed a provenance study of the Muddy Creek Formation in the Meadow Valley Wash, between the Meadow Valley Mountains and the Mormon Mountains (Fig. 6). The Muddy Creek Formation in the Meadow Valley Wash is fine to coarse grained sandstone and is capped by a petrocalcic horizon. Based upon work in the northern part of the Meadow Valley Wash, Dicke (1990) determined that the Muddy Creek Formation was derived from the Moenkopi and Chinle Formations, as well as local Neogene volcanic centers. Dicke (1990) determined that the volcaniclastic sediment of the Muddy Creek Formation was derived from volcanic rocks exposed in the north end of the Meadow Valley Wash (Fig. 6), based on petrographic analyses. Dicke (1990) also concluded that the Muddy Creek Formation was in part derived from the Moenkopi and Chinle Formations as well as local Neogene volcanic centers based on south directed paleocurrent indicators, conglomerate clast compositions, and petrographic thin section analyses.

Schmidt (2000) and Pederson (2001, 2008) conducted provenance studies on the Muddy Creek Formation to determine if it was derived from the Colorado Plateau and deposited by a paleo-Colorado River. Schmidt (2000) hypothesized that the mostly pre-

5.5 Ma Muddy Creek Formation was deposited by a paleo-Colorado River that flowed into the Mesquite basin based on the presence of Colorado Plateau derived conglomerate clasts in the Muddy Creek Formation. Pederson (2001, 2008) petrographically analyzed samples from various outcrops of the Muddy Creek Formation throughout southern Nevada along an east-west transect (Fig. 3). Pederson (2001, 2008) collected seventeen samples, one sample from eight of the outcrop locations and three samples from three of the outcrop locations, and then petrographically analyzed each sample. Pederson (2001, 2008) then compared the Muddy Creek Formation samples to samples from possible sediment source areas, i.e. the Colorado River, the Virgin River, as well as local volcanic, carbonate, and metamorphic sources. Ternary diagrams produced by Pederson (2008) revealed two populations, showing two sediment sources for the Muddy Creek Formation (Fig. 4). One population contained a mixture of local metamorphic, carbonate, and volcanic sources, while the other population contained Colorado Plateau derived material. Pederson (2001, 2008) suggested that most of the Muddy Creek Formation was derived from a volcanic terrain to the north of the Mormon Mountains based on sedimentological, field, and petrographic data (Fig. 4) and that the Muddy Creek Formation was not deposited by a paleo-Colorado River.

The depositional environment of the Muddy Creek Formation was studied by Kowallis and Everett (1986), Scott (1988), and Dicke (1990). Kowallis and Everett (1986) studied the Muddy Creek Formation near Mesquite, Nevada and described the Muddy Creek Formation as discontinuous beds of sandstone and siltstone derived from local mountain ranges that shed detritus into basins. The sediment of the Muddy Creek Formation is pink to orange, texturally immature, poorly sorted, coarse to fine grained

sandstone (Kowallis and Everett, 1986). Kowallis and Everett (1986) found horizontal and vertical burrows, grass impressions, mammal and bird tracks, and mammal bones in certain horizons within the Muddy Creek Formation. Although some trace and body fossils were found within the Muddy Creek Formation, they are rare and the Muddy Creek Formation is predominantly nonfossiliferous. Cross-bedding ranging from a few centimeters to a few meters thick and ripple marks from five to twenty centimeters thick are common in the Muddy Creek Formation (Kowallis and Everett, 1986). Mudcracks, rip-up clasts, and mud balls were found in the Muddy Creek Formation near Mesquite, Nevada, but are quite rare. Kowallis and Everett (1986) determined that the Muddy Creek Formation was deposited in a dry, arid, fluvial, or alluvial environment that is similar to the environment today, but may have had greater periods of rainfall. Scott (1988) conducted a lithofacies analysis of the Muddy Creek Formation near Lake Mead to determine the environment of deposition. Based upon clast supported, tabular conglomerates, cross-bedded sandstones, channel-fill sediments, and fine-grained sandstones Scott (1988) determined that the Muddy Creek Formation was deposited in a fluvial environment. Scott (1988) also conducted a paleocurrent analysis using imbricated clasts and documented an east directed paleocurrent direction. The Muddy Creek Formation in the Meadow Valley Wash contained cross-bedded sandstones, trough cross-bedded sandstones, planar laminations, ripple marks, burrows, and mud cracks. Dicke (1990) determined that the Muddy Creek Formation in the Meadow Valley Wash consists of coarse to fine grained sandstone that was deposited in eolian, fluvial, lacustrine, and alluvial environments. In summary, Kowallis and Everett (1986) and Scott (1988) determined that the Muddy Creek Formation was deposited in a fluvial

environment, but Dicke (1990) determined that the Muddy Creek Formation was deposited in eolian, fluvial, lacustrine, and alluvial environments based upon the sedimentary structures and sediment within the Muddy Creek Formation.

The Muddy Creek Formation has been described as an undeformed post-tectonic basin fill unit. Based on a structural study conducted on the Muddy Creek Formation in the Meadow Valley Wash Dicke (1990) argued that the Muddy Creek Formation is post-Basin and Range basin fill. Dicke (1990) identified the Muddy Creek Formation as an undeformed sequence with no lateral or vertical movements observed in the basin. However, Hanson et al. (2005) argued that the uppermost Pliocene(?) Muddy Creek Formation in the Overton Arm of Lake Mead is syn-tectonic and not post-tectonic basin fill as previously thought. Langenheim et al. (2000) argue that the Muddy Creek Formation is a syn-tectonic formation because even though it may appear continuous at the surface, there are faults that extend into the Muddy Creek Formation in the sub-surface.

CHAPTER 3

GEOLOGIC BACKGROUND

Basin and Range

The Basin and Range province is one of the best exposed and extensive extensional orogens on Earth (Faulds et al., 2001). The Basin and Range province is a continental region in western North America covering 800,000 km^2 in eight states, extending from southern Oregon and Idaho in the north to the Baja California Peninsula in the south, and from the Colorado Plateau in the east to the Sierra Nevada in the west that is characterized by extension (Fig. 1) (Fenneman, 1928, 1931). During the middle Cenozoic, east directed subduction of the Farallon plate resulted in crustal extension, spanning from Canada to Mexico (Atwater, 1970). Basin and Range extension resulted in the crust and upper mantle beneath the Basin and Range province having been stretched up to 100% of its original width (Proffett, 1977). The crust and upper mantle extended along large normal faults, which uplifted mountain ranges and down-dropped basins (Wernicke, 1981). The large normal faults that created the Basin and Range topography dip into the crust at a 60^o angle and create upwards of 3,000 m of vertical relief between the mountain ranges and adjacent basins (Shurbet and Cebull, 1971; Stewart, 1978; Eaton, 1982). The Basin and Range province is characterized by evenly spaced parallel mountain ranges and intervening desert basins created during the Oligocene and Miocene (Stewart, 1978). Southern Nevada is located in the central Basin and Range province, which is a sub-province of the Basin and Range province. The central Basin and Range province underwent predominantly east-west extension and has

many normal, strike-slip, and low-angle detachment faults that were active mainly during the Oligocene and Miocene (Wernicke, 1981; Wernicke et al., 1985; Axen et al., 1990). Although Basin and Range extension began approximately 36 to 37 Ma during the Early Oligocene farther to the north, extension near Mesquite, Nevada in the central Basin and Range province began approximately 16 to 17 Ma during the Middle Miocene (Eaton, 1982; Faulds et al., 2001; Lamb et al., 2005). Major tectonism in southern Nevada occurred during the Miocene, but extension has occurred in this area during the Pliocene and Quaternary.

Transition Zone

The southwestern United States can be sub-divided into three tectonic provinces: (1) the Colorado Plateau, (2) the Basin and Range province, and (3) the Transition Zone (Spencer et al., 2001). The Transition Zone along the northwest portion of the Colorado Plateau in Utah extends between the Colorado Plateau and the Basin and Range province (Fig. 9). Today, the Transition Zone slopes southward from the Colorado Plateau to the Basin and Range Province, but in the early Neogene the Transition Zone sloped toward the Colorado Plateau (Spencer et al., 2001). The Transition Zone locally has been stripped of Paleozoic rocks, exposing 1.1 to 1.8 Ga Proterozoic rocks (Spencer et al., 2001). During the early Neogene rivers carried sediment from what is now the Basin and Range province to the Colorado Plateau (Spencer et al., 2001).

Virgin River Depression

The Muddy Creek Formation is exposed within the central Basin and Range province in southern Nevada (Fig. 1) within the Virgin River Depression and areas to the west and southwest. The study area is located within the Mesquite and Mormon basins, which are two structural Neogene basins within the Virgin River Depression (Fig. 2) (Bohannon et al., 1993; Quigley et al., 2002). The Virgin River Depression is a large, deep basin that straddles Arizona, Nevada, and Utah (Langenheim et al., 2001) and is 31 kilometers wide and 100 kilometers long, with a surface area exceeding 1500 km^2 (Johnson et al., 2002). A buried ridge dividing the Virgin River Depression into the Mesquite and Mormon basins formed between 10 and 13 Ma (Quigley et al., 2002). The Mesquite basin contains six kilometers of Neogene sedimentary fill, which sits upon pre-Cambrian basement rocks (Bohannon et al., 1993). The Neogene sedimentary fill consists of the Muddy Creek Formation, Horse Spring Formation, and Red Sandstone unit, (Bohannon et al. 1993). The rocks stratigraphically beneath the sedimentary basin fill are the Baseline Sandstone, Aztec Sandstone, Moenave Formation, Kayenta Formation, Chinle Formation, Moenkopi Formation, Kaibab Formation, Toroweap Formation, Esplanade Sandstone, Bird Spring Formation, Monte Cristo Formation, Sultan Limestone, and Cambrian dolomite. The Virgin River Depression is surrounded by the Tule Springs Hills to the north, the Virgin Mountains to the south, the Beaver Dam Mountains to the east, and the Mormon Mountains to the west (Fig. 2) (Bohannon et al., 1993; Langenheim et al., 2000; 2001). These mountain ranges contain exposed rocks that range from Proterozoic crystalline basement rocks to Paleozoic carbonate rocks to Mesozoic continental sedimentary rocks (Langenheim et al., 2001). There are low-angle

detachment and normal faults to the north and west of the Virgin River Depression in the Mormon Mountains and Tule Springs Hills, while there are strike slip faults to the south of the Virgin River Depression in the Virgin Mountains (Wernicke, 1981; Wernicke et al., 1985; Axen et al., 1990). The Mesquite basin is fault bounded by the Hen Spring fault and the Lake Mead fault system to the south, the Piedmont fault to the east, and the Mormon basin fault to the west (northeast of Lake Mead) (Bohannon et al., 1993; Duebendorfer et al., 1998; Duebendorfer, 2006). The faults which bound the Virgin River Depression are kinematically linked and accommodate overall extension in this region (Duebendorfer et al., 1998; Duebendorfer and Simpson, 1994).

Provenance Sources

To test the hypotheses regarding the provenance of the Muddy Creek Formation, it is essential to know the age and lithology of the potential sediment source areas, i.e., the Colorado Plateau, the Caliente Caldera complex, the Virgin Mountains, and the Mormon Mountains. The Colorado Plateau is a region characterized by sedimentary rocks that are gently dipping and consist of prominent cliffs and deep canyons (Spencer and Pearthree, 2005). The Colorado Plateau extends across four states and is comprised of sedimentary rocks ranging from Proterozoic sedimentary, volcanic, and crystalline rocks to the Eocene Claron Formation. Detrital zircons in modern Colorado River sediments derived from the Colorado Plateau are varied and span from about 20 Ma to 2.8 Ga (Kimbrough et al., 2007). The Caliente Caldera complex is a Miocene eruptive center located around the town of Caliente, Nevada (Noble and McKee, 1972; Cromme et al., 1997). The Caliente Caldera complex to the north of Mesquite, Nevada was active from 24 Ma to 13

Ma and erupted calc-alkaline and bimodal rocks (Best et al., 1993). While the major-flow eruptions of the Caliente Caldera complex ended around 18 Ma, volcanism persisted in the area until roughly 13 Ma through minor locally distributed eruptions (personal communication E.I. Smith, 2008). The lithologies of rocks from the Caliente Caldera complex vary, but the rocks are predominantly rhyolite flows, airfall tuffs, and extrusive volcanic rocks (Cromme et al., 1997). Although there are other rocks to the northeast of Beaver Dam Wash that could provide detrital zircons with a variety of ages, a northern source (i.e., the Caliente Caldera complex) for sediment in the Muddy Creek Formation is expected to have detrital zircon populations dominated by 13 to 24 Ma ages derived from the Caliente Caldera complex.

Detrital Zircon Sources

Geologic events have produced zircons that were crystallized, subsequently eroded from their source, and deposited within the Muddy Creek Formation. Zircons are durable, resistant minerals that provide information about their source area, if the age of the zircon is determined analytically. The ages of detrital zircons from potential source areas are compared to the ages of detrital zircons analyzed in this study, in order to establish the provenance of the Muddy Creek Formation. In order to determine where a certain zircon comes from it is important to know the major geologic events local to the study area, as well as the major geologic events that occurred throughout North America during the past 4.5 Ga. Detrital zircons shed into the Muddy Creek Formation, inset Pliocene unit, and modern Virgin River from geologic complexes and orogenic events local to the study area could have ages that include the following: 14-12 Ma (River

Mountains/Wilson Ridge pluton), 24-13 Ma (the Caliente Caldera complex), 24-20 Ma (the Pine Valley Mountains in Utah), 70-40 Ma (the Laramide Orogeny), 115-87 Ma (the Sierra Nevada Batholith), 140-50 Ma (the Sevier Orogeny), 180-140 Ma (the Nevadan Orogeny), 270-240 Ma (the Sonoma Orogeny), and 385-345 Ma (the Antler Orogeny). While these orogenic events and complexes are central to the study area, other complexes and orogenic events in North America which could have shed detrital zircons into rocks that were recycled and subsequently deposited in the Muddy Creek Formation, inset Pliocene unit, and modern Virgin River. The ages of detrital zircons from other orogenic events and complexes in North American could have ages that include the following: 300-250 Ma (the Alleghenian Orogeny), 500-310 Ma (the Appalachian Orogeny), 650-600 Ma (the Caledonian Orogeny), 750-650 Ma (the Pan-African Orogeny), 1300-1000 Ma (the Grenville Orogeny), 1470-1400 (the Belt Supergroup), 1750 Ma (the Yavapai Orogeny), 2200-1800 Ma and 3015-2580 Ma (Canadian Shield), and 3700-3200 Ma (the Acasta Gneiss complex). Even though many of these areas are far removed from the field area, studies have shown that detrital zircons from these areas were transported across the craton during earlier times and were then recycled during subsequent uplift and erosion (Gehrels et al., 1995; Rahl et al., 2003; Riggs et al., 2003). The analyzed detrital zircons produce ages similar to known ages of geologic complexes and orogenic events and are used to determine the provenance of the Muddy Creek Formation. Kimbrough et al. (2007) studied detrital zircons from the modern Colorado River delta; Miocene/Pliocene sediments along the lower Colorado River, Miocene to Pleistocene sediments in the Salton Trough, the Miocene Bidahochi Formation (on the southern Colorado Plateau in northeast Arizona and northwest New Mexico), and major tributaries

of the Colorado River to determine how and when the Colorado River became incised. The Bidahochi Formation is interpreted as a paleo-Colorado River deposit (Kimbrough et al., 2007). If detrital zircons analyzed in this study have ages comparable to detrital zircons analyzed by Kimbrough et al. (2007), the results support the hypothesis that the Muddy Creek Formation was deposited by a paleo-Colorado River. However, if the detrital zircon ages are dominantly between 13 and 24 Ma, then the results support the hypothesis that the Muddy Creek Formation was derived from the Caliente Caldera complex.

Age of the Muddy Creek Formation

The age of deposition for the Muddy Creek Formation has been loosely constrained between 8.5 Ma and 4.1 Ma (Metcalf, 1982; Bohannon, 1984; Williams, 1996; Pederson, 2001 and 2008). Stock (1921) originally placed a Pliocene age on the Muddy Creek Formation because it resembled the Panaca Formation, where he found Pliocene mammal bones. The Muddy Creek Formation was identified in literature as Pliocene in age based upon misinterpretation of Chester Longwell's early work on the Muddy Creek Formation by several authors (Longwell, 1946). Williams (1996) dated a basalt flow within the upper portion of the Muddy Creek Formation near Mesquite, Nevada at 4.1 Ma. The basalt flow is contained within the upper Muddy Creek Formation, so most of the Muddy Creek Formation must be older than 4.1 Ma. Metcalf (1982) dated two airfall tuff deposits within the Muddy Creek Formation in the Table Mesa basin at 8.5 Ma and 7.9 Ma using K-Ar dating. Eberly and Stanley (1978) dated basalt interbedded in the Muddy Creek Formation near the Overton Arm of Lake Mead at 8 Ma. Despite the lack of

compelling age control the Muddy Creek Formation was most likely deposited during the late Miocene and early Pliocene (Bohannon 1984; Pederson, 2001 and 2008).

Stratigraphy

Geologic units exposed in the study area consist of Miocene, Pliocene, and Pleistocene siliciclastic fluvial deposits. The stratigraphy near Mesquite, Nevada consists of rocks ranging from the Neogene Muddy Creek Formation to Holocene fluvial and alluvial deposits which are exposed in the vicinity of the study area. Although the exposed units are Neogene and Quaternary in age, there are older units in the subsurface that are not exposed in the field area. Figure 10 is a stratigraphic column derived from well data from the Virgin Oil 1A well on Mormon Mesa which shows the Muddy Creek Formation as well as older Cenozoic, Mesozoic, and Paleozoic age rocks (Bohannon et al., 1993). The Muddy Creek Formation and fluvial Pliocene and Pleistocene units are basin fill in this area. Units older than the Muddy Creek Formation are not exposed in the study area, but are exposed to the west of the study area, near Lake Mead. The Muddy Creek Formation unconformably overlies the older Neogene Horse Spring Formation and Red Sandstone unit (Bohannon, 1984). The main lithologies exposed near Mesquite are fluvial deposits and petrocalcic horizons (resistant carbonate soils).

The Miocene-Pliocene Muddy Creek Formation is the thickest and oldest unit that crops out in the Mesquite basin (Kowallis and Everett, 1986; Williams, 1996). Although 200 to 300 m of the Muddy Creek Formation is exposed, the true thickness of the Muddy Creek Formation is not known because much of the Muddy Creek Formation is in the sub-surface (Bohannon, 1984). The Muddy Creek Formation is extensively exposed and

continuous in southern Nevada (Fig. 7), but confined to basins, valleys, and elevational lows (Bohannon, 1984). The Muddy Creek Formation is comprised of fine to medium grained sandstones and siltstones, with interbedded conglomerates and gypsum deposits, but the Muddy Creek Formation varies compositionally throughout southern Nevada (Bohannon, 1984; Williams, 1996; Langenheim et al., 2000; Hanson et al., 2005). Bohannon (1984) and Beard et al. (2007) described the Muddy Creek Formation near Lake Mead as sandstones, siltstones, and conglomerates. The Muddy Creek Formation consists of pink, fine-grained, thinly bedded, consolidated sandstones and minor siltstones (Bohannon, 1984). Beard et al. (2007) mapped two different conglomerates within the Muddy Creek Formation, one conglomerate to the north of the River Mountains that contains both volcanic and plutonic clasts and one conglomerate west of Lake Mead that predominantly contains volcanic clasts with few sedimentary clasts. Williams (1996) described the Muddy Creek Formation near Mesquite, Nevada as an orange to pink, fine to medium grained, moderately consolidated, poorly to well sorted sandstone with interbedded conglomerates and minor gypsiferous layers. The Muddy Creek Formation locally is capped by a 2 m to 5 m thick petrocalcic horizon (Williams, 1996). Billingsley (1995) described the Muddy Creek Formation near Littlefield, Arizona as light red to brown, fine-grained, sandstone and siltstone with interbedded conglomerates and capping petrocalcic horizons. The sandstone is predominantly unconsolidated, thickly bedded, and weakly cemented with calcite. Billingsley (1995) described conglomerates within the Muddy Creek Formation which contained predominantly volcanic clasts from the ancestral Beaver Dam Wash.

The youngest units exposed in the area are Pliocene-Holocene fluvial deposits and petrocalcic horizons (Billingsley, 1995; Williams, 1996). Inset into the Muddy Creek Formation is a late Pliocene unit that resembles the Muddy Creek Formation. Beard et al. (2007) mapped an inset Pliocene unit near Lake Mead that consists of yellow, fine grained sandstone with interbedded conglomerates consisting of quartzite, chert, limestone, and minor volcanic clasts. This inset basin fill overlies the older Muddy Creek Formation and is composed of medium-fine grained sandstone, calcareous deposits, and interbedded conglomerates (Williams, 1996). The fluvial Pliocene deposits are red to yellow in color, coarse to fine grained, thinly bedded sandstones with interbedded conglomerates and capped by petrocalcic horizons (Billingsley, 1995; Williams, 1996). A Pliocene unit from two different locations laterally, north and south of the Virgin River, was separated into two separate units based on the composition of interbedded conglomerates (Billingsley, 1995; Williams, 1996). Billingsley (1995) determined that sometime after the Muddy Creek Formation was deposited the ancestral Virgin River and Beaver Dam Wash drainages eroded the finer grained deposits of the Muddy Creek Formation causing 200 m of incision. One Pliocene unit contains conglomerates consisting of predominantly volcanic clasts derived from the Beaver Dam Wash drainage, and the second Pliocene unit contains conglomerates consisting of predominantly metamorphic and sedimentary clasts derived from the Virgin River drainage (Billingsley, 1995). Billingsley (1995) concluded that the Muddy Creek Formation was incised and eroded by the ancestral Virgin River and Beaver Dam Wash drainages, which then deposited the inset Pliocene units at Littlefield, Arizona and in the Beaver Dam Wash which were part of this study.

Quaternary alluvium deposited by the Virgin River and local streams is also exposed in the area (Billingsley, 1995; Williams, 1996). The petrocalcic horizons which were first identified on Mormon Mesa by Gardner (1972) cap the Muddy Creek Formation and Pliocene deposits in the Mesquite area. The Mormon Mesa petrocalcic horizon is a pedogenic soil carbonate which started forming roughly 3-4 Ma (Gardner, 1972; Billingsley, 1995; Brock and Buck, 2009). The petrocalcic horizon formed as the result of calcium carbonate precipitation due to the repeated wetting and drying of the upper few meters of soil (Gardner, 1972). In many places the petrocalcic horizon formed in the upper part of reworked Muddy Creek Formation (Gardner, 1972) but in other areas it developed on the inset Pliocene units. The thickness of the petrocalcic horizons ranges from 20 cm to 5 m and is variable depending on location.

CHAPTER 4

METHODOLOGY

This project employed both field and laboratory methods. The field methods consisted of measuring sections, conducting conglomerate clast counts, recording paleocurrent indicators, and collecting samples. The laboratory methods consisted of preparing samples for analyses and then analyzing the samples.

Field Methods

Five stratigraphic sections (three in strata mapped as Muddy Creek Formation and two in younger inset Pliocene units) were measured, described, and sampled. Section locations (two to the north of the Virgin River Gorge, one to the south of the Virgin River Gorge, and two to the west of the Virgin River Gorge) were selected based on exposure quality and accessibility (Fig. 2). Sections were measured using a 1.5 m jacob staff and sight level. Paleocurrent indicators (foresets in cross-bedded sandstones and imbricated clasts in conglomerates) preserved within the sections were measured using a Brunton compass. The preserved paleocurrent indicators were plotted on a stereonet using the Stereowin 1.2 stereonet program developed by Almendinger (2002). Conglomerate clast counts were conducted on conglomerates within the measured sections, and clasts were identified and counted along a horizontal line using a tape measure and a 2 cm interval. Four additional conglomerate clast counts were conducted on conglomerates within the Muddy Creek Formation near Flat Top Mesa and at Mormon Mesa. Small sandstone samples and some unconsolidated sand samples (when consolidated sandstone samples

were not available) were collected for petrographic analysis, while large sandstone samples (mainly unconsolidated sand) were collected for detrital zircon analysis. In all, 39 samples were collected for sandstone petrography and detrital zircon analysis.

Laboratory Methods

Petrography

Hand samples of sandstones and unconsolidated sand samples were prepared for petrographic analysis. The hand samples were cut into billets using a rock saw; thin sections were created and stained for potassium and plagioclase feldspar. Unconsolidated sand samples were impregnated with epoxy; mounted on slides and stained for potassium and plagioclase feldspar. Five hundred points were counted for each of the 32 thin sections using a microscope and mechanical stage. Each thin section was assigned a random number taped over the sample number. The thin sections were randomly chosen by pulling a thin section out of a box to avoid bias. Once all thin sections were counted, the sample number was revealed. For all thirty-two thin sections counted, results are plotted on the chart by Van Der Plos and Tobi (1965) to determine the statistical reliability for framework grains counted. Counting 500 points for each sample from the Muddy Creek Formation and inset Pliocene units would produce a 95% confidence interval for all major framework grains counted.

Detrital Zircons

Detrital zircon samples were separated through a multiple step process, before they were analyzed at the Arizona LaserChron Center at the University of Arizona. The samples were prepared for analysis roughly following the guidelines of the Arizona

LaserChron Center's website for separation of detrital zircon samples with slight variations. Detrital zircon samples were dried and disaggregated using a mortar and pestle and sieved through a 500 μm disposable sieve. Once samples were sieved, they were transferred to the Wilfley Table where the first of two gravity separations occurred. The Wilfley Table separated the dense minerals from the light minerals by running water over the table top, while having sediment introduced through a hopper and chute. Water was decanted from the heavy mineral samples and remaining grains were irrigated with acetone, which was then filtered off. Samples were placed into beakers to dry over night, and then run through a vertical Frantz to separate iron fillings from the sample. A paper funnel was constructed in front of the magnet and the sample was poured into the funnel and collected into a beaker at the bottom. Once the samples were free of iron filings, a second gravity separation was conducted using Methylene Iodide (MI). To separate the dense minerals from the light minerals, the sample was poured into the MI. The resulting dense mineral separates were cleaned with acetone, then passed through a slope Frantz with the magnet set at varying amps with a side slope of 15 degrees. The samples were passed through at 0.3, 0.5, 0.7, 1.0, and 1.7 amps to separate the magnetic minerals from the non-magnetic minerals. After all five passes were completed both the magnetic and non-magnetic samples were looked at under a binocular scope, to ensure that only detrital zircons were in the non-magnetic fraction and no detrital zircons were in the magnetic fraction. The samples were mounted at the Arizona LaserChron Center by laboratory staff, following the Arizona LaserChron Center's guidelines for mounting and epoxying samples for analysis. The samples were then analyzed at the Arizona LaserChron Center

using U/Pb Laser-Ablation Multicollector Inductively Coupled Plasma Mass Spectrometry (La-ICPMS).

CHAPTER 5

RESULTS

Stratigraphy

To determine the stratigraphic relationships within the Muddy Creek Formation stratigraphic sections were measured in strata previously mapped as Muddy Creek Formation and within Pliocene units inset into the Muddy Creek Formation (Fig. 2). Three Muddy Creek Formation sections were measured from location F at Flat Top Mesa, at location H in the Beaver Dam Wash, and at location A on Mormon Mesa, and two stratigraphic sections were measured in Pliocene inset units at location G at Littlefield, Arizona and at location I in the Beaver Dam Wash (Fig. 2).

The Muddy Creek Formation at location F (Fig. 2) at Flat Top Mesa consists of dominantly orange to yellow, unconsolidated sandstone with interbedded conglomerates at the top of the section (Fig. 11). The sandstone in this section consists of moderately sorted, sub-angular to sub-rounded, fine to medium sandstone that is poorly cemented with calcite. This section contains ~90% sandstone, ~7% conglomerate, and ~ 3% shale. The sandstone within this section is massively bedded with beds ranging from 0.5 m to 5 m in thickness. The sandstone at location F (Fig. 2) at Flat Top Mesa is predominantly massively bedded sandstone, but locally muddy interbeds and some cross-bedded sandstone occur within this section and interrupt the massively bedded sandstone. The contacts between the beds are planar and laterally continuous.

The Muddy Creek Formation at location H (Fig. 2) in the Beaver Dam Wash is predominantly composed of orange, unconsolidated sandstone with interbedded

conglomerates near the top of the section (Fig. 12). The sandstone in this section is moderately sorted, angular to sub-angular, medium to coarse sandstone that is poorly cemented with calcite. This section contains ~90% sandstone, ~5% shale, and ~5% conglomerate. The sandstone is massively bedded with beds ranging from 0.3 m to 3.5 m in thickness. There are locally thin muddy interbeds, planar foresets, laminated sandstones, and mud cracks that interrupt the massively bedded sandstone. The contacts between the beds are mostly laterally continuous with some erosional contacts.

The Muddy Creek Formation at location A on Mormon Mesa (Fig. 2) predominantly consists of orange to yellow, unconsolidated sandstone with interbedded conglomerates near the top of the section (Fig. 13). The sandstone in this section consists of moderately sorted, fine to medium, sub-angular to sub-rounded sandstone cemented with calcite. This section contains ~95% sandstone and ~5% conglomerate. The sandstone is massively bedded with beds ranging from 0.5 m to 3 m in thickness. There are very few muddy interbeds and planar laminated sandstones that interrupt the massively bedded sandstone in this section. The contacts between the beds are laterally continuous.

The inset Pliocene unit at location G (Fig. 2) in Littlefield, Arizona is composed of mainly yellow, moderately consolidated sandstone with interbedded conglomerates at the base and the top of the section (Fig. 14). The sandstone in this section contains fine sub-rounded grains, is moderately sorted, and is cemented with calcite cement. This section contains ~70% sandstone, ~15% shale, and ~15% conglomerate. The sandstone is thinly to medium bedded with beds ranging from 0.25 m to 1.5 m in thickness. There are some nodular calcrete deposits, imbricated clasts within the conglomerates, and planar laminations within the sandstone. The contacts between the beds are laterally continuous.

The inset Pliocene unit at location I (Fig. 2) in the Beaver Dam Wash predominantly consists of orange, unconsolidated sandstone with interbedded conglomerates near the top of the section (Fig. 15). This section consists of poorly sorted, angular, and fine to medium sandstone that is cemented with calcite. This section contains ~90% sandstone, ~5% shale, and ~5% conglomerate. The sandstone is medium to massively bedded with beds ranging from 0.25 m to 2.25 m in thickness. There are laterally accreting foresets and laminated sandstones in this section. The contacts between the beds are mostly planar and laterally continuous, but there are some erosionally scoured contacts. Between the Muddy Creek Formation and the inset Pliocene unit is an obvious erosional unconformity separating the Muddy Creek Formation and the inset Pliocene unit. The lower 16 m of the section is the Muddy Creek Formation; the rest of the section is the inset Pliocene unit.

Petrographic Analyses

Thirty-two thin sections from strata previously mapped as Muddy Creek Formation and the inset Pliocene units were petrographically analyzed and point-counted to determine the provenance of the stratigraphic units of interest. Thin sections were petrographically analyzed, with 500 points counted for each thin section. Compositional data for each sample are included in Appendix I.

Figure 16 is a ternary diagram that shows the relative percentage of monocrystalline quartz (Qm), feldspar (F), and total lithic fragments (Lt) in each sample. Dickinson and Suczek (1982) first developed ternary diagrams for use in determining the provenance of sedimentary rocks. Different ternary diagrams (i.e., Q/F/L, Qm/F/Lt, Qp/Lv/Ls, Qm/P/K,

etc.) are used for different purposes. Qm/F/Lt ternary diagrams are the most useful for determining provenance and data from this study are shown on figure 16. The ternary diagram shows three very distinct groups that are separated based on composition. One group (shown as solid diamonds) consisting of samples from the inset Pliocene unit from location G (Fig. 2) plots near the Qm pole within the upper 35% of the diagram. The second group (shown as solid squares) plots near the Qm pole but below the first group of samples and contains samples from the Muddy Creek Formation from location A (Fig. 2). The third group (shown as red filled circles, green filled diamonds, and x's) plots near the Lt pole and contains samples from the Muddy Creek Formation from locations F and H (Fig. 2), as well as from the inset Pliocene unit at location I (Fig. 2).

Eight samples from the Muddy Creek Formation at location F (Fig. 2) were counted (circles on Fig. 16). Framework grains are composed of predominantly quartz and volcanic lithic fragments. There were few feldspar minerals (< 5%) present in these samples. Three of the sandstone samples counted were unconsolidated and had to be epoxied; therefore there is no cement in these samples. Five sandstone samples from this section were moderately cemented with calcite cement. These samples contained little to no matrix. The samples were dominated by volcanic lithic fragments, which comprised ~50% of the framework grains. There were ~1% sedimentary lithic fragments and ~2% carbonate grains. About ~45% of the grains consisted of quartz. In summary, the samples from location F (Fig. 2) are composed primarily of volcanic lithic fragments and quartz.

Seven samples from the Muddy Creek Formation at location H (Fig. 2) were counted (x's on Fig. 16). Framework grains are composed of predominantly volcanic lithic

fragments and quartz. The samples are composed of ~60% volcanic lithic fragments, ~40% quartz minerals, and ~5% feldspar minerals. Two sandstone samples that were point counted were unconsolidated samples and contained no cement because these samples were epoxied. The other five sandstone samples from this section were moderately consolidated and were cemented with calcite cement. The samples from this section contained almost no matrix. The samples contained ~33% more plagioclase feldspar then potassium feldspar. All the samples contained sedimentary lithic fragments, carbonate grains, and few metamorphic grains, but overall these grains represented a small percentage of the overall sample (~4%). The composition of the Muddy Creek Formation at location H (Fig. 2) consisted of mainly volcanic lithic fragments and quartz.

Seven samples from the measured section of the Muddy Creek Formation from location A (Fig. 2) were counted (squares on Fig. 16). Framework grains are composed of ~55-60% quartz, ~30% sedimentary and volcanic lithic fragments, and ~10-15% feldspar minerals. All the sandstone samples were unconsolidated and epoxied so they contain no cement. The samples contained almost equal amounts of sedimentary lithic fragments and volcanic lithic fragments. There were also almost equal amounts of plagioclase and potassium feldspar in the samples. The samples also contained minor amounts of carbonate grains, metamorphic lithic fragments, amphibole, and opaque minerals (~8%). The Muddy Creek Formation from location A (Fig. 2) is composed of quartz, sedimentary and volcanic lithic fragments, and feldspar grains.

Six samples from the inset Pliocene unit at location G (Fig. 2) were counted (triangles on Fig. 16). All of the sandstone samples that were point counted from this section were

well consolidated and well cemented with calcite cement. These samples were dominated by quartz (~75%). The samples also contained about equal amounts of feldspar grains and lithic fragments. There were ~15% feldspar minerals (plagioclase and potassium feldspar) and ~20% lithic fragments, which were mainly volcanic lithic fragments. These samples also contained some mica (~1%). The samples from the inset Pliocene unit at location G (Fig. 2) are comprised of quartz with some volcanic lithic fragments and feldspar grains.

Four samples from the inset Pliocene unit at location I (Fig. 2) were counted (diamonds on Fig. 16). Framework grains consisted of predominantly volcanic lithic fragments and quartz. Two of the sandstone samples that were point counted were unconsolidated, so they were epoxied and contained no cement. The other two sandstone samples were poorly consolidated with some calcite cement, but were not fully cemented. These samples contained almost no matrix. The dominant grains in these samples were volcanic lithic fragments (~55%) and quartz (~40%). Subequal amounts of plagioclase and potassium feldspar grains were seen in the samples, but they were not a dominant grain type (~5%). These samples contained (~1%) opaque minerals. The inset Pliocene unit at location I (Fig. 2) primarily consists of volcanic lithic fragments and quartz.

In summary, the data from the Muddy Creek Formation and the inset Pliocene units produced varied results. The results from the Muddy Creek Formation at locations F and H (Fig. 2) show that it is composed of 50% volcanic lithic fragments, 45% quartz, and 5% feldspar. In contrast the Muddy Creek Formation from location A (Fig. 2) has a higher percentage of quartz (55%), fewer lithic fragments (30%), and more feldspar (15%). Unlike the Muddy Creek Formation at locations F and H (Fig. 2) which have

dominantly volcanic lithic grains, the Muddy Creek Formation from location A (Fig. 2) contains lithic fragments with subequal amounts of sedimentary and volcanic lithic fragments. The results from the inset Pliocene unit at location G (Fig. 2) show that it is composed of 75% quartz, 20% feldspar and volcanic lithic fragments, and 5% other minerals. In contrast, the inset Pliocene unit at location I (Fig. 2) has higher volcanic lithic fragments (55%), with fewer quartz (45%) and minor amounts of feldspar and plots with samples of the Muddy Creek Formation from locations F and H (Fig. 2).

Detrital Zircon Analyses

Seven detrital zircon samples from the Muddy Creek Formation at locations F and H (Fig. 2), an inset Pliocene unit at location G (Fig. 2), the modern Virgin River at location J (Fig. 2), and the modern Beaver Dam Wash were analyzed by LA-ICPMS to determine the statistically definable age peaks of detrital zircons present in these samples. Concordia diagrams and data tables showing U/Pb isotope ratios and apparent ages for all detrital zircon samples are included in Appendix II. No detrital zircons were analyzed from the Muddy Creek Formation at location A (Fig. 2) or the inset Pliocene unit at location I (Fig. 2). Sample 08MC21 from the modern day Beaver Dam Wash only yielded three detrital zircons. The data for sample 08MC21 are included in Appendix II, but because this sample produced limited results it was excluded from further discussion.

The detrital zircon data for six samples were plotted on a cumulative probability plot (Fig. 17) so that samples could be compared to each other. The dark blue line (08MC29) is the cumulative probability plot for a sample from the base of the exposed section of the Muddy Creek Formation at location F (Fig. 2) at Flat Top Mesa and the dark green line

(08MC36) is the cumulative probability plot for a sample from the top of the Muddy Creek Formation at the same location. Sample 08MC36 contains more zircons younger than 1000 Ma than sample 08MC29, while sample 08MC29 contains more zircons older than 1000 Ma. The light purple/pink line (08MC11) is a cumulative probability plot for a sample from the base of the exposed section of the Muddy Creek Formation at location H (Fig. 2) in the Beaver Dam Wash and the light blue line (08MC18) is a cumulative probability plot of a sample from the top of the Muddy Creek Formation at location H (Fig. 2) in the Beaver Dam Wash. Unlike the Muddy Creek Formation at location F (Fig. 2), the detrital zircon cumulative probability plots of samples from the top and bottom of the Muddy Creek Formation at location H (Fig. 2) are very similar from 1000 Ma to 3000 Ma. The lime green line (08MC09) is the cumulative probability plot for a sample from the base of the inset Pliocene unit at location G (Fig. 2) at Littlefield, Arizona and the orange line (08MC20) is a cumulative probability plot for a sample from the modern day Virgin River at location J (Fig. 2) in the Virgin River Gorge. These two lines are intertwined and almost identical over the entire age spectrum and differ from the curves representing the Muddy Creek Formation between 1000 Ma and 2000 Ma. The cumulative probability plot shows that for all detrital zircons analyzed from the samples 20% of detrital zircons are younger than 500 Ma, 70% of the detrital zircons are between 500 Ma and 2000 Ma, and 10% of detrital zircons older than 2000 Ma.

The detrital zircon data for the six samples were placed into an overlap-similarity program to determine if two age probabilities overlap and whether proportions of overlapping ages are similar (Tables 1 and 2). The degree of overlap is the degree to which two age probabilities overlap. To determine the degree of overlap, values from

zero to one are assigned to the samples. A value of one is given to samples that have perfect overlap and a value of zero is given to samples that have no overlap.

The degree of similarity is a measure of whether proportions of overlapping ages are similar. To determine the degree of similarity values are assigned to samples. A value up to one is given to samples that reflect similar proportions of overlapping ages and a value down to zero is given to samples that reflect different proportions of ages that may or may not overlap.

All of the samples overlap each other well, but none of the samples have perfect overlap with each other. Overlap values range from 0.89 to 0.72, while similarity values range from 0.84 to 0.60. The overlap values show statistical correlation between some of the samples. Samples from the inset Pliocene unit at location G (Fig. 2) (08MC09), the top of the Muddy Creek Formation at location H (Fig. 2) (08MC18), the modern Virgin River at location J (Fig. 2) (08MC20), and the base of the Muddy Creek Formation at location F (Fig. 2) (08MC29) show 81-89% overlap with respect to each other. There is less than 80% overlap between samples from the base of the Muddy Creek Formation at location H (Fig. 2) (08MC11) and the top of the Muddy Creek Formation at location F (Fig. 2) (08MC36) as well as with samples 08MC09, 08MC18, 08MC20, and 08MC29. The samples analyzed in this study have more overlap with each other, than similarity with each other. Sample 08MC20 had 84% similarity with sample 08MC09 and 80% similarity with 08MC29. There was less than 70% overlap between the other samples.

Figure 18 is a relative probability plot of all detrital zircons analyzed in this study. This plot shows the major detrital zircon age populations when all data are summed. This relative probability plot shows thirteen statistically defined age peaks at 20 Ma, 96 Ma,

182 Ma, 246 Ma, 358 Ma, 436 Ma, 618 Ma, 1096 Ma, 1470 Ma, 1758 Ma, 2668 Ma, 2736 Ma, and 2816 Ma.

Figure 19 is a normalized probability plot that shows the range of detrital zircon ages within each sample. Four samples from the Muddy Creek Formation (two at location F (Fig. 2) and two at location H (Fig. 2)), one sample from the inset Pliocene unit at location G (Fig. 2), and one sample from the modern day Virgin River at location J (Fig. 2) are stacked on top of each other to view similarities and differences between the samples. Sample 08MC29 was collected from the base of the Muddy Creek Formation at location F (Fig. 2) at Flat Top Mesa and sample 08MC36 was collected from the top of the Muddy Creek Formation at location F (Fig. 2) at Flat Top Mesa (Fig. 11). Ninety five detrital zircons from sample 08MC29 were analyzed, while only twenty eight detrital zircons from sample 08MC36 were analyzed. Figures 20 and 21 are relative probability plots of all detrital zircons in samples 08MC29 and 08MC36, respectively. A normalized probability plot of sample 08MC29 shows six statistically defined age peaks at 19 Ma, 1174 Ma, 1461 Ma, 1680 Ma, 1747 Ma, and 2095 Ma (Fig. 20), determined by a detrital age pick program. Unlike sample 08MC29, a normalized probability plot of sample 08MC36 shows four statistically defined age peaks determined by a detrital zircon age pick program at 555 Ma, 609 Ma, 1166 Ma, and 2786 Ma (Fig. 21). The age peak at 1166 Ma from the bottom of the Muddy Creek Formation is similar to the age peak at 1174 Ma age peak from the top of the Muddy Creek Formation. There are no other correlative statistically defined age peaks between the top and bottom of the Muddy Creek Formation at location F (Fig. 2).

Samples 08MC11 and 08MC18 were collected from the base and top of a 73 m section of the Muddy Creek Formation at location H (Fig. 2) in the Beaver Dam Wash (Fig. 12). Forty detrital zircons were analyzed in sample 08MC11 and one hundred detrital zircons were analyzed in sample 08MC18. Figures 22 and 23 are relative probability plots of all detrital zircons analyzed from the Muddy Creek Formation at location H (Fig. 2) in the Beaver Dam Wash. When sample 08MC11 was mounted at the University of Arizona, the sample was not fully sanded down and therefore most of the detrital zircons were under epoxy when the sample was analyzed. A relative probability plot of sample 08MC11 shows six statistically defined age peaks determined by a detrital zircon age peak program at 1017 Ma, 1178 Ma, 1437 Ma, 1747 Ma, 1839 Ma, and 1986 Ma (Fig. 22). A relative probability plot of sample 08MC18 shows twelve statistically defined age peaks at 15 Ma, 21 Ma, 442 Ma, 593 Ma, 618 Ma, 679 Ma, 700 Ma, 1127 Ma, 1466 Ma, 1737 Ma, 1834 Ma, and 2754 Ma (Fig. 23). The bottom of the Muddy Creek Formation at location H (Fig. 2) has statistically defined age peaks at 1178 Ma, 1437 Ma, 1747 Ma, and 1839 Ma and the top of the Muddy Creek Formation at location H (Fig. 2) has similar statistically defined age peaks at 1127 Ma, 1466 Ma, 1737 Ma, and 1834 Ma.

Sample 08MC09 was collected from the base of the inset Pliocene unit at location G (Fig. 2) in Littlefield, Arizona (Fig. 14) and is the only detrital zircon sample from the inset Pliocene units in this study. One hundred detrital zircons were analyzed for this sample. Figure 24 is a relative probability plot of all detrital zircons from this sample, showing ten statistically defined age peaks at 376 Ma, 428 Ma, 601 Ma, 1062 Ma, 1072 Ma, 1376 Ma, 1449 Ma, 1736 Ma, 1855 Ma, and 2734 Ma (Fig. 23), determined by a

detrital age peak program. Statistically defined age peaks at 428 Ma, 601 Ma, 1062 Ma, 1449 Ma, 1736 Ma, 1855 Ma, and 2734 Ma are similar to statistically defined age peaks within samples taken at the top of the Muddy Creek Formation at locations F and H (Fig. 2).

Sample 08MC20 is a modern sand sample from the Virgin River at location J (Fig. 2) in the Virgin River Gorge. Detrital zircon ages from this sample presumably characterize a modern detrital zircon provenance for the portion of the Colorado Plateau drained by the Virgin River. One hundred detrital zircons were analyzed in this sample. Figure 25 is a relative probability plot of all detrital zircons in this sample, showing seventeen statistically defined age peaks determined by a detrital zircon age peak program at 19 Ma, 20 Ma, 24 Ma, 272 Ma, 357 Ma, 410 Ma, 453 Ma, 535 Ma, 617 Ma, 1015 Ma, 1095 Ma, 1396 Ma, 1467 Ma, 1701 Ma, 1886 Ma, 1943 Ma, and 2814 Ma (Fig. 25). This sample produced nine statistically defined age peaks at 357 Ma, 453 Ma, 617 Ma, 1095 Ma, 1396 Ma, 1467 Ma, 1701 Ma, 1886 Ma, and 2814 Ma that are similar to statistically defined age peaks within the sample in the inset Pliocene unit at location G (Fig. 2). Twelve of the statistically defined age peaks from the modern Virgin River at location J (Fig. 2) are similar to statistically defined age peaks from the top and bottom of the Muddy Creek Formation at locations F and H (Fig. 2).

Paleocurrent Indicators

The Muddy Creek Formation at locations F and H (Fig. 2) and inset Pliocene unit at location G (Fig. 2) contain paleocurrent indicators which record paleoflow directions. Paleocurrent indicators preserved within cross-bedded planar foreset sandstones in the

Muddy Creek Formation were measured at locations F and H (Fig. 2). Preserved paleocurrent indicators from imbricated clasts within interbedded conglomerates were measured in an inset Pliocene unit at location G (Fig. 2). The paleocurrent indicators from within the Muddy Creek Formation and the inset Pliocene unit were plotted on rose diagrams using the Stereowin 1.2 stereonet program created by Almendinger (2002). The paleoflow direction preserved in the Muddy Creek Formation at location F (Fig. 2) at Flat Top Mesa is south-southwest directed (Fig. 26) and the paleoflow direction at location H (Fig. 2) in the Beaver Dam Wash was south-southeast directed (Fig. 27). The paleoflow direction of an inset Pliocene unit at location G (Fig. 2) at Littlefield, Arizona was to the south-southwest (Fig. 28). Evidence from the measured paleocurrent indicators, indicates a strong southward directed paleocurrent direction in the Muddy Creek Formation as well as in the inset Pliocene unit throughout both units.

Conglomerate Clast Counts

Clast counts were performed on conglomerates interbedded within the Muddy Creek Formation and the younger inset Pliocene units in order to determine their composition (Fig 2). The results help constrain the provenance of the Muddy Creek Formation. Studied sections include the Muddy Creek Formation at location F at Flat Top Mesa, at location H in the Beaver Dam Wash, and from locations A-E at Mormon Mesa (Fig. 2). Figure 29 shows conglomerate clast count results from the measured sections at location F at Flat Top Mesa and from location A at Mormon Mesa as well as four additional conglomerates conducted at locations B-E at Mormon Mesa (Fig. 2). Conglomerate clasts were also counted on interbedded conglomerates within two inset Pliocene units at

location G at Littlefield, Arizona and at location I in the Beaver Dam Wash (Fig. 2). Compositional data for each clast count are included in Appendix III as histograms, showing which clasts were counted.

Two conglomerate clast counts were conducted in the measured section in the Muddy Creek Formation at location F (Fig. 2) and both clast counts show similar results. The conglomerates were composed of predominantly volcanic clasts (80-85%), with some sedimentary clasts (15%), and few metamorphic clasts (0-5%) (Figs. 30 and 31). The conglomerate clast count conducted at location H (Fig. 2) yielded results similar to those at location F (Fig. 2). The clasts were predominantly volcanic clasts (73%), with some sedimentary clasts (23%), and few metamorphic clasts (4%) (Fig. 32). Two conglomerate clast counts were conducted in the measured section of the Muddy Creek Formation from location A (Fig. 29) and both counts produced similar results. Unlike the results from locations F and H (Fig. 2), conglomerates from location A (Fig. 29) consist of 50-60% igneous clasts, 20-30% sedimentary clasts, and 15-25% metamorphic clasts (Figs. 33 and 34). A key difference between the compositions from location A (Fig. 29) compared to locations F and H (Fig. 2) is that one third of the igneous clasts from location A (Fig. 29) are plutonic whereas 100% of the igneous clasts at locations F and H (Fig. 2) are volcanic clasts. There is also an order of magnitude higher percentage of metamorphic clasts from location A (Fig. 29). Four additional conglomerate clast counts from locations B-E (Figs. 2, 29) were conducted to determine how the conglomerates at location F (Fig. 2) and from location A (Fig. 2) are related (Figs. 35-38). The conglomerate from location B (Fig. 29) consists of 45% volcanic clasts, 35% metamorphic clasts, 10% sedimentary clasts, and 10% plutonic clasts, while the

conglomerate from location C (Fig. 29) contains 48% igneous clasts, 40% sedimentary clasts, and 12% metamorphic clasts (Figs. 35 and 36). Clasts in conglomerates from locations D and E (Fig. 29) consist of 65-75% volcanic clasts, 22-27% sedimentary clasts, and 3-8% metamorphic clasts (Figs. 37 and 38). Conglomerate clasts within two inset Pliocene units were counted at location G (Fig. 2) and at location I (Fig. 2) (Figs. 39 and 40). Unlike any of the previously mentioned results, conglomerate clasts from location G (Fig. 2) consisted of predominantly sedimentary clasts (44%) and metamorphic clasts (38%) and some volcanic clasts (18%) (Fig. 39). Conglomerate clasts from the inset Pliocene unit at location G (Fig. 2) consist of primarily sedimentary and metamorphic derived material, with little volcanic derived material. Despite being demonstrably younger than the Muddy Creek Formation, conglomerates within the inset Pliocene unit at location I (Fig. 2) are most similar to the Muddy Creek Formation at locations F and H (Fig. 2) and consist almost entirely of volcanic clasts (94%) with almost no sedimentary (4%) or metamorphic clasts (2%) (Fig. 40). In summary, despite stratigraphic age differences the conglomerate data from the Muddy Creek Formation at locations F and H (Fig. 2) and the inset Pliocene unit at location I (Fig. 2) are similar. Results from the Muddy Creek Formation from location A (Fig. 29) are intermediate between results from other Muddy Creek Formation sections at locations F and H (Fig. 2) and the inset Pliocene unit at location G (Fig. 2). Results from the interbedded conglomerates from locations B-E (Fig. 29) are gradational and show a compositional change from the northeast to the southwest.

The five stratigraphic sections were compiled to create a southwest-northeast transect to show the stratigraphic relationship between the Muddy Creek Formation and inset

Pliocene units (Fig. 41). Conglomerate clast counts have been added to the stratigraphic columns to show the change in the composition of the Muddy Creek Formation from the southwest to the northeast as well as the change in composition of the inset Pliocene units.

CHAPTER 6

INTERPRETATIONS AND CONCLUSIONS

Interpretations

The sedimentological, petrographic, detrital zircon, paleocurrent, and conglomerate clast count data are interpreted to determine the provenance of the Muddy Creek Formation as well as the inset Pliocene units. Figure 42 shows all stratigraphic columns measured in the Muddy Creek Formation and inset Pliocene units correlated along a southwest to northeast transect. All stratigraphic sections are hung from an upper datum because all sections are capped by a petrocalcic horizon, which is presumed to be correlative throughout the study area. A dashed line separates sections in the Muddy Creek Formation from Pliocene units which are inset into the Muddy Creek Formation. Pliocene units previously determined to be age correlative by Billingsley (1995) are separated by a vertical dashed line, because even though they are age correlative units, compositionally they are not the same and therefore are represented as two separate units. Conglomerate data from all measured sections, as well as from locations B-E (Fig. 29) on Mormon Mesa, show how the composition of the interbedded conglomerates of the Muddy Creek Formation and inset Pliocene units varies from southwest to northeast.

The predominance of volcanic lithic fragments and quartz in the Muddy Creek Formation from location F (Fig. 2) at Flat Top Mesa and location H (Fig. 2) in the Beaver Dam Wash indicate derivation from a volcanic source. Samples that are rich in quartz and volcanic lithic fragments could not have been derived from the Colorado Plateau as sediments derived from the Colorado Plateau have very different compositions (Peterson

and Turner-Peterson, 1989; Baars, 2000). Rocks on the Colorado Plateau consist of predominantly sedimentary and metamorphic rocks with some plutonic rocks (Peterson and Turner-Peterson, 1989; Baars, 2000). The Muddy Creek Formation at locations F and H (Fig. 2) is interpreted as derived from the volcanic Caliente Caldera complex which lies to the north because sediment derived from the Caliente Caldera complex would produce sediment compositions like those seen in thin-section in this study. Derivation of sediment from the Caliente Caldera complex would also result in south directed paleocurrent indicators like those documented at locations F and H (Fig. 2). Some of the conglomerate clasts contained within the Muddy Creek Formation from locations F and H (Fig. 2) contain flow banded textures that are common in rocks from the Caliente Caldera complex (personal communication E.I. Smith, 2008). Other clasts are also similar to rocks from the Caliente Caldera complex; e.g., basalts, ryholites, and andesites. Based upon the high abundance of volcanic clasts within the conglomerates the clasts are interpreted as being derived from the Caliente Caldera complex. Petrographically, the Muddy Creek Formation at locations F and H (Fig. 2) was derived from a transitional recycled orogen (Fig. 16). These results indicate derivation from a volcanic source (the Caliente Caldera complex) as well as quartzose continental crust.

Figure 43 is a cumulative probability plot of detrital zircons ages from the bottom of the Muddy Creek Formation from locations F and H (Fig. 2), the Bidahochi Formation, and known Colorado River deposits. Detrital zircons from the Bidahochi Formation represent detrital zircons from a paleo-Colorado River. If detrital zircons from the bottom of the Muddy Creek Formation at locations F and H (Fig. 2) are comparable to detrital zircons from the Bidahochi Formation, then the Muddy Creek Formation was

deposited by a paleo-Colorado River. The cumulative probability plot shows some similarity between the base of the Muddy Creek Formation at locations F and H (Fig. 2) and known Colorado River deposits. However, there is no similarity between the base of the Muddy Creek Formation at locations F and H (Fig. 2) and the Bidahochi Formation. These results show that the base of the Muddy Creek Formation from locations F and H (Fig. 2) was not derived from the Colorado Plateau and deposited by a paleo-Colorado River, and these data are consistent with paleocurrent, petrographic, or conglomerate clast count data that show the Muddy Creek Formation from locations F and H (Fig. 2) was derived from the Caliente Caldera complex.

Figure 44 is a cumulative probability plot of samples from the top of the Muddy Creek Formation from locations F and H (Fig. 2), the Bidahochi Formation, and known Colorado River deposits. The cumulative probability plots of detrital zircons from the top of the Muddy Creek Formation at locations F and H (Fig. 2) are not comparable to the cumulative probability plot of known Colorado River detrital zircons. The cumulative probability plots of detrital zircons from the top of the Muddy Creek Formation at locations F and H (Fig. 2) are similar to detrital zircons from the Bidahochi Formation because all three cumulative probability plots contain a high percentage (30%-40%) of detrital zircons younger than 500 Ma (Fig. 44). These are the only samples that contain a large percentage of young zircons. The cumulative probability plots from top of the Muddy Creek Formation at locations F and H (Fig. 2) are similar to the cumulative probability plot of detrital zircons from the Bidahochi Formation. However, a paleo-Colorado River could not have deposited the top of the Muddy Creek Formation at locations F and H (Fig. 2) because the top of the Muddy Creek Formation at locations F

and H (Fig. 2) is loosely constrained to have been deposited by 4.1 Ma. The cumulative probability plots for both samples are similar, showing that the top of the Muddy Creek Formation from locations F and H (Fig. 2) contains similar detrital zircons that were derived from similar sources. Comparing the cumulative probability plots it is clear that detrital zircons from the top of the Muddy Creek Formation from locations F and H (Fig. 2) are different than those from the bottom of the Muddy Creek Formation and they are not comparable to known Colorado River detrital zircons. This shows that the Muddy Creek Formation from locations F and H (Fig. 2) was not deposited by a paleo-Colorado River. Even though there is only partial overlap, partial similarity, and a lack of similar statistically definable age peaks between the top and bottom of the Muddy Creek Formation from locations F and H (Fig. 2) both sections are Muddy Creek Formation based upon sedimentological, conglomerate, and petrographic data. The normalized probability plots of detrital zircons analyzed in this study show significant differences between the top (08MC36) and bottom (08MC29) of the Muddy Creek Formation from location F (Fig. 2) at Flat Top Mesa (Figs. 20 and 21) and the top (08MC18) and the bottom (08MC11) of the Muddy Creek Formation from location H (Fig. 2) in the Beaver Dam Wash (Figs. 22 and 23). The biggest difference between the top and bottom of the Muddy Creek Formation at locations F and H (Fig. 2) is that the top of the Muddy Creek Formation in both sections contains Paleozoic and Proterozoic age zircons, whereas the base of the Muddy Creek Formation in both sections contains predominantly Proterozoic age zircons. This finding suggests a changing detrital zircon provenance within the Muddy Creek Formation through time.

Preserved paleocurrent indicators and sedimentological data indicate that the Muddy Creek Formation at locations F and H (Fig. 2) was mainly derived from the Caliente Caldera complex and transported south via high energy, fluvial systems. Southerly directed paleocurrent directions at locations F and H (Fig. 2) argue against a paleo-Colorado River flowing through the Virgin River Gorge because north-directed paleocurrent indicators would have been produced in the Beaver Dam Wash section. Sub-rounded to sub-angular conglomerate clasts indicate that the clasts traveled a modest distance from their source.

The Muddy Creek Formation from location A at Mormon Mesa (Fig. 2) is dominated by quartz and subequal amounts of volcanic lithic fragments and sedimentary lithic fragments, which indicate that this unit could not be derived solely from a volcanic source like the Muddy Creek Formation at locations F and H (Fig. 2). Due to the reduced abundance of volcanic lithic fragments and increased abundance of sedimentary lithic fragments, the Muddy Creek Formation at location A (Fig. 2) on Mormon Mesa is most likely derived from a mixed provenance, which includes the Caliente Caldera complex and the Colorado Plateau. Petrographic data indicate that the Muddy Creek Formation from location A (Fig. 2) was derived from a quartzose recycled orogen (Fig. 16). The conglomerate clast count results from the Muddy Creek Formation at locations A-E on Mormon Mesa (Fig. 29) show a gradational change from the northeast to the southwest and show a mixing of material from two lithologically distinct areas. Conglomerates from locations D and E (Fig. 29) were derived from the Caliente Caldera complex due to the high abundance of volcanic clasts and similarity to conglomerates from location F (Fig. 2) at Flat Top Mesa and location H (Fig. 2) in the Beaver Dam Wash. The volcanic

clasts are similar in composition to clasts within the Muddy Creek Formation from locations F and H (Fig. 2) and suggest that the volcanic clasts at location D and E (Fig. 2) were derived from the Caliente Caldera complex. The conglomerates on Mormon Mesa gradually change from being dominated by volcanic clasts in the northeast at locations D and E (Fig. 2) to being dominated by more sedimentary and metamorphic clasts in the southwest at locations B and C (Fig. 2). Conglomerate clasts from locations B and C (Fig. 29) were derived from both the Caliente Caldera complex and the Colorado Plateau because the conglomerates contain clasts that are similar to rocks from the Caliente Caldera complex and rocks that crop out on the Colorado Plateau. The wide range of clast composition shows that the conglomerates within the Muddy Creek Formation at location A (Fig. 2) are significantly more diverse than the conglomerates from locations F and H (Fig. 2). Many of the conglomerate clasts are similar in composition to rocks that crop out on the Colorado Plateau and suggest that some of the clasts were derived from the Colorado Plateau. The conglomerates within the Muddy Creek Formation at location A (Fig. 2) contain clasts that are sub-rounded to sub-angular and therefore traveled a modest distance from their sources, which include the Caliente Caldera complex and the Colorado Plateau. Like the Muddy Creek Formation from location F (Fig. 2) at Flat Top Mesa and location H (Fig. 2) in the Beaver Dam Wash, the Muddy Creek Formation at location A (Fig. 2) on Mormon Mesa was deposited in a high energy fluvial environment based on the sedimentological data. The Muddy Creek Formation at location A (Fig. 2) is presumed to have south-southwest directed paleocurrent indicators based on paleocurrent indicators in the Muddy Creek Formation at locations F and H (Fig. 2), although no paleocurrent indicators were measured in this section.

The inset Pliocene unit at location I (Fig. 2) in the Beaver Dam Wash predominantly contained volcanic lithic fragments and quartz suggesting that this unit was derived from a volcanic source area. The percentages of volcanic lithic fragments and quartz are similar to samples from the Muddy Creek Formation from locations F and H (Fig. 2), suggesting that despite different ages, these units were derived from the same source, i.e., the Caliente Caldera complex and quartzose areas to the north of the field area. Although the conglomerate within the inset Pliocene unit from location I (Fig. 2) has slightly more volcanic clasts, it is reasonable to assume that the conglomerate clasts are derived from the same source as the conglomerate clasts within the Muddy Creek Formation at locations F and H (Fig. 2). Angular to sub-angular conglomerate clasts indicate that the clasts traveled a short distance from their source. Petrographic data indicate that the inset Pliocene unit from location I (Fig. 2) was derived from a transitional recycled orogen (Fig. 15). The inset Pliocene unit at location I (Fig. 2) was deposited in a high energy fluvial environment based on the sedimentological evidence.

The Pliocene unit from location G (Fig. 2) at Littlefield, Arizona is predominantly composed of quartz with minor sub-equal amounts of feldspar and volcanic lithic fragments indicating that this inset Pliocene unit was primarily derived from a quartz-rich location with minor input from a volcanic source area. Therefore, this Pliocene unit has a distinctly different provenance than the inset Pliocene unit at location I (Fig. 2) in the Beaver Dam Wash. The inset Pliocene unit from location G (Fig. 2) was likely derived from the Colorado Plateau because rocks on the Colorado Plateau have compositions rich in quartz and low in volcanic lithic fragments (Peterson and Turner-Peterson, 1989; Baars, 2000). Petrographic data indicates that the inset Pliocene unit at Littlefield,

Arizona was derived from a quartzose recycled orogen (Fig. 16). Therefore the inset Pliocene unit from location G (Fig. 2) is interpreted as being derived from the Colorado Plateau based on petrographic data. The conglomerate clasts in the inset Pliocene unit at location G (Fig. 2) consist of dominantly sedimentary and metamorphic clasts, with few volcanic clasts and therefore I interpret that the clasts are derived from the Colorado Plateau. The conglomerate clast data are also consistent with petrographic data and support derivation from the Colorado Plateau. Detrital zircons from the inset Pliocene unit at location G (Fig. 2) at Littlefield, Arizona, the modern Virgin River, the Bidahochi Formation, and known Colorado River deposits are compared on a cumulative probability plot (Fig. 45). The cumulative probability plots of detrital zircons from the inset Pliocene unit from location G (Fig. 2), the Virgin River, the Bidahochi Formation, and Colorado River deposits are not comparable. Therefore, the inset Pliocene unit at location G (Fig. 2) was not deposited by a paleo-Colorado River. The cumulative probability plots (Fig. 45) of detrital zircons from the inset Pliocene unit from location G (Fig. 2) at Littlefield, Arizona and at location J (Fig. 2) from the modern Virgin River are intertwined and similar over geologic time. The normalized probability plots of detrital zircons from the inset Pliocene unit from location G (Fig. 2) and from the modern Virgin River in location J (Fig. 2) show that the samples have similar probability plots and contain similar statistically definable age peaks (Figs. 24 and 25). I interpret that the inset Pliocene unit at location G (Fig. 2) was not deposited by a paleo-Colorado River, but rather was deposited by a paleo-Virgin River because detrital zircons from the inset Pliocene unit and Virgin River are very similar. Based on the sedimentological evidence and the southwest paleocurrent direction preserved within the inset Pliocene unit at location G

(Fig. 2), this unit could have been deposited by a paleo-Virgin River or from the Caliente Caldera complex, but petrographic data rule out the Caliente Caldera complex and support the paleo-Virgin River origin interpretation. A paleo-Virgin River flowing through the Virgin River Gorge would have brought sediment from northeast of Littlefield, Arizona and deposited it in this region and produced paleocurrent indicators that show transport to the southwest.

The Muddy Creek Formation from location A at Mormon Mesa (Figs. 2, 29) was derived from both the Caliente Caldera complex and the Colorado Plateau based on petrographic and conglomerate clast count data, but the provenance of the Muddy Creek Formation at location A (Figs. 2, 29) is different than the provenance of the Muddy Creek Formation at locations F and H (Fig. 2). There are two explanations for the Muddy Creek Formation from location A (Fig. 2): 1) The studied section from location A (Fig. 2) is Muddy Creek Formation, is late Miocene-early Pliocene in age, and is a mixture of two sources; or 2) The studied section from location A (Fig. 2) is not Muddy Creek Formation, is not late Miocene-early Pliocene in age, but rather is inset into the Muddy Creek Formation. I interpret that the strata at location A on Mormon Mesa (Fig. 2) are part of the Muddy Creek Formation, are late Miocene-early Pliocene in age, and were derived from both the Caliente Caldera complex and Colorado Plateau based on petrographic and conglomerate clast count data. Despite differences between the provenance of the Muddy Creek Formation at locations F and H (Fig. 2) when compared to location A (Fig. 2) there are similar volcanic clasts within the conglomerates at all three locations. The Muddy Creek Formation at location A on Mormon Mesa (Fig. 2) is a combination of material derived from the Caliente Caldera complex and the Colorado

Plateau, which was deposited by a paleo-Virgin River because conglomerates within the Muddy Creek Formation at location A (Fig. 2) have a composition similar to conglomerates within the inset Pliocene unit at location G (Fig. 2). Petrographic analyses and conglomerate clast counts show that a portion of the Muddy Creek Formation at location A (Fig. 2) on Mormon Mesa is similar in composition to the inset Pliocene unit at Littlefield, Arizona. Therefore, a portion of the Muddy Creek Formation at location A (Fig. 2) was derived from the Colorado Plateau and deposited by a paleo-Virgin River. The petrocalcic horizon above the Muddy Creek Formation from location A at Mormon Mesa (Fig. 2) formed about 3 Ma (Brock and Buck, 2009), meaning that the Muddy Creek Formation from location A (Fig. 2) is at least older than 3 Ma. However, this line of argument is circular in that the petrocalcic horizon is assumed to be as much as 3 Ma in part because it is assumed that it is developed in Miocene-Pliocene Muddy Creek Formation. The Muddy Creek Formation at location A (Fig. 2) on Mormon Mesa is Muddy Creek Formation, even though the provenance is different than the provenance of the Muddy Creek Formation at locations F and H (Fig. 2). This conclusion is in agreement with previous researchers who have mapped this unit at location A (Fig. 2) as Muddy Creek Formation (Billingsley, 1995; Pederson, 2008).

Figures 46 and 47 show how the study area near Mesquite evolved during the Miocene and Pliocene when the Muddy Creek Formation and inset Pliocene units were deposited. Figure 46 shows the study area near Mesquite during the Miocene when the Muddy Creek Formation was deposited. The Muddy Creek Formation at Flat Top Mesa and in the Beaver Dam Wash was deposited by sediment derived from the Caliente Caldera complex. Sediment derived from the Caliente Caldera complex was transported

to the southwest of Flat Top Mesa and the Beaver Dam Wash to Mormon Mesa. Colorado Plateau derived sediments transported by a paleo-Virgin River, mixed and interfingered with sediment derived from the Caliente Caldera complex to deposit the Muddy Creek Formation at Mormon Mesa. Sometime after the Muddy Creek Formation was deposited at Flat Top Mesa, Mormon Mesa, and in the Beaver Dam Wash, the Muddy Creek Formation was incised and cut by Pliocene faults that allowed a Pliocene unit to become inset within the Muddy Creek Formation. Figure 47 shows the study area near Mesquite during the Pliocene after the Muddy Creek Formation was deposited and when the Pliocene units were deposited. Sediment derived from the Caliente Caldera complex was deposited in the Beaver Dam Wash. Colorado Plateau derived sediments transported by a paleo-Virgin River were deposited at Littlefield, Arizona. Sediment from the Caliente Caldera complex and Colorado Plateau mixed and interfingered to presumably deposit Pliocene units to the southwest of the study area that are similar in composition to the Muddy Creek Formation at Mormon Mesa. During the Pleistocene the Muddy Creek Formation and inset Pliocene units were incised by the modern Beaver Dam Wash and Virgin River drainages.

This study determined that the Muddy Creek Formation from location F (Fig. 2) at Flat Top Mesa and location H (Fig. 2) in the Beaver Dam Wash was derived from the Caliente Caldera complex, while the Muddy Creek Formation from location A (Fig. 2) at Mormon Mesa was derived from the Caliente Caldera complex and the Colorado Plateau, which was deposited by a paleo-Virgin River. This study also determined that the Muddy Creek Formation was not deposited by a paleo-Colorado River. This interpretation is similar to the conclusion made by Pederson (2008). Pederson (2008)

determined via petrographic analysis that the Muddy Creek Formation was derived from local volcanic sources (i.e., the Caliente Caldera complex and Kane Springs volcanic center) and was not deposited by a paleo-Colorado River (Fig. 4). While Pederson (2008) suggested that the Muddy Creek Formation was derived from local volcanic sources and not the Colorado Plateau, results from his samples 2, 4, 6, 7, 8, 9, and 10 indicate that the Muddy Creek Formation has a Colorado Plateau derivation (Fig. 4). However, the results of this study are different than results from the Meadow Valley Wash that was previously studied by Dicke (1990). Dicke (1990) concluded that the Muddy Creek Formation in the Meadow Valley Wash was derived from the Moenkopi and Chinle Formations as well as local volcanic centers. Results from the Muddy Creek Formation in the Meadow Valley Wash are similar to results from locations A-C (Fig. 28), as they were both derived from multiple sources including a volcanic complex. The results from the Meadow Valley Wash are different from the results in this study because the Muddy Creek Formation from locations F and H (Fig. 2) was derived entirely from the Caliente Caldera complex. The results of this study are also different from results from the western edge of Lake Mead previously studied by Scott (1988). Scott (1988) concluded that the interbedded conglomerates in the Muddy Creek Formation around Lake Mead were derived from the River Mountains. The results from Lake Mead are different from the results in this study because the Muddy Creek Formation from locations F and H (Fig. 2) was derived from the Caliente Caldera complex.

Conclusions

The purpose of this study was to determine the depositional history, provenance, and stratigraphy of the Muddy Creek Formation. This study also attempted to constrain the age of deposition of the Muddy Creek Formation. Based upon sedimentological evidence the Muddy Creek Formation and the inset Pliocene units are all interpreted as high energy fluvial deposits. The Muddy Creek Formation at location F (Fig. 2) on Flat Top Mesa and at location H (Fig. 2) in the Beaver Dam Wash and inset Pliocene unit at location I (Fig. 2) in the Beaver Dam Wash were derived from north of the Beaver Dam Wash and transported southward to their current location. The Muddy Creek Formation at location A (Fig. 2) on Mormon Mesa was derived from north of the Beaver Dam Wash and east of the Virgin River Gorge and deposited at its current location. The inset Pliocene unit at location G (Fig. 2) at Littlefield, Arizona was derived from east of the Virgin River Gorge and deposited near Littlefield, Arizona.

Previous research has determined that the provenance of the Muddy Creek Formation varies throughout southern Nevada. Pederson (2008) studied an east-west transect of the Muddy Creek Formation throughout southern Nevada and determined that Muddy Creek Formation was derived from local volcanic centers, although some of the data show that some portions of the Muddy Creek Formation were derived from the Colorado Plateau. Dicke (1990) determined that the Muddy Creek Formation in the Meadow Valley Wash was derived from the Moenkopi and Chinle Formations as well as local volcanic centers. Scott (1988) studied the Muddy Creek Formation around Lake Mead and determined that the conglomerate clasts were derived from the River Mountains. Kowallis and Everett (1986) determined that the Muddy Creek Formation near Mesquite, Nevada was derived

from local mountain ranges that shed detritus into basins. This study shows that the Muddy Creek Formation is not just derived from local mountain ranges that shed detritus into the basin. The Muddy Creek Formation from locations F and H (Fig. 2) was derived from the Caliente Caldera complex, while the Muddy Creek Formation from location A (Fig. 2) was derived from both the Caliente Caldera complex and the Colorado Plateau.

Kowallis and Everett (1986) studied the Muddy Creek Formation near Mesquite, Nevada and determined the Muddy Creek Formation consisted predominantly of immature, poorly sorted, coarse to fine grained sandstone. The Muddy Creek Formation at locations A, F, and H (Fig. 2) was predominantly unconsolidated, massively bedded, medium grained, sub-angular sandstone. The sedimentology of the Muddy Creek Formation at locations A, F, and H (Fig. 2) is similar to the sedimentology described in the Muddy Creek Formation by Kowallis and Everett (1986).

Detrital zircon analyses show that the detrital zircons within the Muddy Creek Formation are not comparable to the detrital zircons in known Colorado River deposits or the Bidahochi Formation which were analyzed by Kimbrough et al. (2007); therefore a paleo-Colorado River did not deposit the upper portion of the Muddy Creek Formation. However, no data generated as part of this study rule out the possibility that a paleo-Colorado River deposited the basal Muddy Creek Formation at location A (Fig. 2) on Mormon Mesa. Detrital zircon analyses show that detrital zircons from the inset Pliocene unit from location G (Fig. 2) in Littlefield, Arizona and from location J (Fig. 2) in the modern day Virgin River are comparable and that the inset Pliocene unit from location G (Fig. 2) at Littlefield, Arizona was deposited by a paleo-Virgin River. Based upon the statistical populations of detrital zircons in this study, it was determined that the Muddy

Creek Formation was deposited sometime after 15 Ma. The post-15 Ma deposition age for the Muddy Creek Formation is in agreement with previous research which determined that the Muddy Creek Formation was deposited between approximately 8.5 and 4.1 Ma (Metcalf, 1982; Bohannon, 1984; Williams, 1996; Pederson, 2008).

If the Muddy Creek Formation was deposited as late as 4.1 Ma, then the upper portion of the Muddy Creek Formation could not have been deposited by a paleo-Colorado River because the Colorado River was flowing through the Grand Wash Trough and into Lake Mead between 4.3 Ma and 5 Ma (Howard and Bohannon, 2001). While this study determined that the Muddy Creek Formation was not deposited by a paleo-Colorado River, it did not determine how the Colorado River formed. It is possible that the Colorado River formed via headward erosion, antecedence, superimposition, stream piracy, or lake overflow. There is insufficient evidence from this study to determine which river-forming process formed the Colorado River. However, it seems unlikely that a lake overflow process caused a paleo-Colorado River to ever flow into the Mesquite basin and deposit the Muddy Creek Formation.

This study shows that the Muddy Creek Formation from location F (Fig. 2) at Flat Top Mesa and from location H (Fig. 2) in the Beaver Dam Wash was derived from the Caliente Caldera complex and not the Colorado Plateau. Consequently, a paleo-Colorado River did not flow into the Mesquite basin and deposit the Muddy Creek Formation at locations F and H (Fig. 2). The Muddy Creek Formation at location A (Fig. 2) was derived from both the Caliente Caldera complex and the Colorado Plateau, which was deposited by a paleo-Virgin River. The inset Pliocene unit at location I (Fig. 2) was

derived from the Caliente Caldera complex, while the inset Pliocene unit from location G (Fig. 2) was derived from the Colorado Plateau and deposited by a paleo-Virgin River.

EXHIBITS

Figures

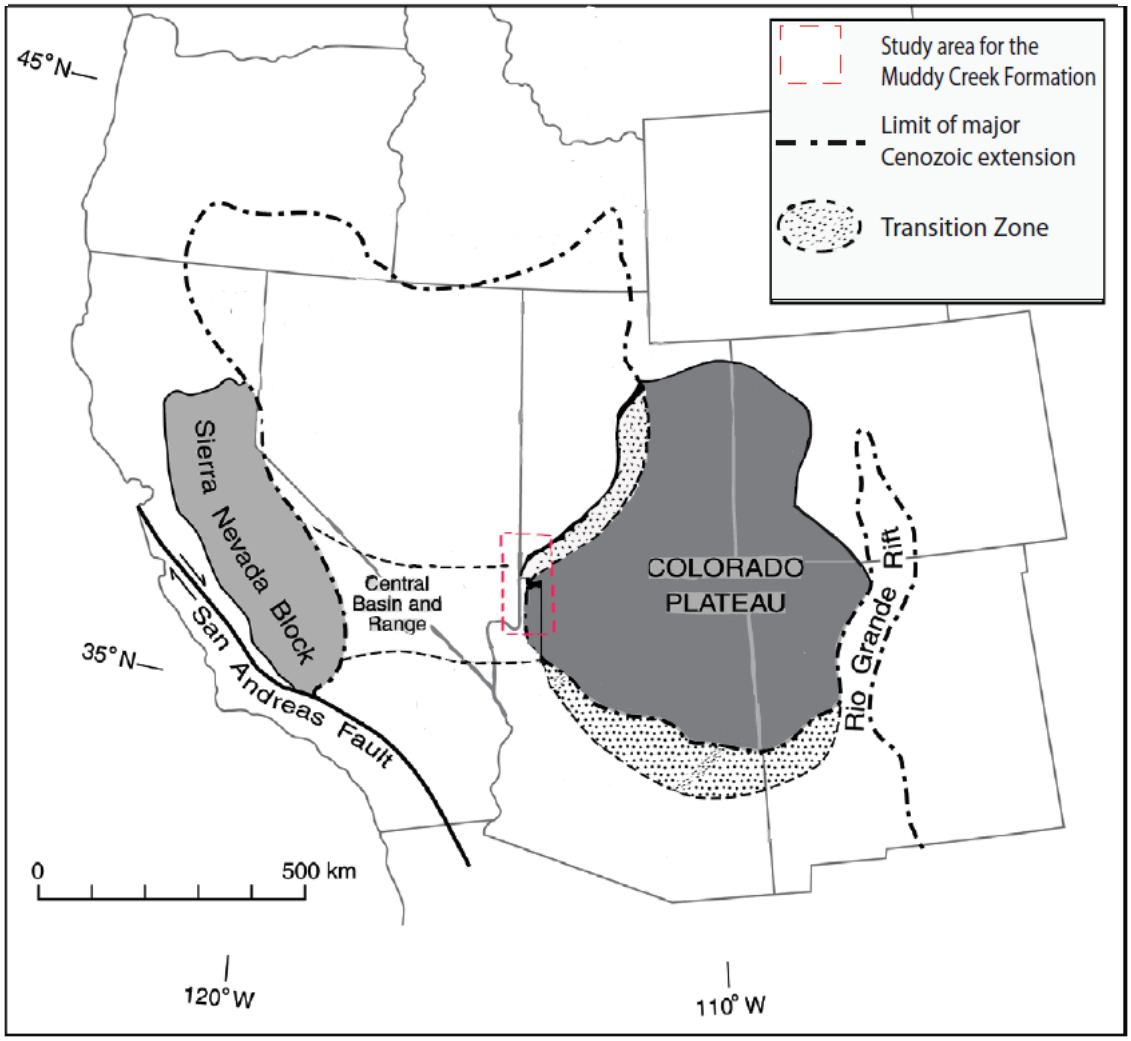

Figure 1. Map of central Basin and Range province. The field area is located within the red box (modified from Faulds et al., 2001).

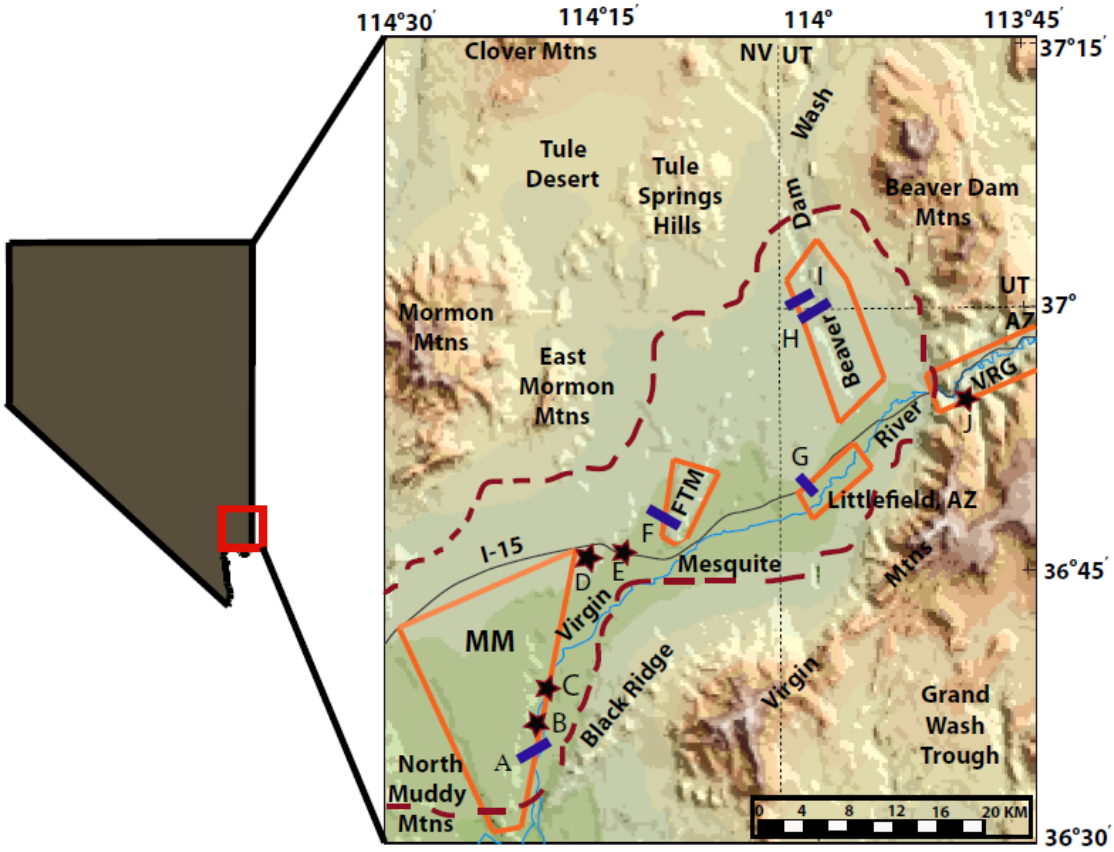

Figure 2. Map of southern Nevada showing field locations in orange where sample sites and stratigraphic sections were measured for this study. The Virgin River Depression is outlined in red. Stars denote locations on Mormon Mesa where conglomerate clast counts were conducted and the location in the Virgin River Gorge where a detrital zircon sample was collected. Mormon Mesa locations are broken up into five locations (A-E). Location A represents a measured stratigraphic section site at Mormon Mesa and locations B-E represent conglomerate clast count locations. Location F represents the measured section at Flat Top Mesa. Location G represents the location of the stratigraphic section at Littlefield, Arizona. Location H represents the stratigraphic section in the Muddy Creek Formation while location I represents the stratigraphic section of the inset Pliocene unit in the Beaver Dam Wash. Location J represents the location of the detrital zircon sample from the modern Virgin River in the Virgin River Gorge. VRG = Virgin River Gorge. MM = Mormon Mesa. FTM = Flat Top Mesa. NV = Nevada. UT = Utah. AZ = Arizona. Figure was modified from Langenheim et al. (2000).

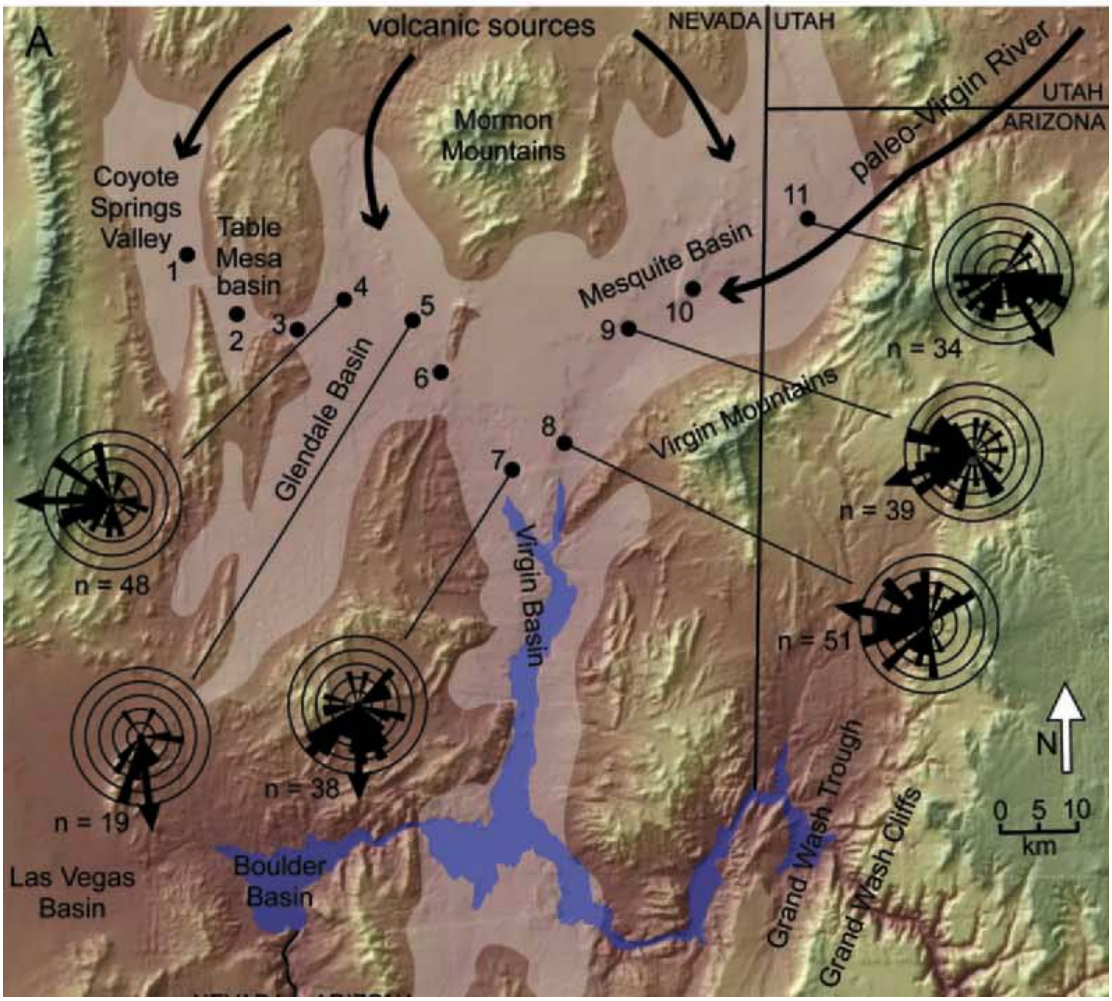

Figure 3. Diagram showing the location of Muddy Creek Formation outcrops which Pederson (2008) sampled for a provenance study of the Muddy Creek Formation.

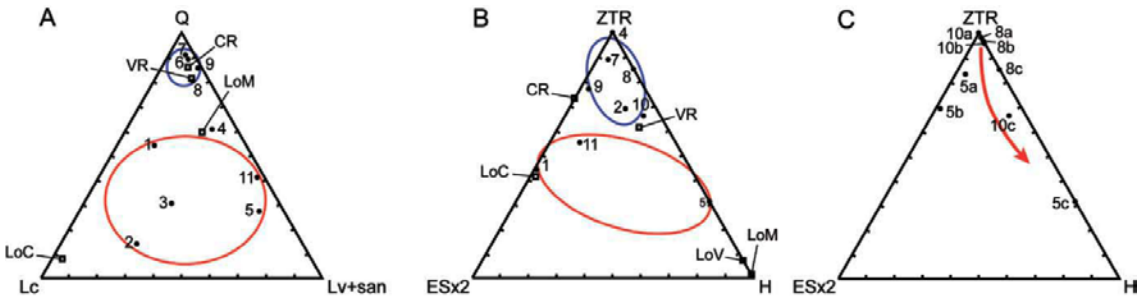

Figure 4. Ternary diagrams created by Pederson (2008) for Muddy Creek Formation samples representing possible sediment source areas. Ternary diagram A is a plot to distinguish the possible sediment source areas. The blue oval shows a population that has a mature exotic river source and the red oval contains a population that has a combination of local and volcanic sources. Ternary diagram B is a plot of heavy minerals showing two populations that are similar to populations in ternary diagram A. Ternary diagram C is a heavy mineral plot showing vertical transect samples at three locations from the base to the top of the exposed middle member of the Muddy Creek Formation. The red arrow shows a trend of increasing volcanic input going up section at all three locations. CR = Colorado River. ESx2 = Epidote and Sphene multiplied by 2. H = Hornblende. Lc = Carbonate lithic fragments. LoC = Local carbonate source. LoM = Local metamorphic source. LoV = Local volcanic source. Lv+san = Volcanic lithic fragments and sanidine. Q = Quartz. VR = Virgin River. ZTR = Zircon, Tourmaline, and Rutile. Numerical values correspond to sample locations shown in Figure 3.

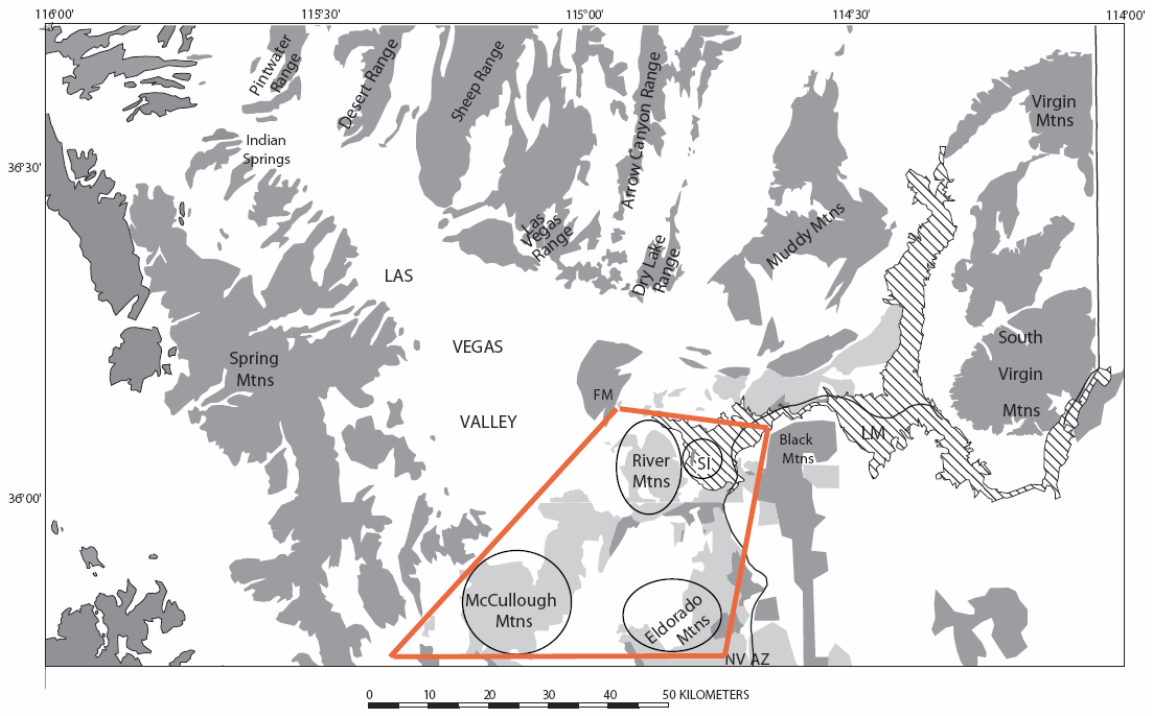

Figure 5. Map of southern Nevada showing Lake Mead and the study area (red box) of Scott (1988). Scott (1988) studied conglomerates within the Muddy Creek Formation around Lake Mead. The black circles are the locations Scott (1988) studied as provenance sources for the Muddy Creek Formation. SI = Saddle Island. FM = Frenchman Mountain. LM = Lake Mead. Figure was modified from Page et al. (2005).

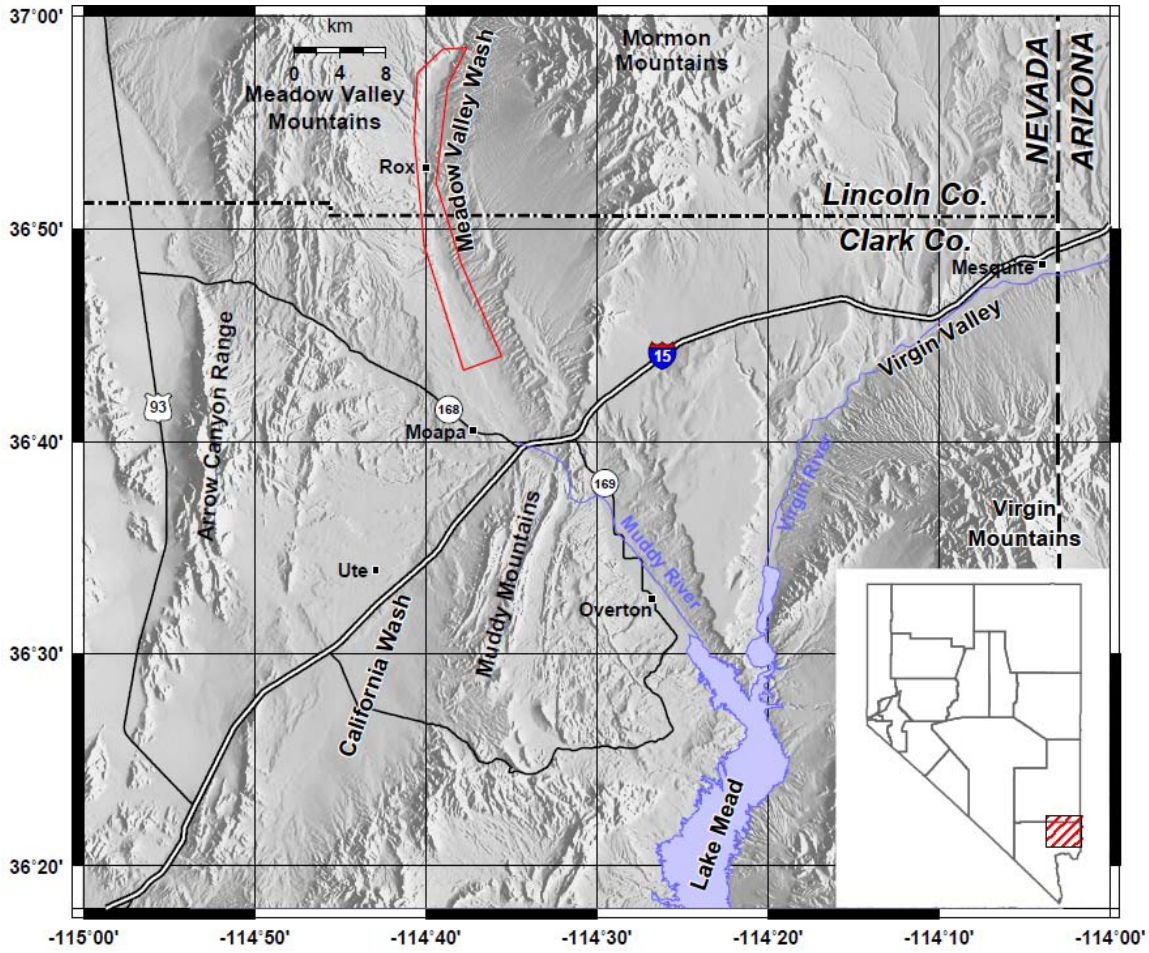

Figure 6. Map of southern Nevada northwest of Lake Mead where Dicke (1990) studied the provenance of the Muddy Creek Formation. Dicke (1990) worked in the Meadow Valley Wash, outlined in red, which is located between the Meadow Valley Mountains and Mormon Mountains. Figure was modified from Scheirer and Andreasen (2008).

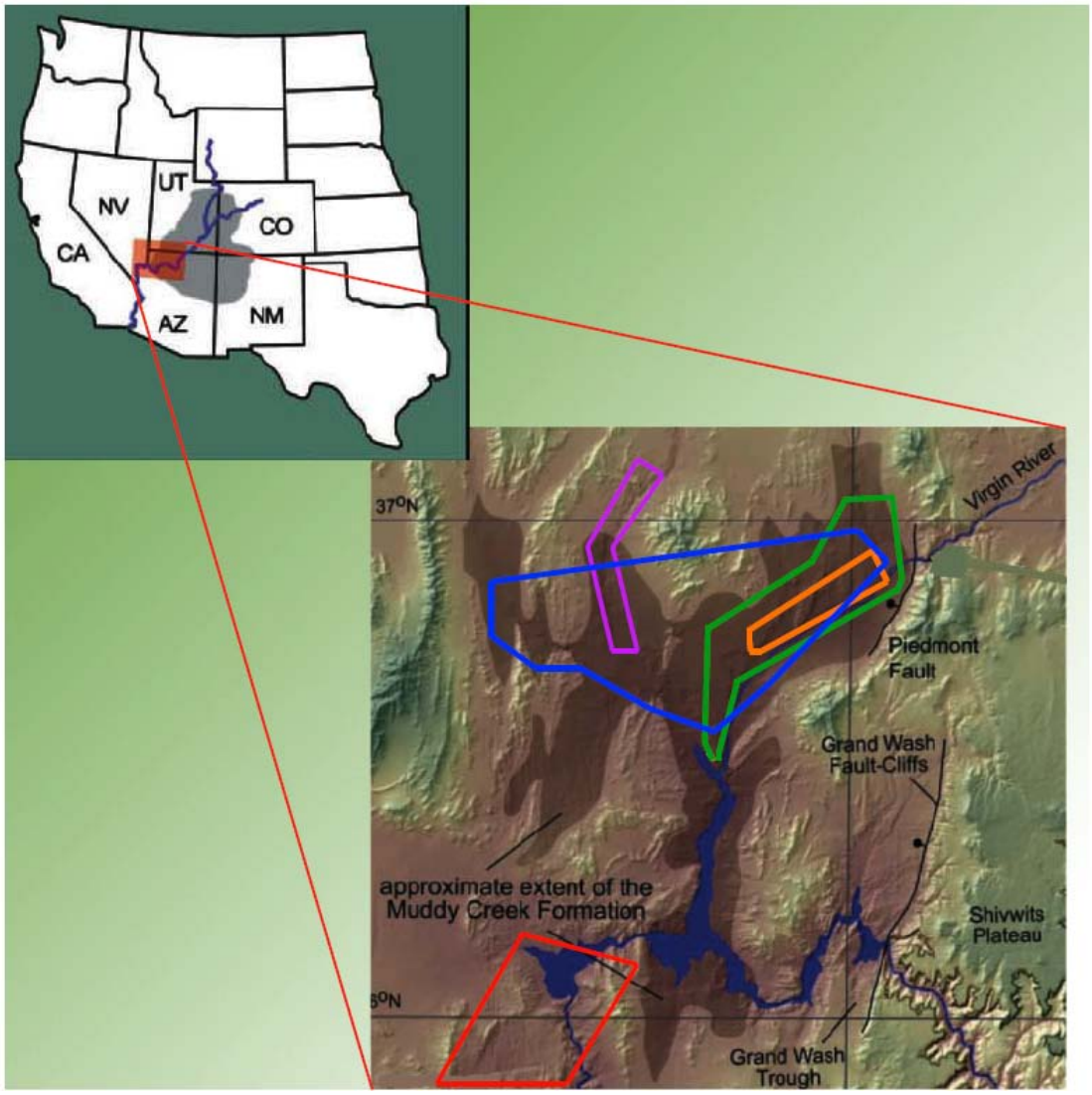

Figure 7. Map showing the extent of the Muddy Creek Formation in the vicinity of Mesquite and Lake Mead, NV. The modern-day path of the Colorado River flowing through the Grand Canyon, off the Colorado Plateau, into the Grand Wash Trough, and out to sea is shown. The orange polygon is the outline of the study for Kowallis and Everett (1986). The red polygon is the outline of the study area for Scott (1988). The purple polygon is the outline of the study area for Dicke (1990). The blue polygon is the outline of the study area for Pederson (2008). The green polygon is the outline of the study area for this thesis. The dark brown area is the extent of the Muddy Creek Formation in southern Nevada (modified from Pederson, 2008).

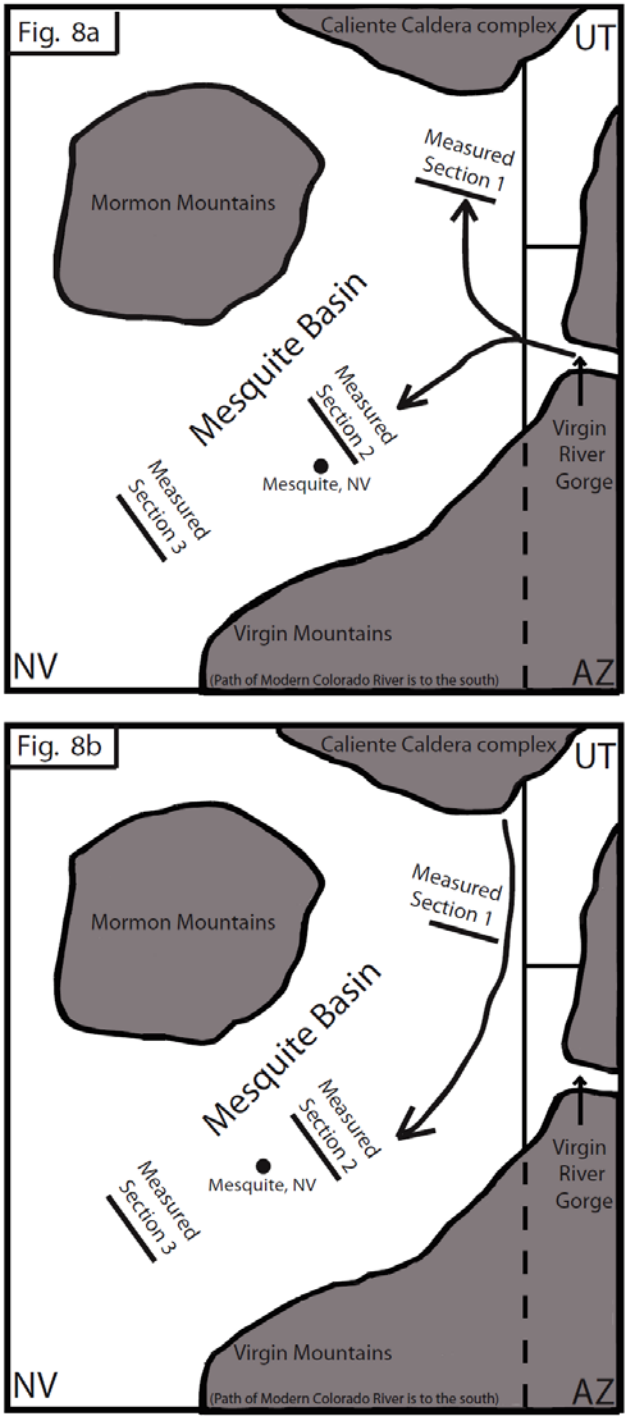

Figure 8a and 8b. Cartoons showing the hypothesis (a) and alternative hypothesis (b) which are tested in this study. Shown are two possible sediment sources for the Muddy Creek Formation. One hypothesis (a) is that the Muddy Creek Formation was derived from the Colorado Plateau and deposited by a paleo-Colorado River. The alternative hypothesis (b) is that the Muddy Creek Formation was derived from the Caliente Caldera complex.

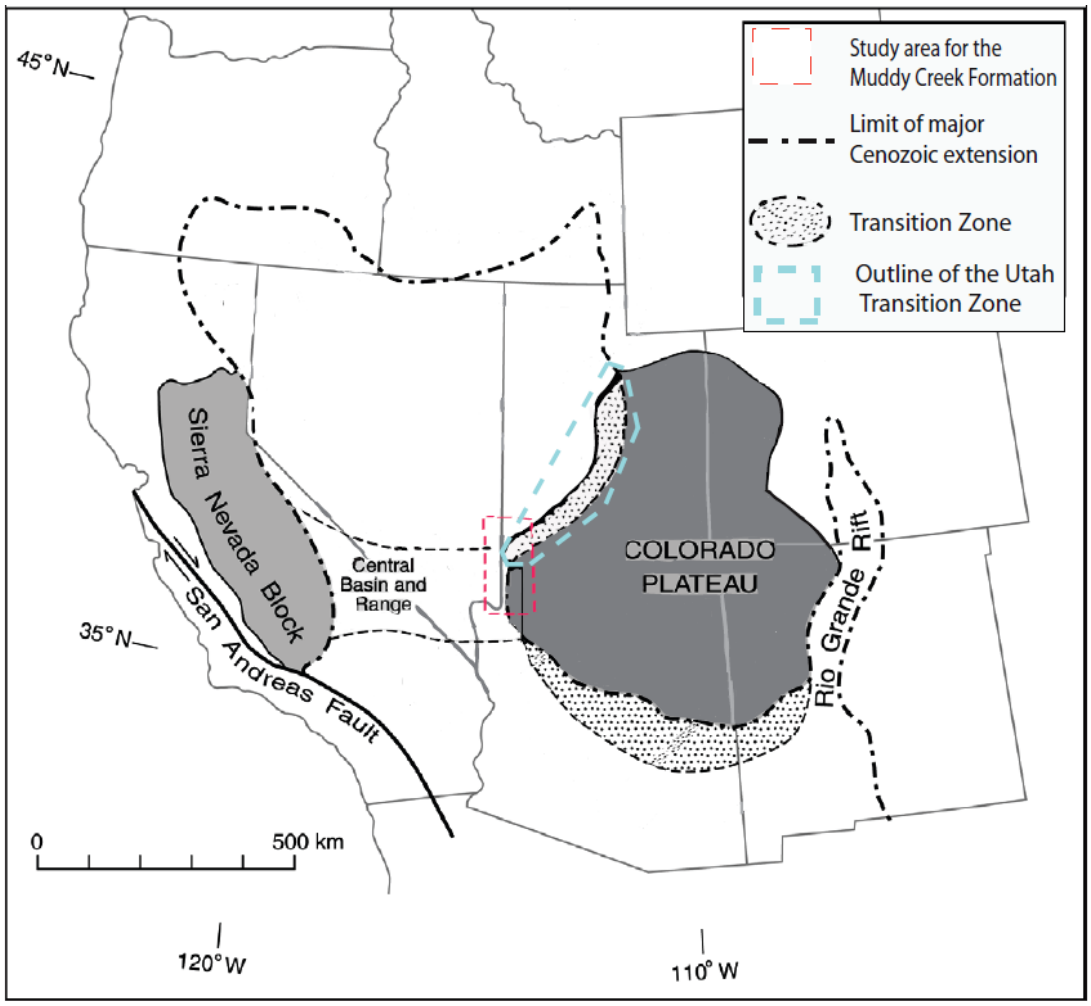

Figure 9. Map of southern Nevada showing the Utah Transition Zone between the Colorado Plateau and the Basin and Range province (modified from Faulds et al., 2001).

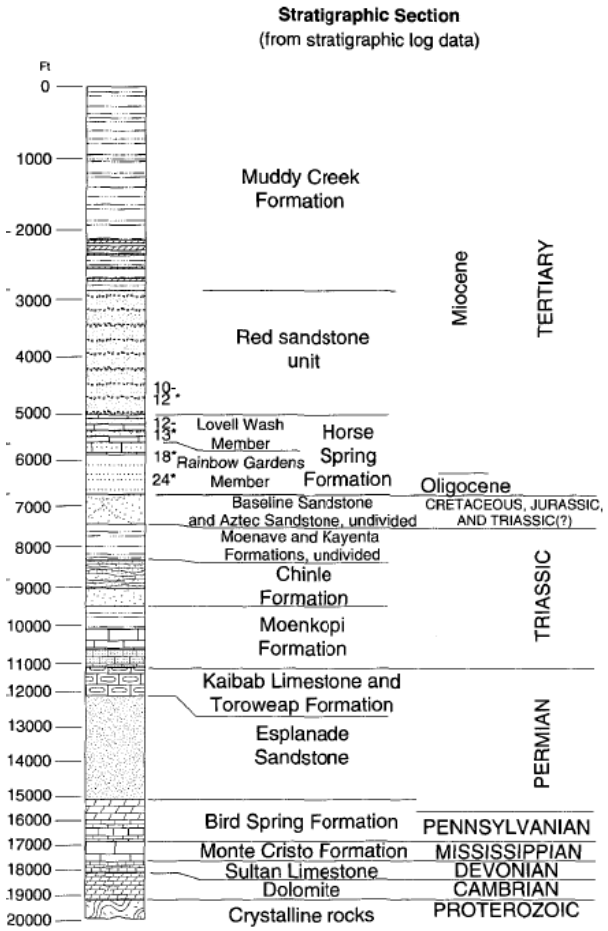

Figure 10. Stratigraphic column from the Mobil Oil Virgin 1A test well at Mormon Mesa. Stratigraphic section shows stratigraphy based on well data. Figure was modified from Bohannon et al. (1993).

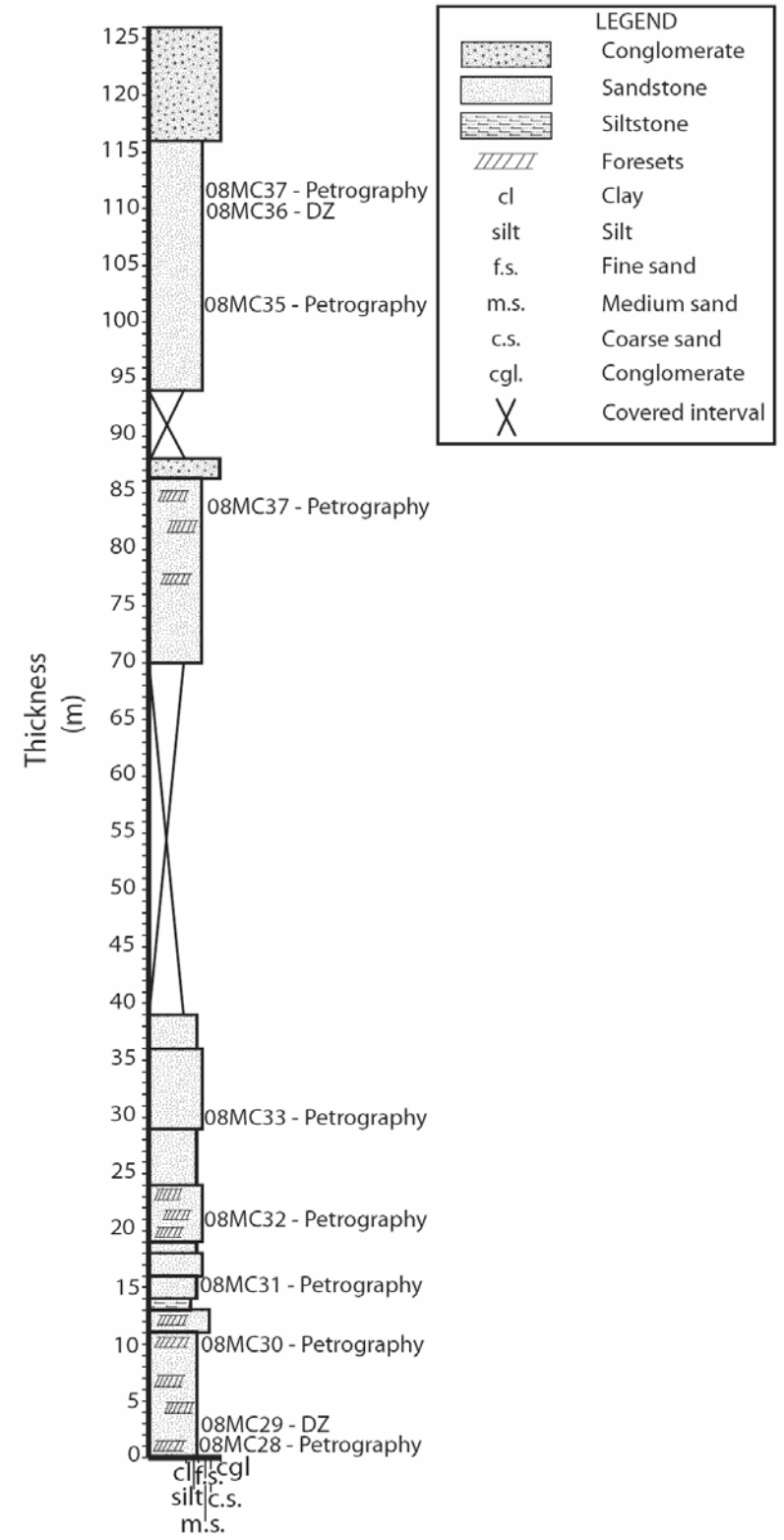

Figure 11. Measured section of the Muddy Creek Formation from location F (Fig. 2) at Flat Top Mesa near Mesquite, Nevada. Sample locations for sandstone petrography and detrital zircon (DZ) analyses are labeled.

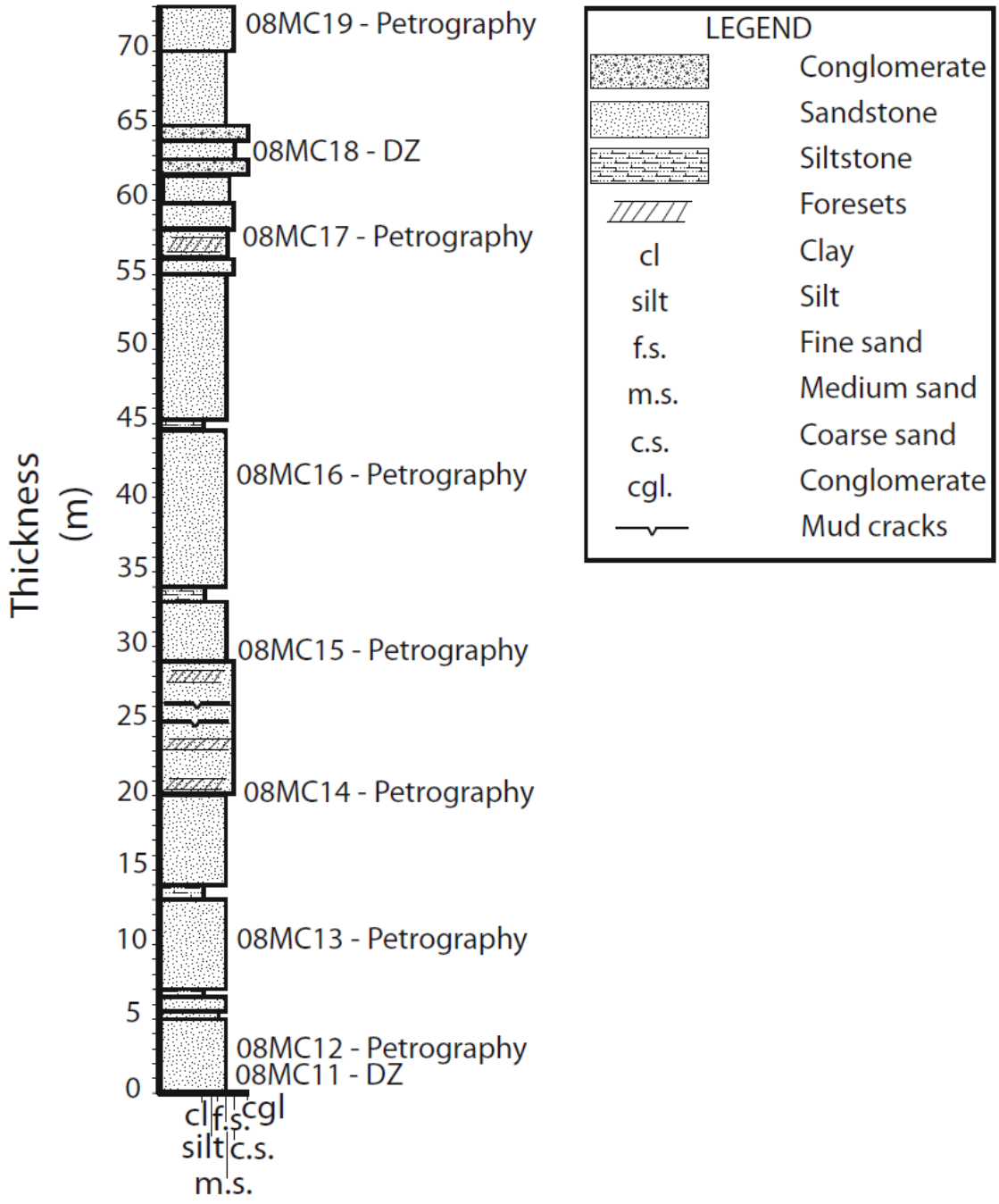

Figure 12. Measured section of the Muddy Creek Formation from location H (Fig. 2) in the Beaver Dam Wash. Sandstone petrography and detrital zircon (DZ) sample locations are labeled.

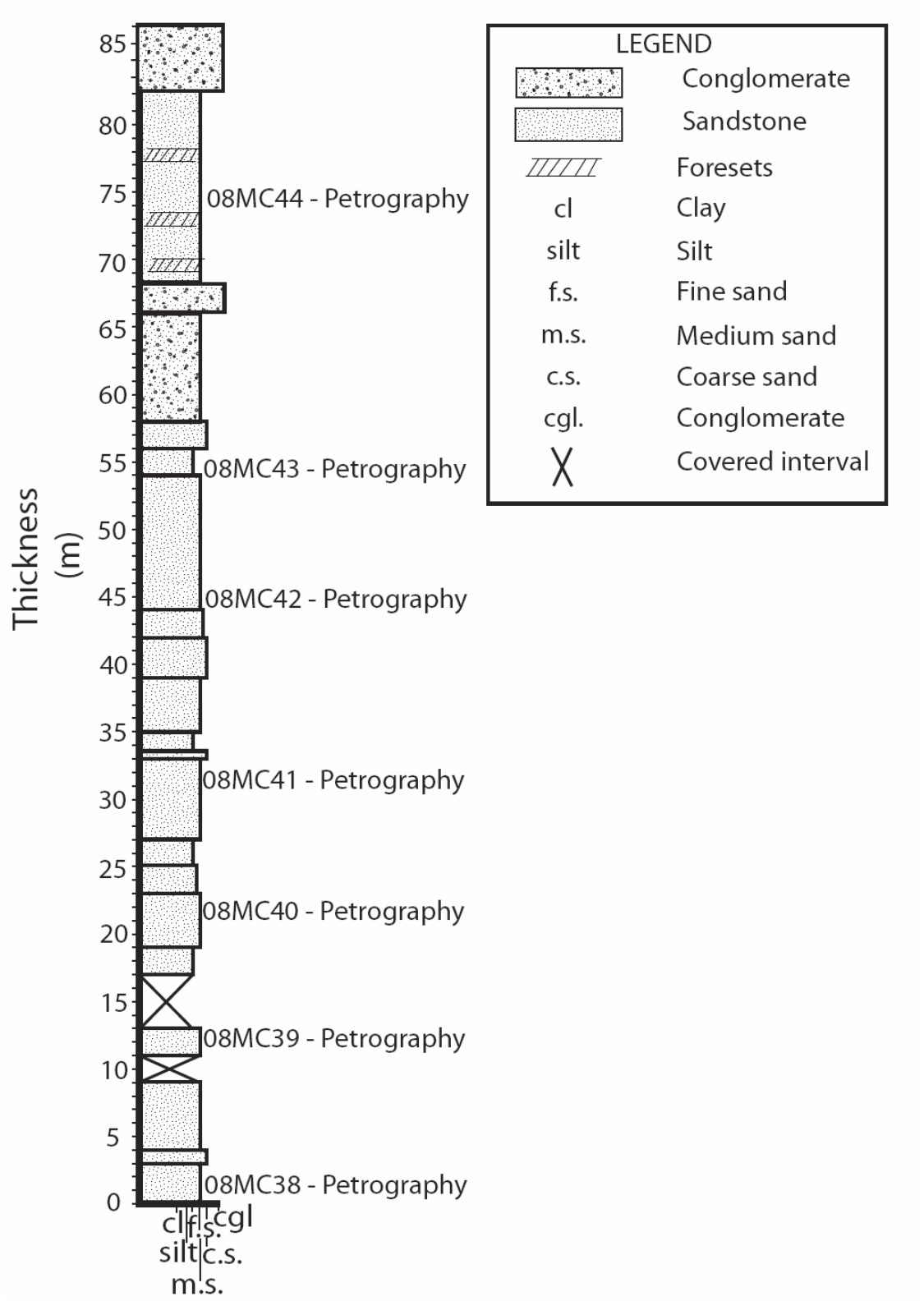

Figure 13. Measured section from the Muddy Creek Formation at location A (Fig. 2) at Mormon Mesa west of Mesquite, Nevada. Sample locations for sandstone petrography are labeled.

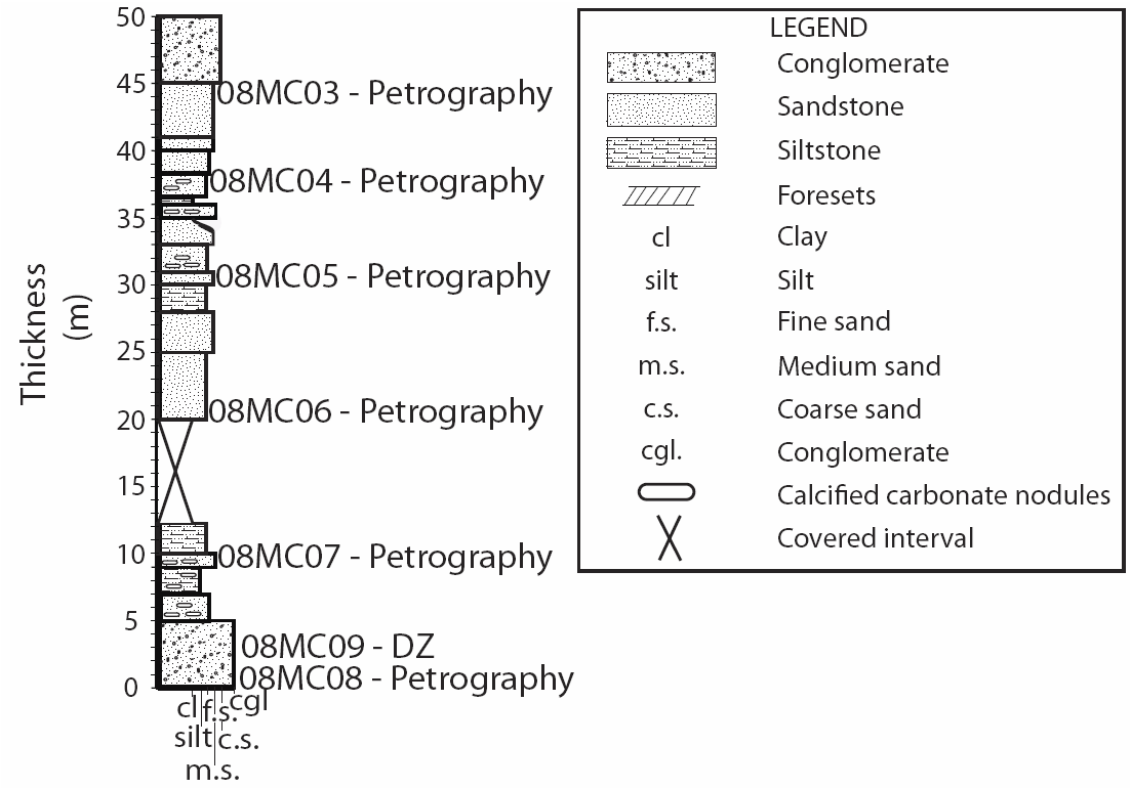

Figure 14. Measured section from location G (Fig. 2) of an inset Pliocene unit near Littlefield, Arizona. Sandstone petrography and detrital zircon (DZ) sample locations are labeled.

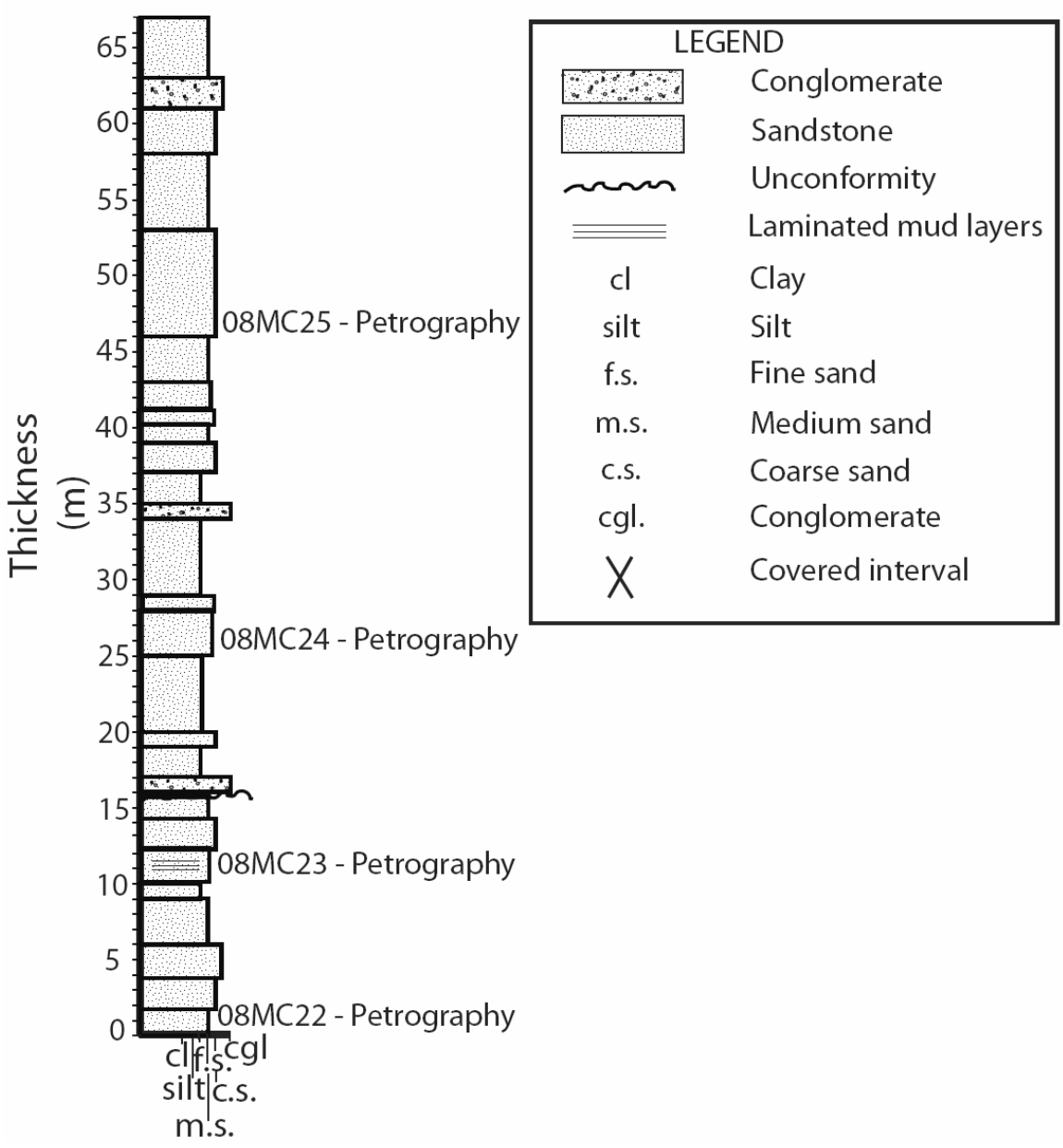

Figure 15. Measured section from location I (Fig. 2) of an inset Pliocene unit (above the unconformity) and Muddy Creek Formation (below the unconformity) in the Beaver Dam Wash. Sandstone petrography samples are labeled.

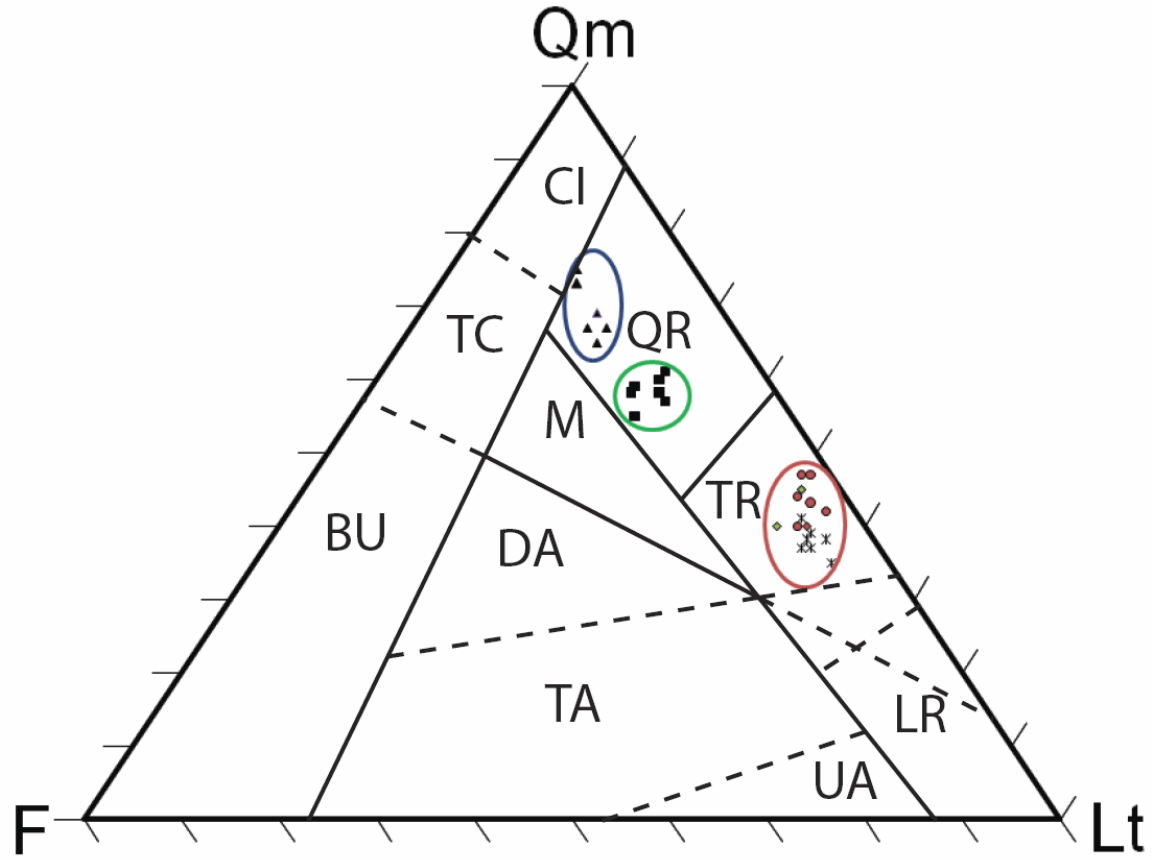

Figure 16. Ternary diagram with provisional compositional fields showing the relative percentage of monocrystalline quartz (Qm), feldspar (F), and total lithic fragments (Lt) in samples from the Muddy Creek Formation and inset Pliocene units. Circles = Location F at Flat Top Mesa (Fig 2). X's = Location H at Beaver Dam Wash (Fig. 2). Squares = Location A at Mormon Mesa (Fig. 2). Triangles = Location G of inset Pliocene unit at Littlefield, AZ (Fig. 2). Diamonds = Location I of inset Pliocene unit in Beaver Dam Wash (Fig. 2). BU = Basement Uplift. CI = Craton Interior. DA = Dissected Arc. LR = Lithic Recycled. M = Mixed. QR = Quartzose Recycled. TA = Transitional Arc. TC = Transitional Continental. TR = Transitional Recycled. UA = Undissected Arc.

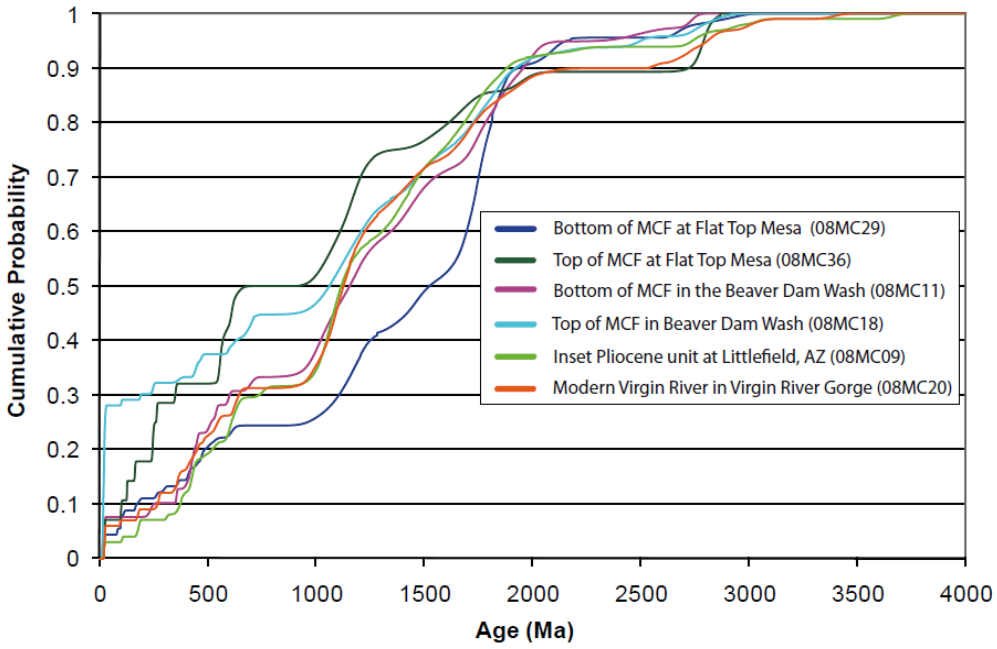

Figure 17. Cumulative probability plot of all detrital zircon samples in this study. This plot shows the probability of detrital zircons from each section over geologic time.

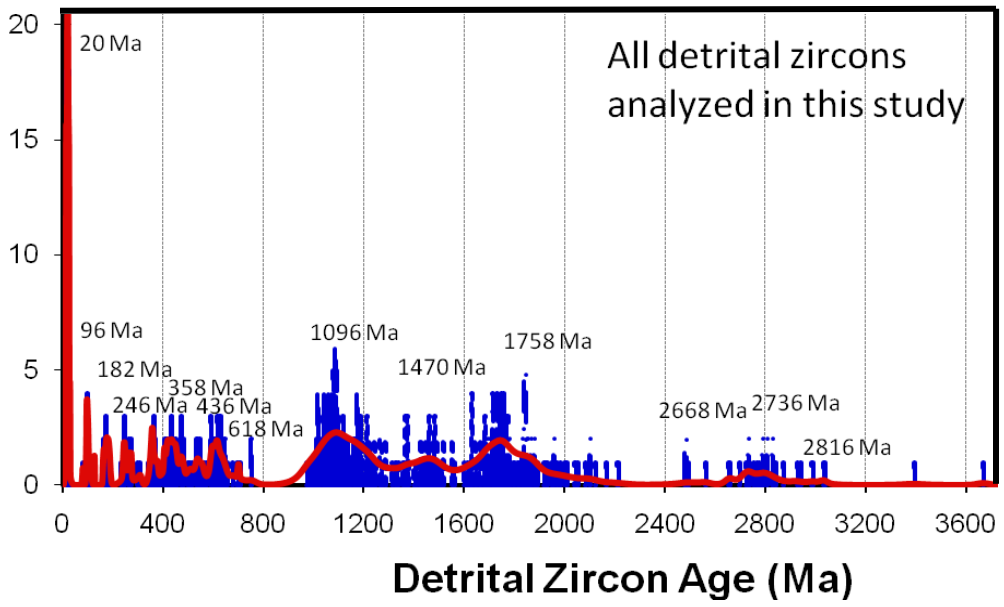

Figure 18. Relative probability plot of all detrital zircons from the Muddy Creek Formation at Flat Top Mesa and in the Beaver Dam Wash; inset Pliocene unit in Littlefield, Arizona; and Virgin River Gorge. This plot also shows the thriteen statistically defined age peaks that were determined for the six samples. The y-axis shows the number of detrital zircons within the sample.

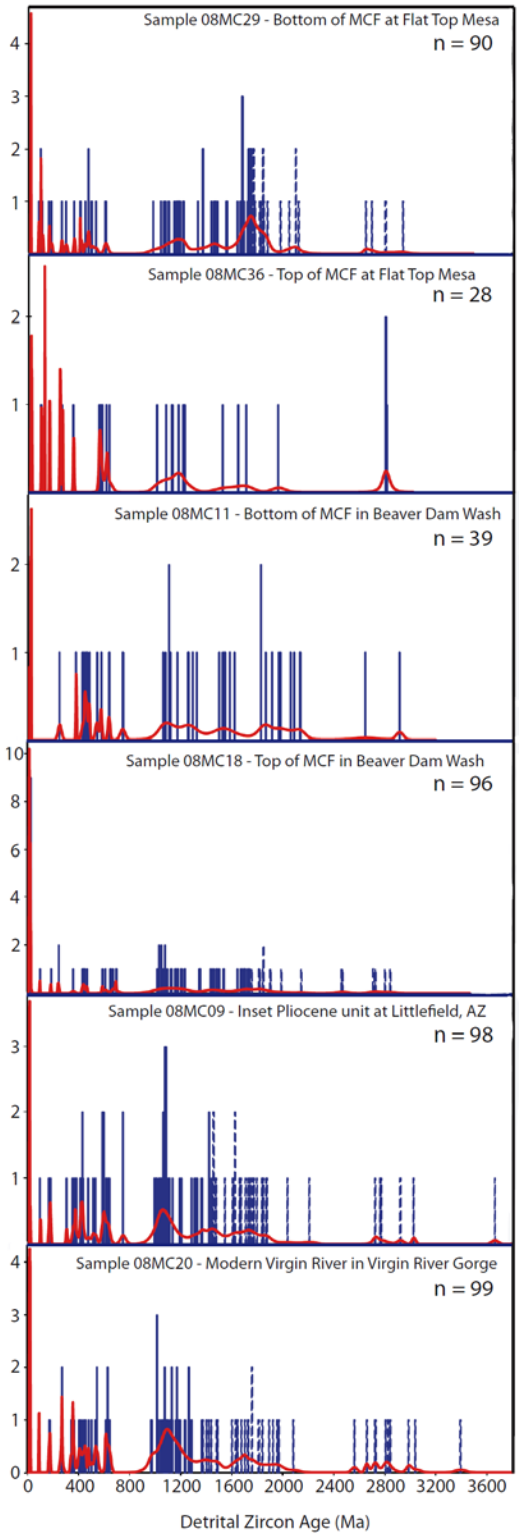

Figure 19. Normalized probability plot of detrital zircons from the Muddy Creek Formation, an inset Pliocene unit, and the Virgin River. Plot shows detrital zircon ages from each section analyzed stacked on top of each other for easier comparison. For each sample, the y-axes are not the same scale.

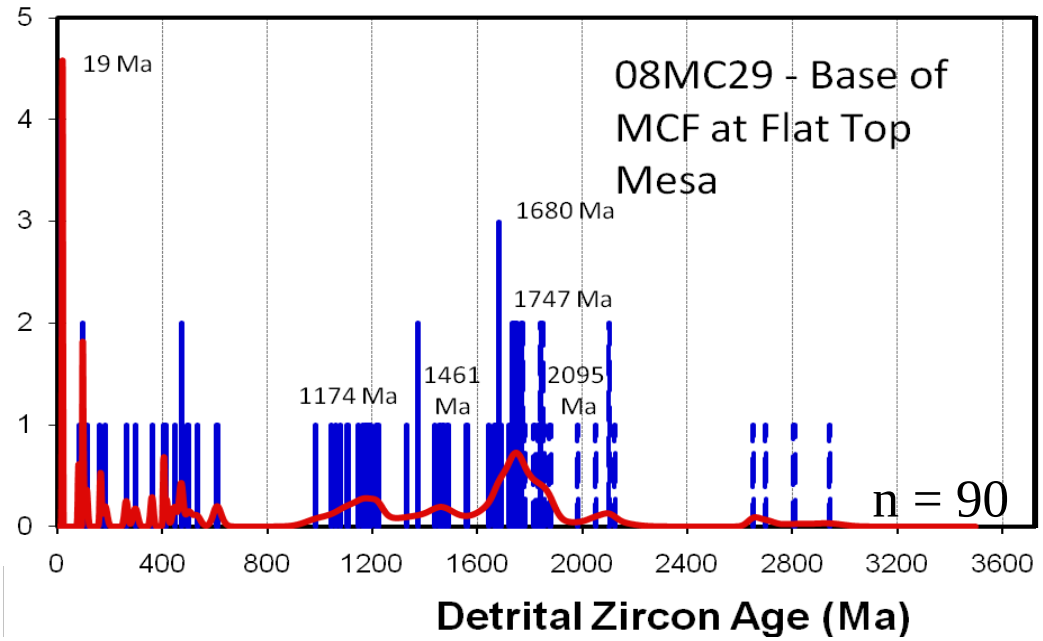

Figure 20. Relative probability plot of detrital zircons from the base of the Muddy Creek Formation from location F (Fig. 2) at Flat Top Mesa, showing six statistically defined age peaks at 19 Ma, 1174 Ma, 1461 Ma, 1680 Ma, 1747 Ma, and 2095 Ma.

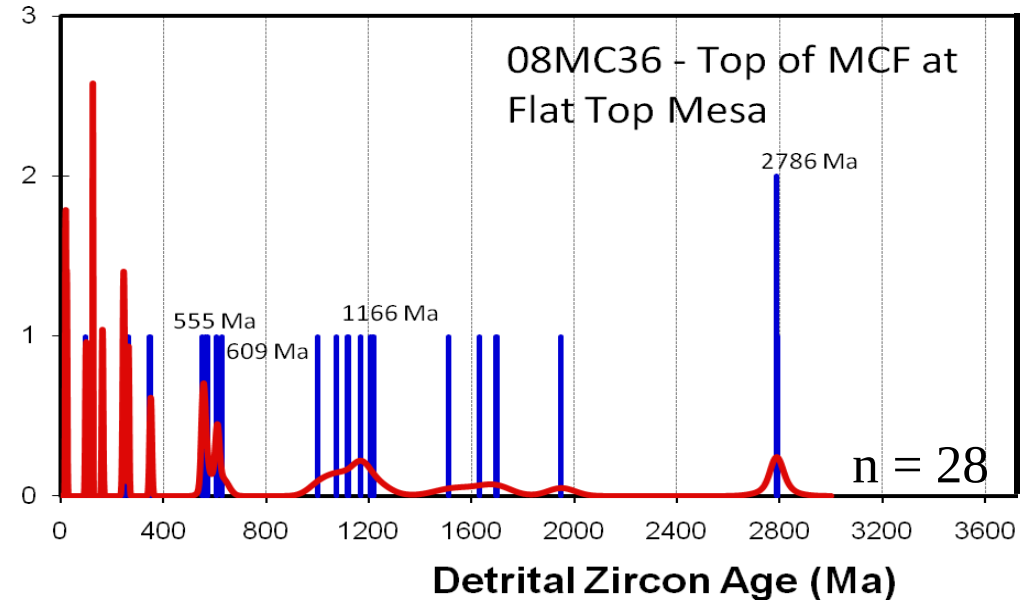

Figure 21. Relative probability plot of detrital zircons from the top of the Muddy Creek Formation from location F (Fig. 2) at Flat Top Mesa. Four statistically defined age peaks were determined for this sample.

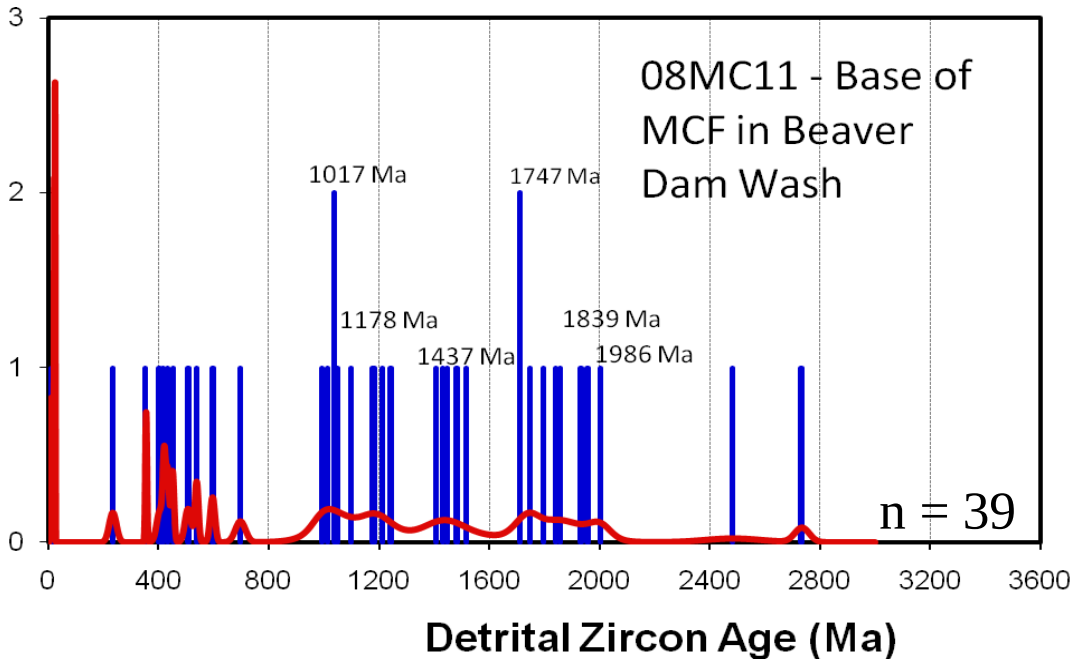

Figure 22. Relative probability plot of detrital zircons from the base of the Muddy Creek Formation from location H (Fig. 2) in the Beaver Dam Wash. This plot shows six statistically defined age peaks.

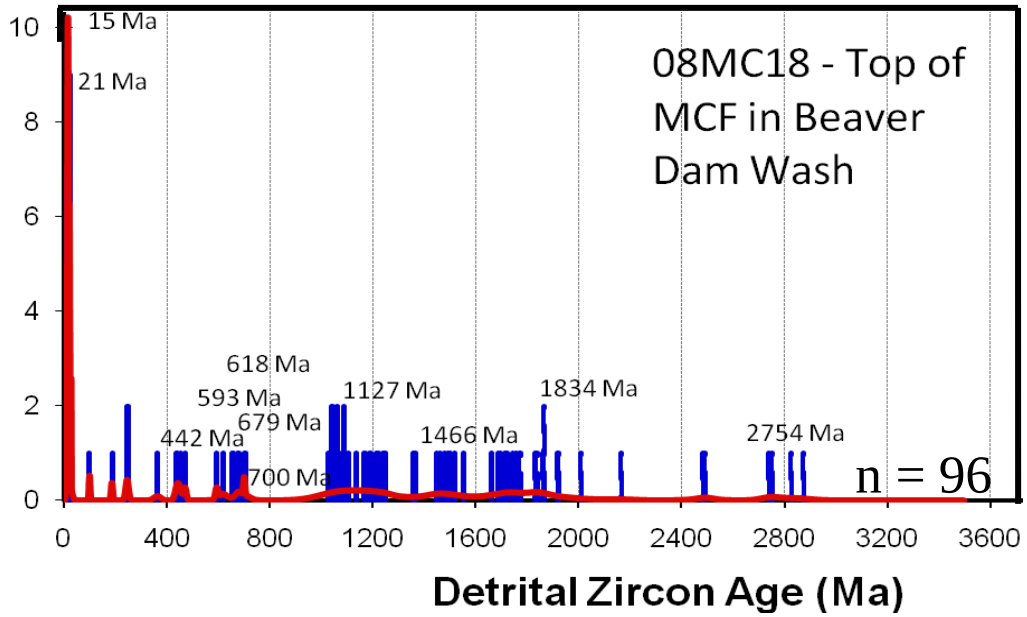

Figure 23. Relative probability plot of detrital zircons from the top of Muddy Creek Formation from location H (Fig. 2) in the Beaver Dam Wash showing eleven statistically defined age peak at 15 Ma, 21 Ma, 442 Ma, 593 Ma, 618 Ma, 679 Ma, 700 Ma, 1127 Ma, 1466 Ma, 1834 Ma, and 2754 Ma.

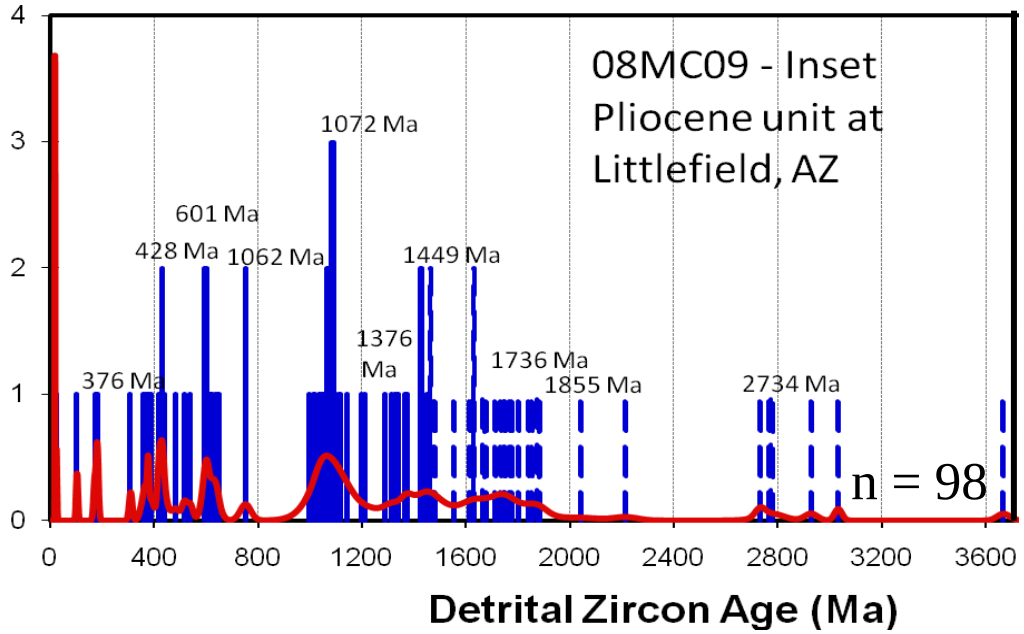

Figure 24. Relative probability plot of detrital zircons from the base of inset Pliocene unit from location G (Fig. 2) at Littlefield, Arizona showing ten statistically defined age peaks.

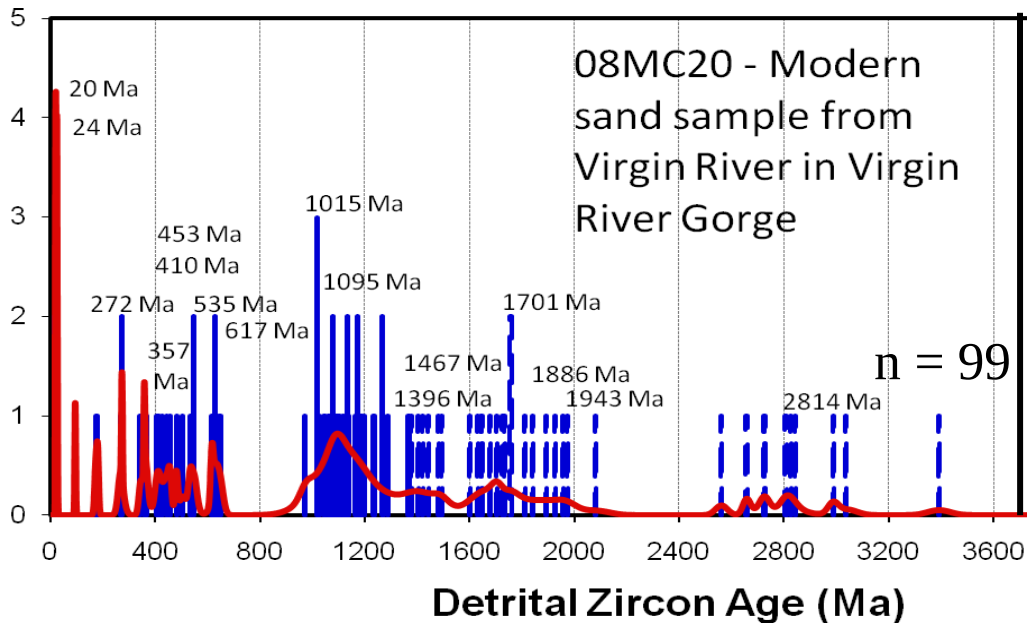

Figure 25. Relative probability plot of detrital zircons in the Virgin River Gorge from location J (Fig. 2) of the Virgin River, showing sixteen statistically defined age peaks at 20 Ma, 24 Ma, 272 Ma, 357 Ma, 410 Ma, 453 Ma, 535 Ma, 617 Ma, 1015 Ma, 1095 Ma, 1396 Ma, 1467 Ma, 1701 Ma, 1886 Ma, 1943 Ma, and 2814 Ma.

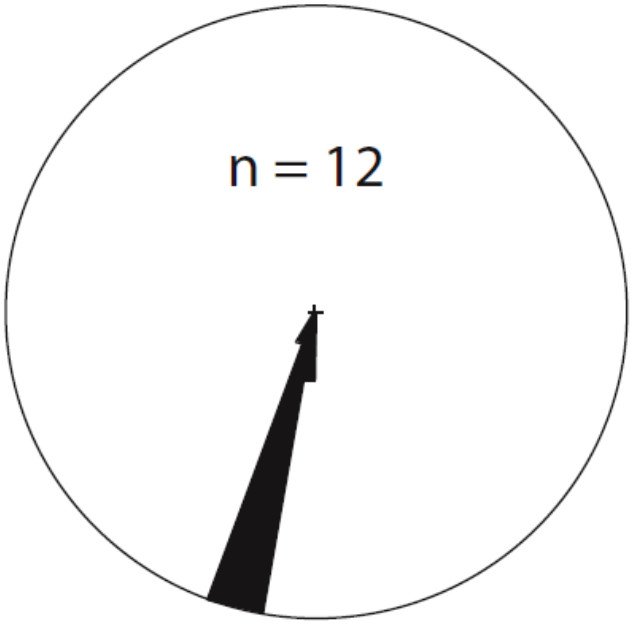

Figure 26. Rose diagram of cross-bedded planar foresets from the Muddy Creek Formation from location F (Fig. 2) at Flat Top Mesa indicating a paleoflow direction to the south-southwest.

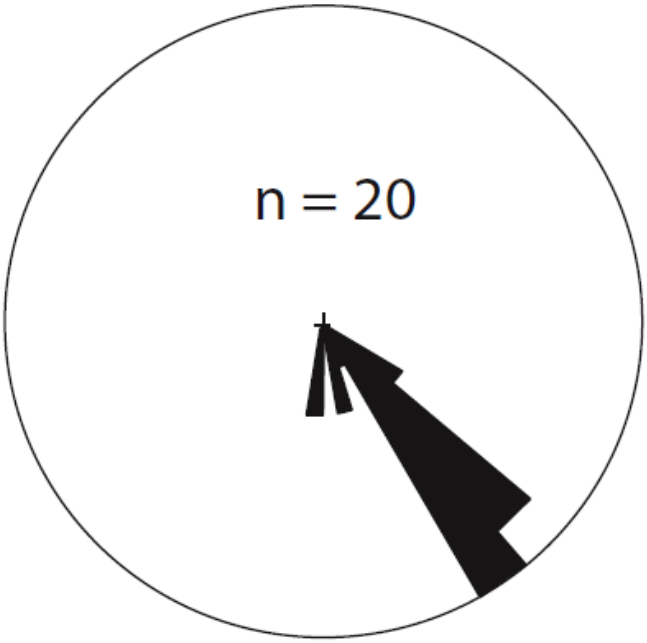

Figure 27. Rose diagram of cross-bedded sandstones in the Muddy Creek Formation from location H (Fig. 2) in the Beaver Dam Wash showing a south-southeast directed paleocurrent direction.

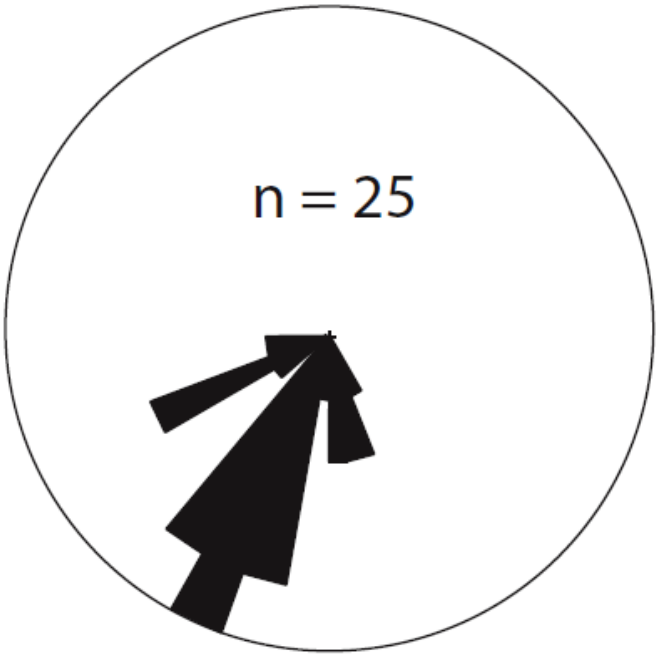

Figure 28. Rose diagram of imbricated clasts in an inset Pliocene unit from location G (Fig. 2) in Littlefield, Arizona showing a paleoflow direction to the southwest.

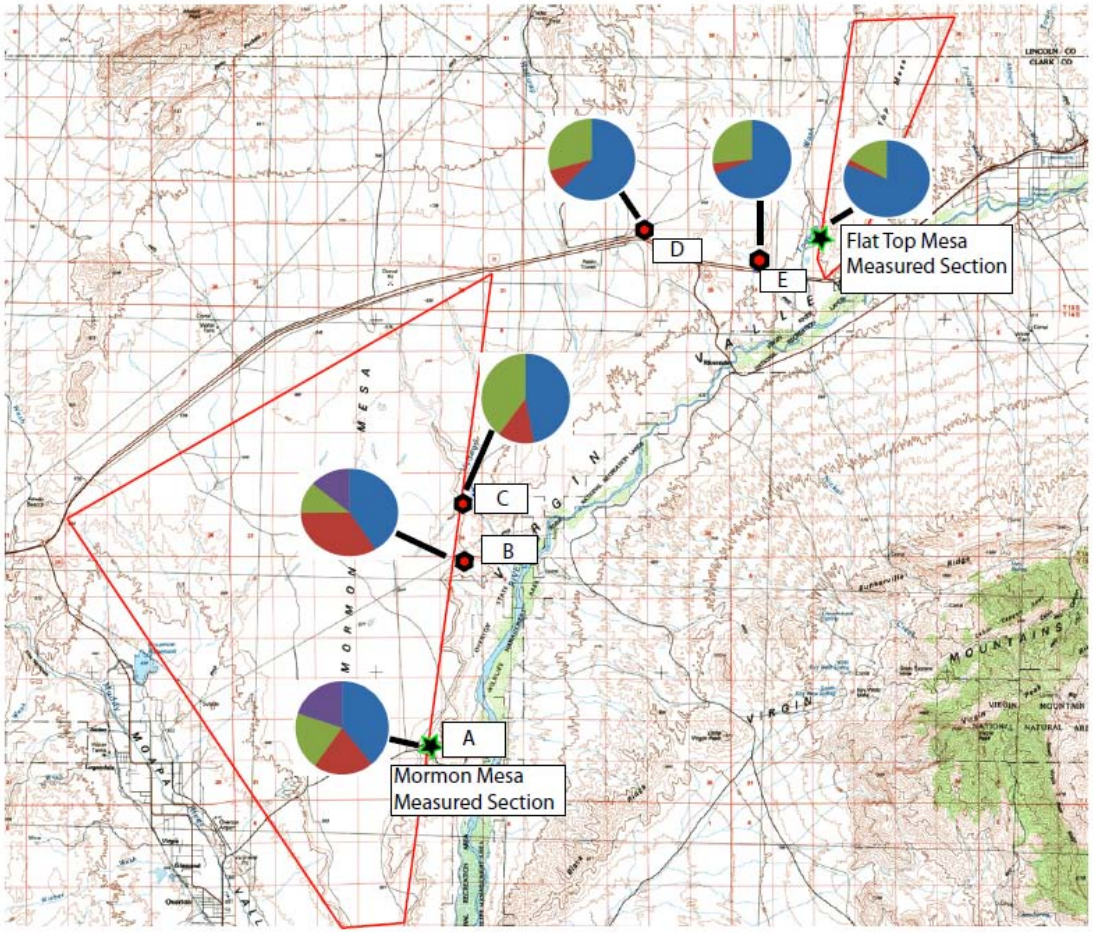

Figure 29. Topographic map of the Muddy Creek Formation at Flat Mesa and Mormon Mesa. Conglomerate clast count data from the measured sections at location F (Fig. 2) at Flat Top Mesa, location A (Fig. 2) on Mormon Mesa, and four additional interbedded conglomerates on Mormon Mesa showing how the composition changes from the northeast to the southwest. Flat Top Mesa and Mormon Mesa are outlined in red boxes, and conglomerates are represented by a pie chart. The conglomerate clast count conducted at the measured section of Mormon Mesa is labeled A. The additional conglomerate clast counts shown with an octagon are labeled B, C, D, and E.

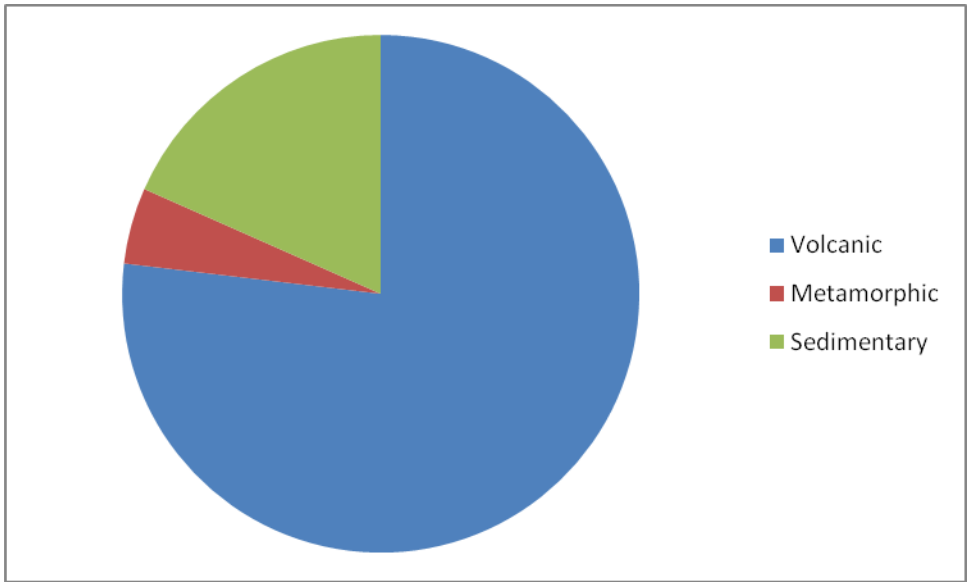

Figure 30. One conglomerate clast count from Muddy Creek Formation at location F (Fig. 2) at Flat Top Mesa showing that the conglomerates are composed of predominantly volcanic clasts.

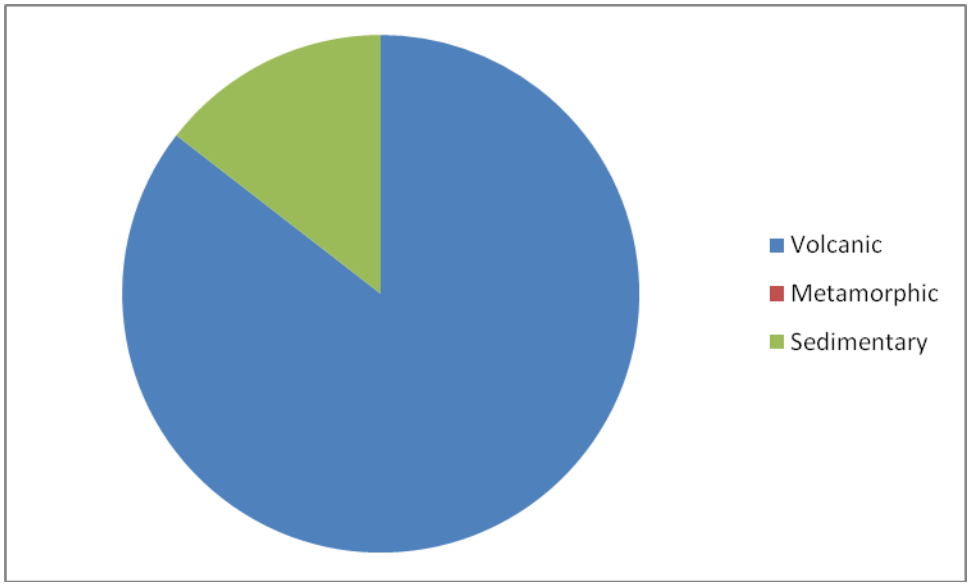

Figure 31. A second conglomerate clast count from Muddy Creek Formation from location F (Fig. 2) at Flat Top Mesa showing that the conglomerates are composed of predominantly volcanic clasts.

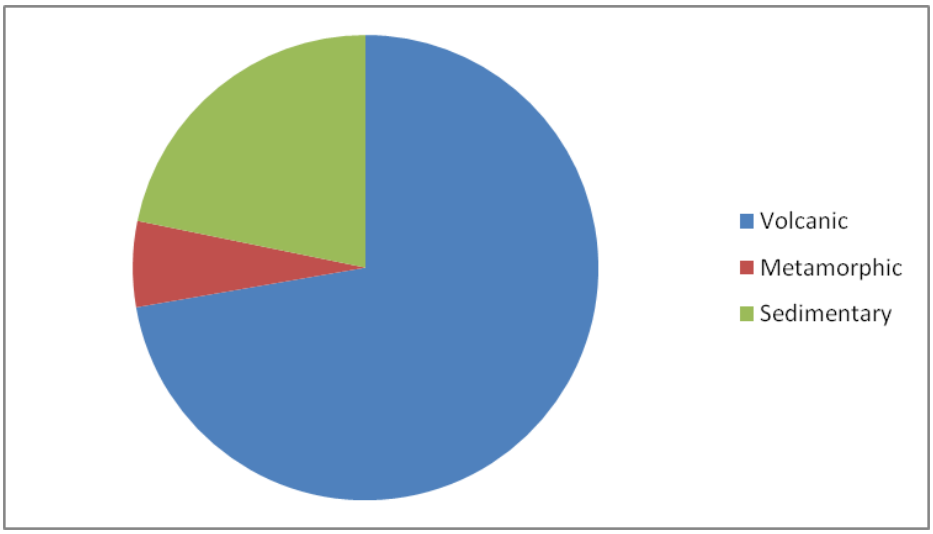

Figure 32. Pie chart of the Muddy Creek Formation from location H (Fig. 2) in the Beaver Dam Wash showing that the interbedded conglomerate is predominantly composed of volcanic clasts with some sedimentary clasts.

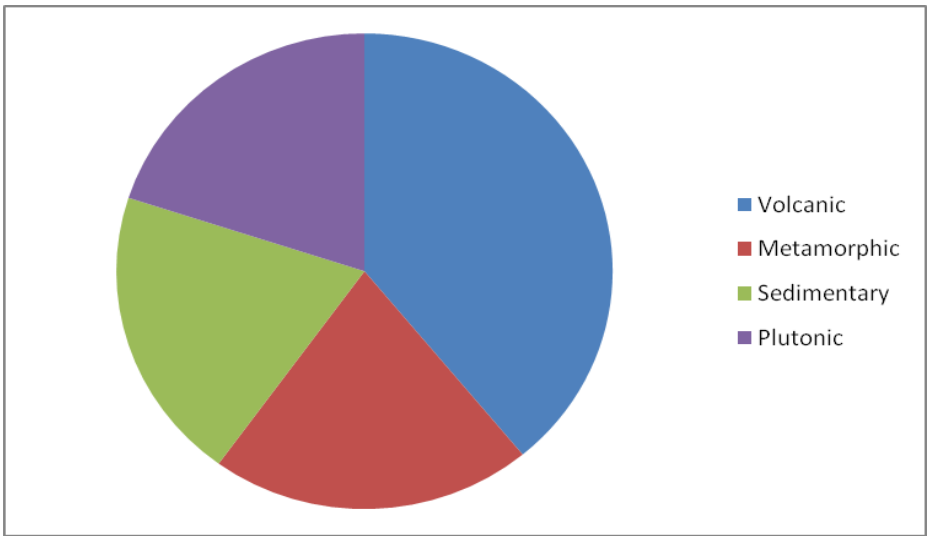

Figure 33. One conglomerate clast count from the measured section of the Muddy Creek Formation from location A at Mormon Mesa (Fig. 28), indicating a mixture of volcanic, plutonic, metamorphic, and sedimentary clasts.

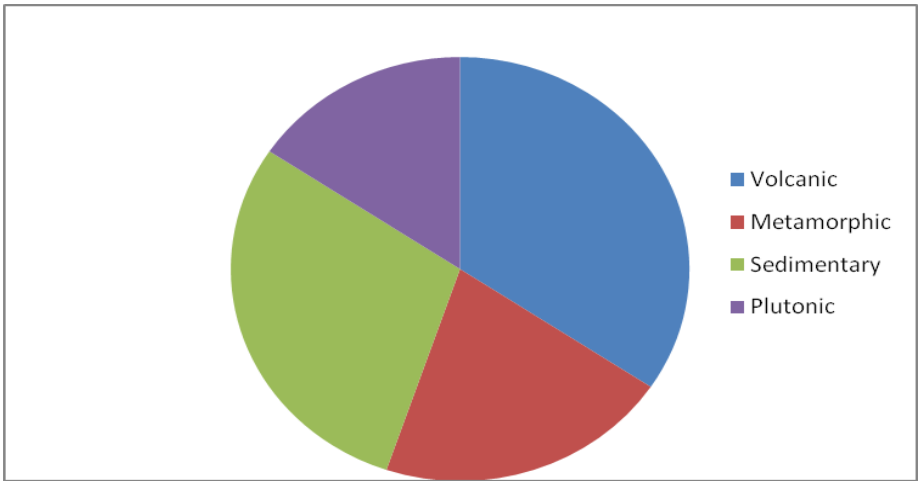

Figure 34. A second conglomerate clast count from the measured section of the Muddy Creek Formation from location A at Mormon Mesa (Fig. 28), indicating a mixture of volcanic, plutonic, metamorphic, and sedimentary clasts.

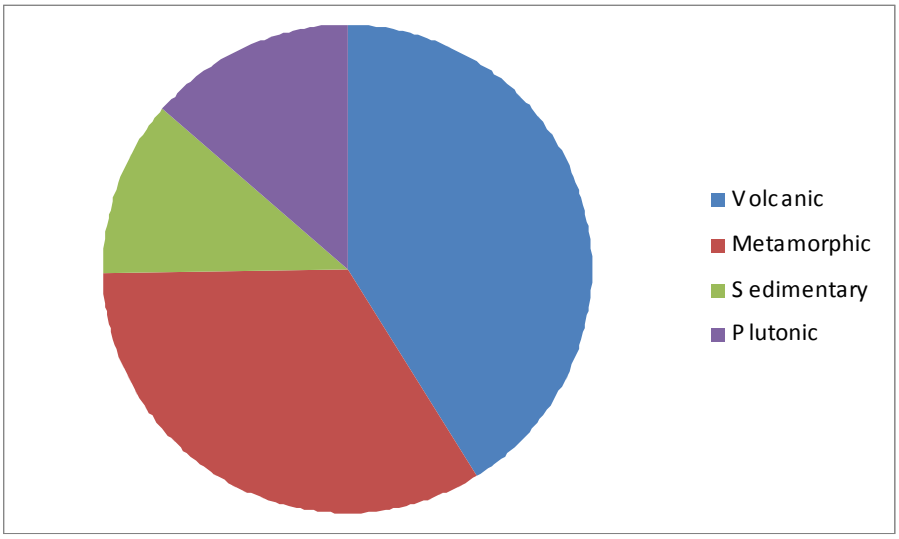

Figure 35. One conglomerate clast count from the Muddy Creek Formation at location B (Fig. 28) at Mormon Mesa, indicating a mixture of volcanic, plutonic, metamorphic, and sedimentary clasts.

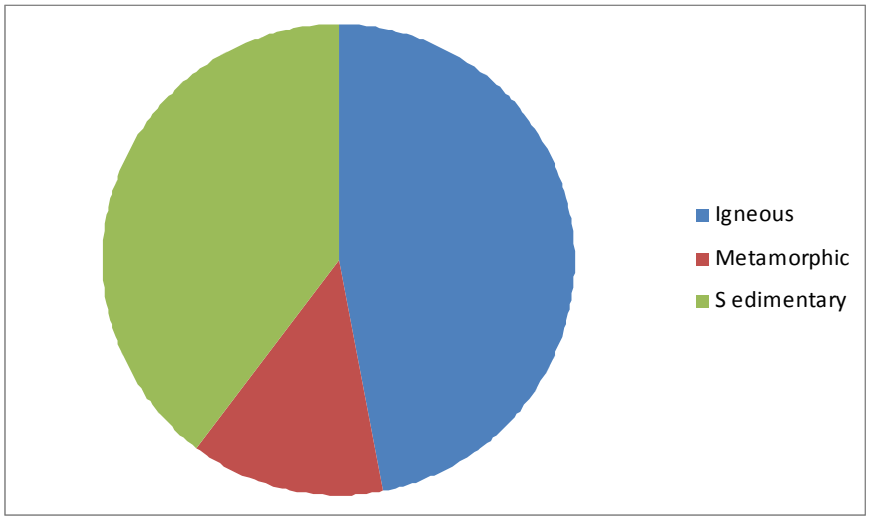

Figure 36. One conglomerate clast count from location C (Fig. 28) within the Muddy Creek Formation at Mormon Mesa indicating a mixture of igneous, metamorphic, and sedimentary clasts.

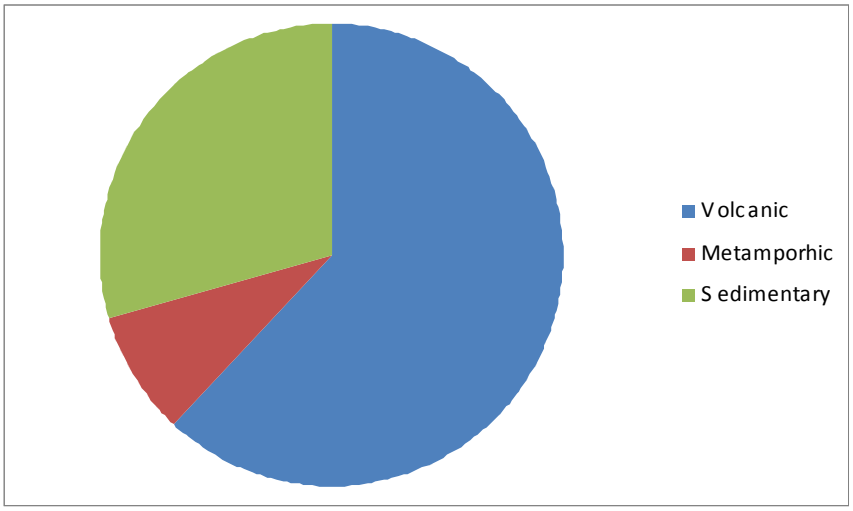

Figure 37. One conglomerate clast count from location D (Fig. 28) within the Muddy Creek Formation at Mormon Mesa showing that the itnerbedded conglomerate is predominantly composed of volcanic clasts and some sedimentary clasts.

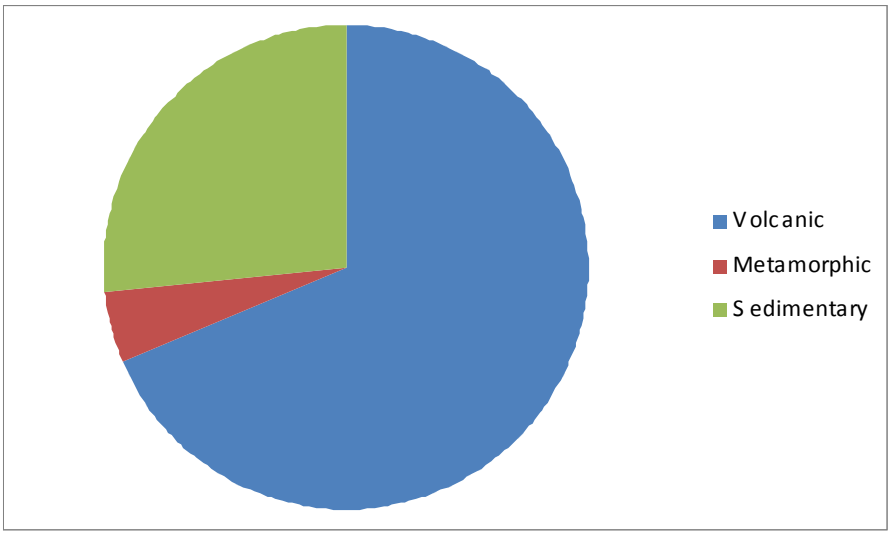

Figure 38. One conglomerate clast count from the Muddy Creek Formation at location E (Fig. 28) at Mormon Mesa indicating that the interbedded conglomerate consists of predominantly volcanic clasts with some sedimentary clasts.

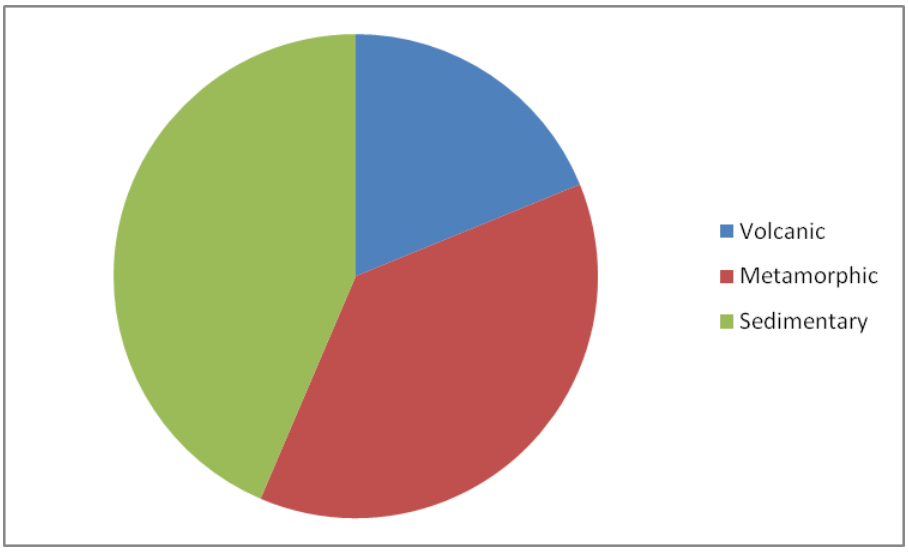

Figure 39. Pie chart from the inset Pliocene unit from location G (Fig. 2) at Littlefield, Arizona showing that conglomerate clasts within interbedded conglomerates are mainly sedimentary and metamorphic clasts.

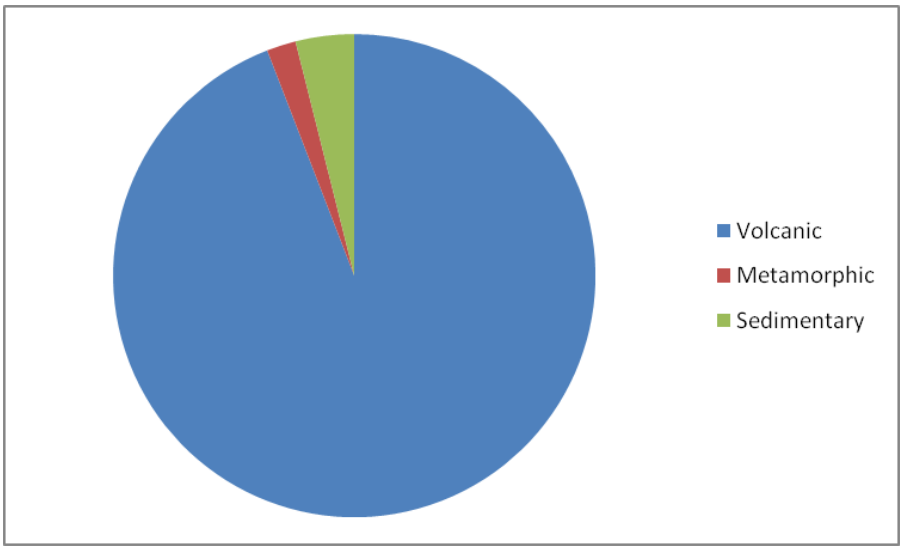

Figure 40. Conglomerate clast count from the inset Pliocene unit from location I (Fig. 2) in the Beaver Dam Wash showing that the conglomerate is composed of almost entirely volcanic clasts.

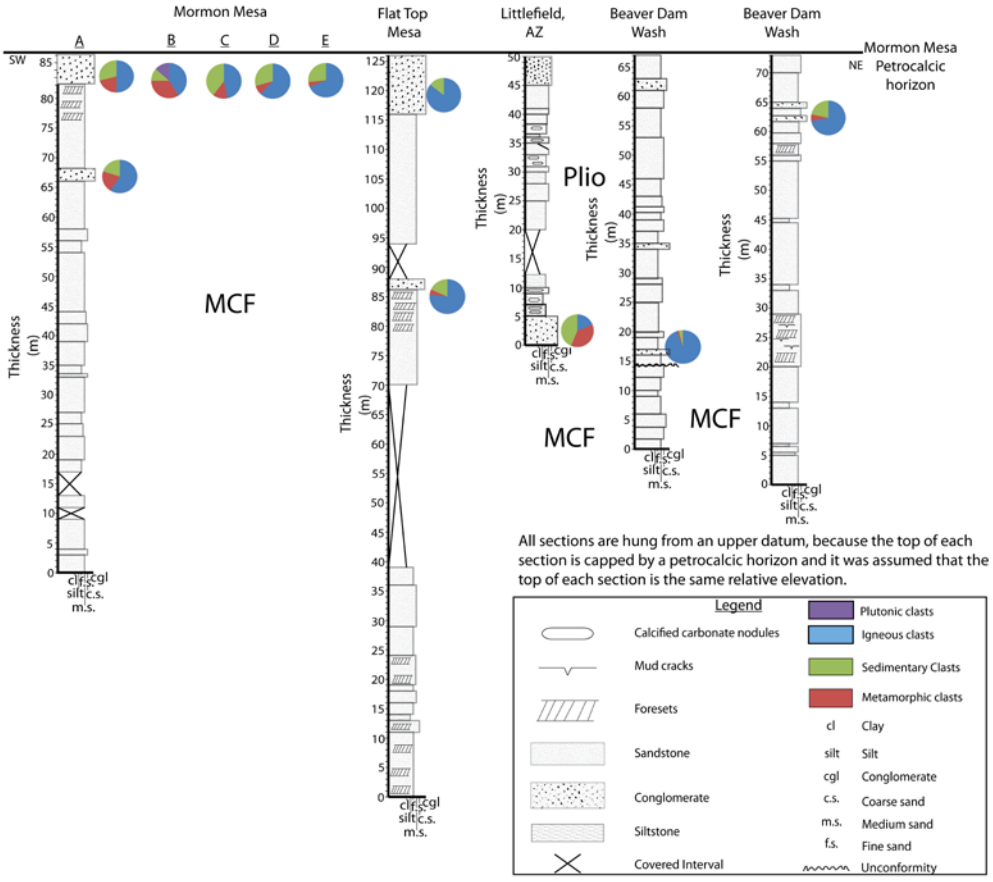

Figure 41. Combined stratigraphic columns, arranged from the southwest to the northeast of the study area. From southwest to northeast, the stratigraphic sections are from Mormon Mesa, Flat Top Mesa, Littlefield, Arizona, and the Beaver Dam Wash. The conglomerate clast count data within each section and from locations B-E at Mormon Mesa are included on the diagram to show where the conglomerate clast counts were conducted and to show the compositional variability.

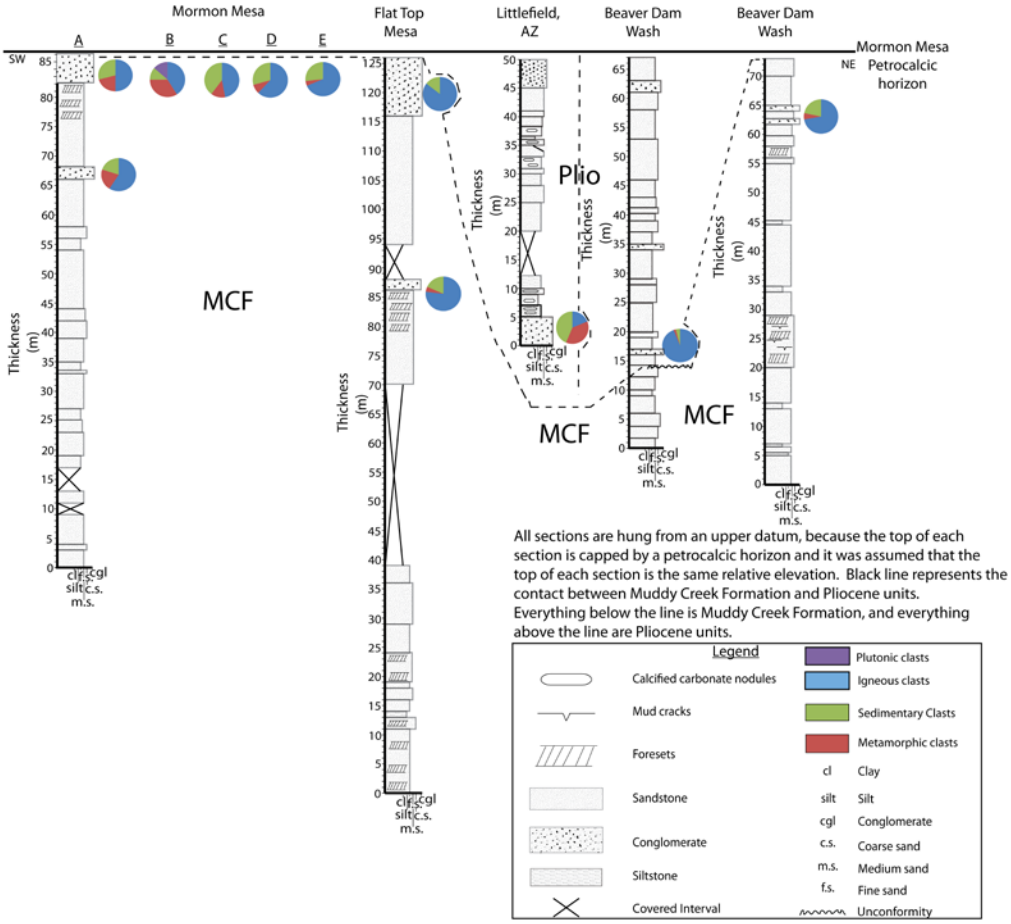

Figure 42. Stratigraphic data from Mormon Mesa, Flat Top Mesa, Littlefield, Arizona, and the Beaver Dam Wash. The stratigraphic columns are arranged from southwest to northeast and are separated by a dotted line, representing the contact between the Muddy Creek Formation and the younger inset Pliocene units. The conglomerate clast count pie charts from each section and from locations B-E at Mormon Mesa are shown to indicate the differences in composition of the Muddy Creek Formation and inset Pliocene units.

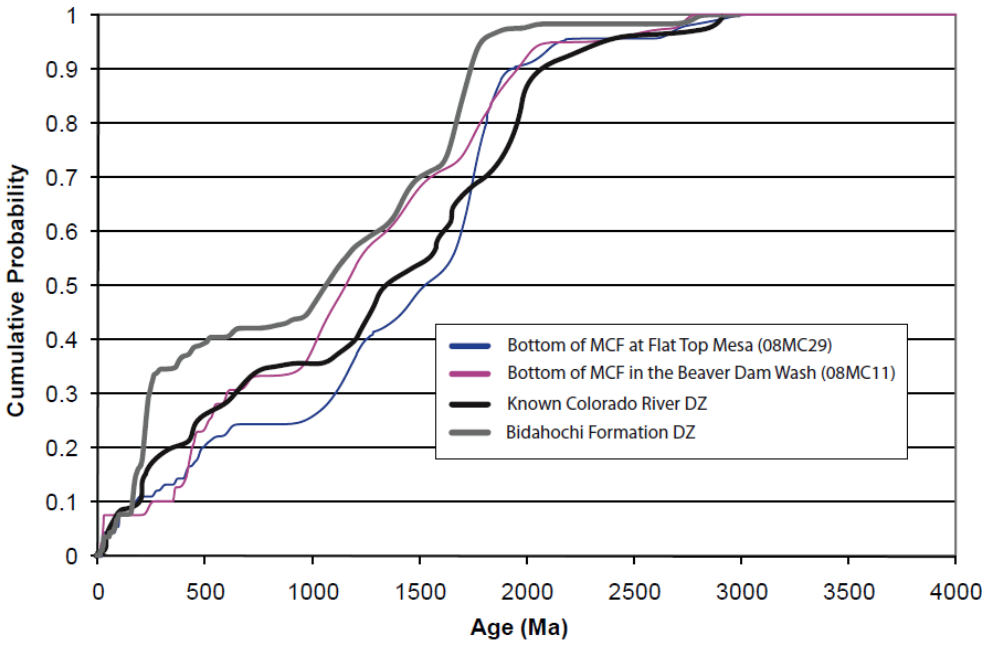

Figure 43. Cumulative probability plot of detrital zircons from the bottom of the Muddy Creek Formation from location F (Fig. 2) at Flat Top Mesa, the bottom of the Muddy Creek Formation from location H (Fig. 2) in the Beaver Dam Wash, the Bidahochi Formation, and known Colorado River deposits (Kimbrough et al., 2007).

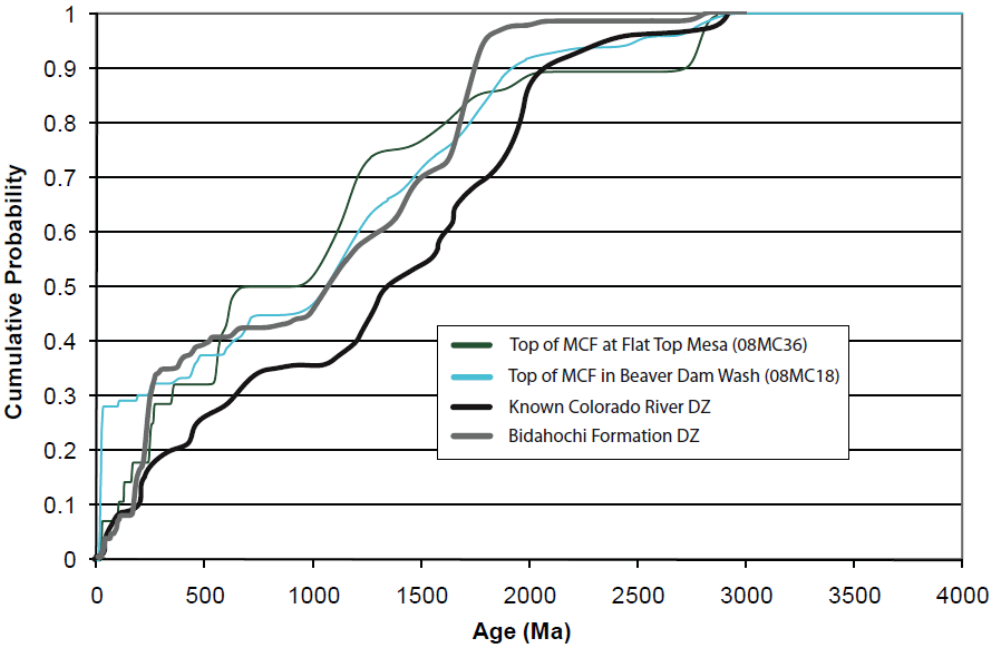

Figure 44. Cumulative probability plot of detrital zircons from the top of the Muddy Creek Formation at Flat Top Mesa and the Beaver Dam Wash, the Bidahochi Formation, and known Colorado River deposits (Kimbrough et al., 2007).

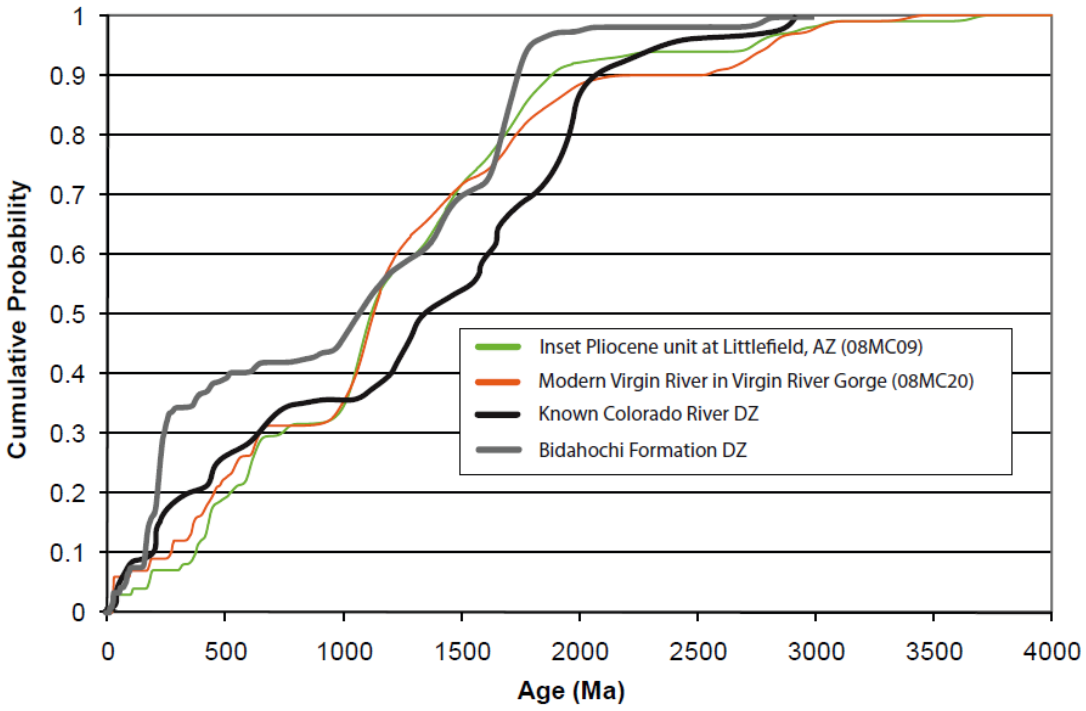

Figure 45. Cumulative probability plot of detrital zircons from the inset Pliocene unit from location G (Fig. 2) at Littlefield, Arizona, location J (Fig. 2) in the Virgin River Gorge, the Bidahochi Formation, and known Colorado River deposits (Kimbrough et al., 2007).

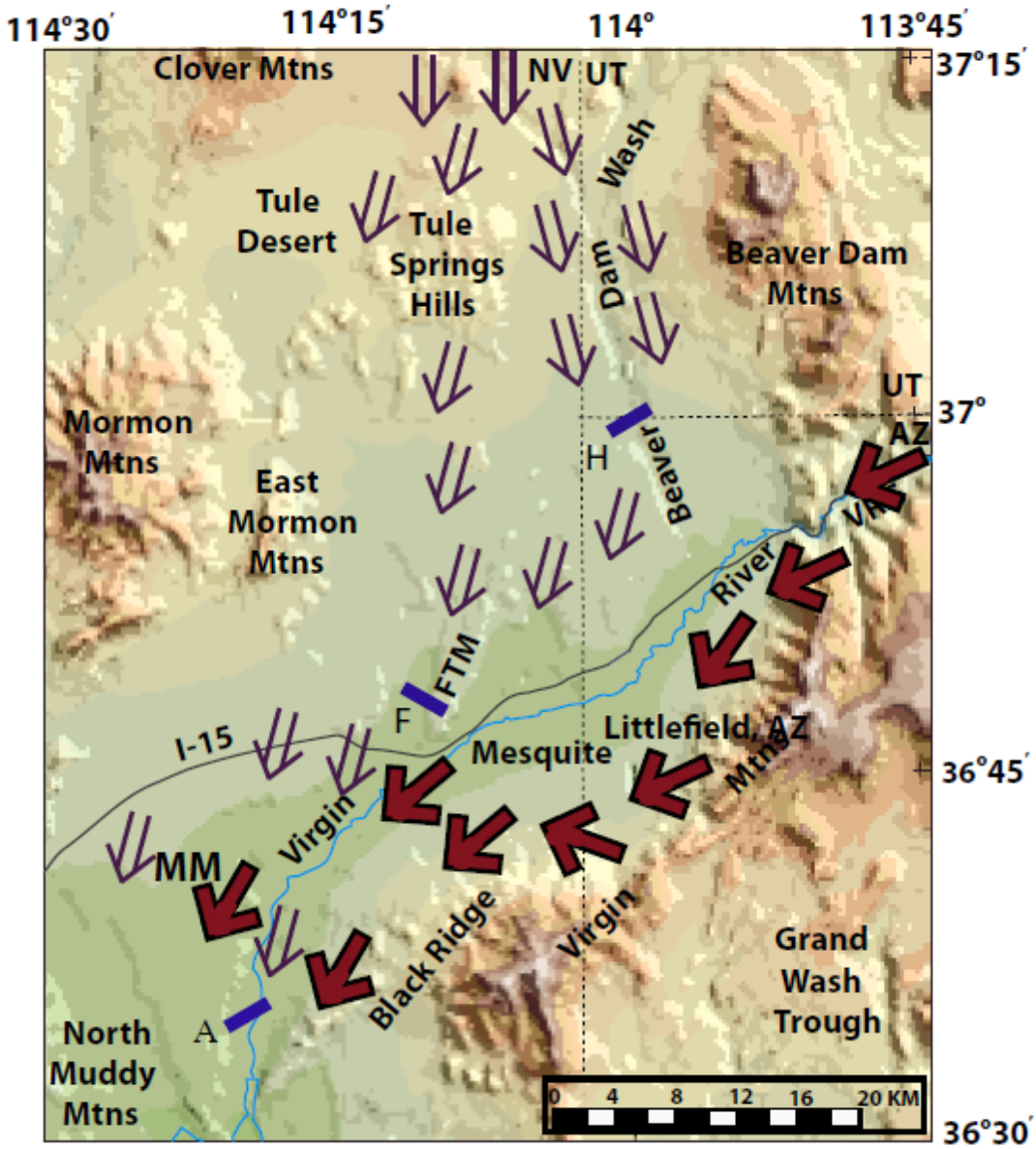

Figure 46. Map of southern Nevada during the Miocene showing deposition of the Muddy Creek Formation at Flat Top Mesa, Mormon Mesa, and the Beaver Dam Wash. Open purple arrows show sediment derived from the Caliente Caldera complex and closed red arrows show sediment derived from the Colorado Plateau. Figure was modified from Langenheim et al. (2000).

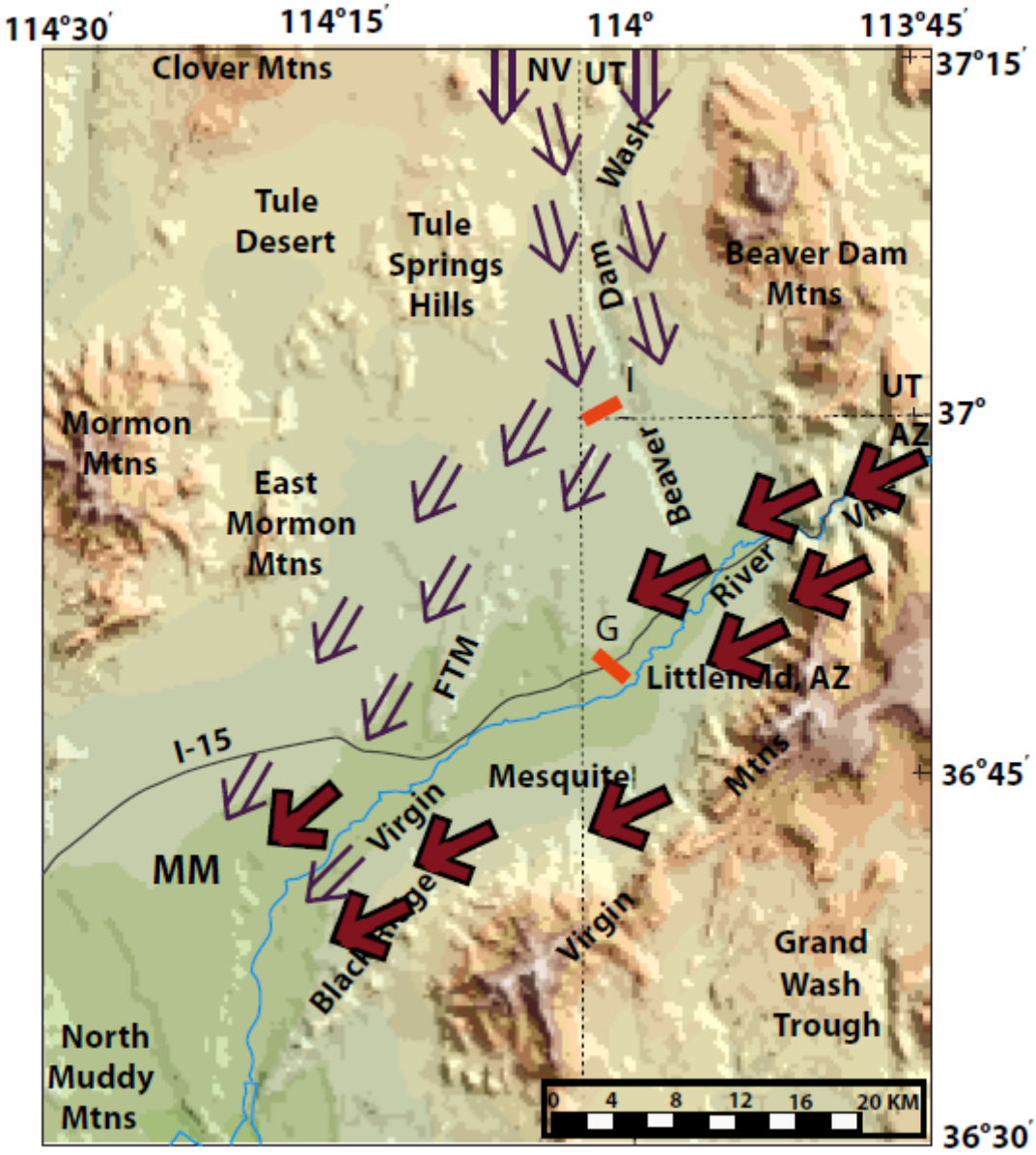

Figure 47. Map of southern Nevada during the Pliocene showing deposition of the Inset Pliocene units at Littlefield, Arizona and in the Beaver Dam Wash. Open purple arrows show sediment being derived from the Caliente Caldera complex and closed red arrows show sediment derived from the Colorado Plateau. Figure was modified from Langenheim et al. (2000).

Tables

Table 1. Overlap program data showing how much the detrital zircon samples overlap each other.

OVERLAP						
Samples						
08MC09	08MC09					
08MC11	0.733	08MC11				
08MC18	0.845	0.831	08MC18			
08MC20	0.834	0.749	0.817	08MC20		
08MC29	0.895	0.735	0.828	0.863	08MC29	
08MC36	0.766	0.727	0.772	0.756	0.799	08MC36

Table 2. Similarity program data showing how similar/dissimilar the detrital zircon samples are relative to each other.

SIMILARITY						
Samples						
08MC09	08MC09					
08MC11	0.770	08MC11				
08MC18	0.748	0.764	08MC18			
08MC20	0.847	0.773	0.746	08MC20		
08MC29	0.805	0.734	0.730	0.802	08MC29	
08MC36	0.658	0.602	0.662	0.712	0.626	08MC36

APPENDIX I

PETROGRAPHIC ANALYSES DATA

This study analyzed thirty two thin sections to determine the provenance of the Muddy Creek Formation. For each sample 500 grains were counted to determine the composition of each sample. The percentage of each grain counted within each sample is shown.

Table of point count data showing the composition of sandstones from the Muddy Creek Formation and inset Pliocene units. Qm = Monocrystalline quartz. Qp = Polycrystalline quartz. K = Potassium feldspar. P = Plagioclase feldspar. Feldspar = Other feldspar minerals besides, Potassium or Plagioclase feldspar. Lv = Volcanic lithic fragments. Lslt = Sedimentary lithic fragments. Xb CO_3 = Carbonate grains. Lm = Metamorphic lithic fragments. Unid L = Unidentified lithic fragments. Bt = Biotite mica. Ms = Muscovite mica. Chl = Chlorite. Heav. = Heavy minerals. Cmt = Cement. Matr. = Matrix. Por = Porosity. Unid T = Total unidentified minerals. Opaq = Opque minerals. CHK = Check to make sure the total number of grains counted equals 500 grains.

Sample#	Q m	Q p	K	P	Feld	Lv	Lslt	xb CO_3	Lm	unid L	bt	ms	chl	heav.	Cmt	Matr.	Por	Unid T	Opaq	CHK
08MC03	193	3	25	21	0	32	10	7	8	0	3	0	0	2	161	4	17	2	12	500
08MC04	194	1	20	16	0	19	8	4	7	0	2	0	0	3	172	2	41	0	11	500
08MC05	199	3	18	15	0	17	7	2	6	0	4	0	0	2	181	3	39	0	4	500
08MC06	189	0	20	21	0	36	8	3	4	0	2	0	0	4	188	0	15	0	10	500
08MC07	179	1	19	16	0	31	10	4	8	0	3	0	0	5	180	2	30	3	9	500
08MC08	195	1	18	19	0	27	9	10	3	0	0	0	0	1	183	2	18	1	13	500
08MC12	172	4	14	24	0	237	6	12	2	0	3	2	0	3	0	7	0	1	13	500
08MC13	136	2	8	18	0	184	2	16	3	0	0	1	0	5	90	5	20	2	8	500
08MC14	179	2	10	19	0	232	5	15	2	0	3	0	0	9	0	4	0	3	17	500

Sample#	Q m	Q p	K	P	Feld	Lv	Lslt	xb CO_3	Lm	unid L	bt	ms	chl	heav.	Cmt	Matr.	Por	Unid T	Opaq	CHK
08MC15	143	15	9	11	0	204	4	12	2	0	4	0	0	1	84	2	4	0	5	500
08MC16	150	4	13	16	0	198	5	10	2	0	2	1	0	6	85	0	5	0	3	500
08MC17	162	2	9	12	0	193	3	13	0	0	3	1	0	0	88	0	6	0	8	500
08MC19	133	9	8	14	0	206	7	15	0	0	3	0	0	0	84	2	6	1	12	500
08MC22	190	0	14	16	0	233	5	16	2	0	3	1	0	7	0	3	0	1	9	500
08MC22	190	0	14	16	0	233	5	16	2	0	3	1	0	7	0	3	0	1	9	500
08MC23	169	1	14	12	0	209	6	9	1	0	2	0	0	3	50	2	12	2	8	500
08MC24	192	1	15	30	0	236	0	5	2	0	0	0	0	5	0	0	5	3	6	500
08MC25	170	1	11	13	0	212	7	9	3	0	2	0	0	6	52	3	8	0	3	500
08MC28	174	0	7	8	0	185	5	8	1	0	1	0	0	1	85	2	12	0	11	500
08MC30	212	2	12	8	0	226	6	8	2	0	2	0	0	4	0	5	0	0	13	500
08MC31	179	0	4	6	0	182	4	7	1	0	2	0	0	3	82	3	12	1	14	500
08MC32	169	2	10	7	0	178	5	10	4	0	4	0	0	2	80	4	17	2	6	500
08MC33	189	1	20	15	0	241	4	7	1	0	1	0	0	5	0	0	5	3	8	500
08MC34	160	1	8	4	0	189	5	12	0	0	1	0	0	0	94	6	12	1	7	500
08MC35	165	0	9	5	0	184	4	14	1	0	1	1	0	4	92	4	5	1	10	500
08MC37	223	3	8	4	0	224	6	7	2	0	1	0	0	5	0	4	0	2	11	500
08MC38	274	0	38	33	0	57	51	11	12	0	2	0	0	2	0	9	0	2	9	500
08MC39	255	2	30	44	0	51	56	18	8	0	4	0	0	4	0	14	0	2	12	500
08MC40	266	5	27	30	0	60	57	11	11	0	3	0	0	3	0	12	0	3	12	500
08MC41	285	0	31	35	0	57	59	6	6	0	2	0	0	6	0	6	0	1	6	500
08MC42	269	1	25	29	0	59	55	15	10	0	2	1	0	3	0	13	0	2	16	500
08MC43	280	4	20	25	0	52	54	14	12	0	3	0	0	1	0	21	0	1	13	500
08MC44	277	0	25	23	0	60	53	15	6	0	3	0	0	3	0	24	0	1	10	500

Table showing ternary diagram percentages for each sample from the Muddy Creek Formation and inset Pliocene units. F= Feldspar grains. L = Lithic grains. Lt = Total lithic grains. Qm = Monocrystalline quartz. Q = Total quartz grains. Qp = Polycrystalline quartz. Lsm = Sedimentary and metamorphic lithic grains. P = Plagioclase feldspar grains. K = Potassium feldspar grains. Mic = Mica grains. Hv = Heavy mineral grains. CO_3 = Carbonate grains.

Sample#	F	L	Lt	QM	F	Lt	Q	F	L	QP	LV	LSM	QM	P	K	P/F	%Mic	%hv	% CO_3
08MC03	46	57	60	64.5	15.4	20.1	64.9	15.2	19.9	5.7	60.4	34.0	80.8	8.8	10.5	0.5	0.6	0.4	0.4
08MC04	36	38	39	72.1	13.4	14.5	72.2	13.3	14.4	2.9	54.3	42.9	84.3	7.0	8.7	0.4	0.4	0.6	0.6
08MC05	33	32	35	74.5	12.4	13.1	74.8	12.2	13.0	9.1	51.5	39.4	85.8	6.5	7.8	0.5	0.8	0.4	0.4
08MC06	41	51	51	67.3	14.6	18.1	67.3	14.6	18.1	0.0	75.0	25.0	82.2	9.1	8.7	0.5	0.4	0.8	0.8
08MC07	35	53	54	66.8	13.1	20.1	66.9	13.0	20.1	2.0	62.0	36.0	83.6	7.5	8.9	0.5	0.6	1.0	1.0
08MC08	37	49	50	69.1	13.1	17.7	69.3	13.1	17.7	2.5	67.5	30.0	84.1	8.2	7.8	0.5	0.0	0.2	0.2
08MC12	38	257	261	36.5	8.1	55.4	37.1	8.0	54.9	1.6	95.2	3.2	81.9	11.4	6.7	0.6	1.0	0.6	0.6
08MC13	26	205	207	36.9	7.0	56.1	37.2	7.0	55.8	1.0	96.3	2.6	84.0	11.1	4.9	0.7	0.2	1.0	1.0
08MC14	29	254	256	38.6	6.3	55.2	38.8	6.2	54.9	0.8	96.3	2.9	86.1	9.1	4.8	0.7	0.6	1.8	1.8
08MC15	20	222	237	35.8	5.0	59.3	38.1	4.8	57.1	6.7	90.7	2.7	87.7	6.7	5.5	0.6	0.8	0.2	0.2
08MC16	29	215	219	37.7	7.3	55.0	38.3	7.2	54.5	1.9	94.7	3.3	83.8	8.9	7.3	0.6	0.6	1.2	1.2
08MC17	21	209	211	41.1	5.3	53.6	41.4	5.3	53.3	1.0	97.5	1.5	88.5	6.6	4.9	0.6	0.8	0.0	0.0
08MC19	22	228	237	33.9	5.6	60.5	35.4	5.5	59.1	4.1	92.8	3.2	85.8	9.0	5.2	0.6	0.6	0.0	0.0
08MC22	30	256	256	39.9	6.3	53.8	39.9	6.3	53.8	0.0	97.1	2.9	86.4	7.3	6.4	0.5	0.8	1.4	1.4
08MC23	26	225	226	40.1	6.2	53.7	40.3	6.2	53.6	0.5	96.3	3.2	86.7	6.2	7.2	0.5	0.4	0.6	0.6
08MC24	45	243	244	39.9	9.4	50.7	40.0	9.3	50.6	0.4	98.7	0.8	81.0	12.7	6.3	0.7	0.0	1.0	1.0
08MC25	24	231	232	39.9	5.6	54.5	40.0	5.6	54.3	0.4	95.1	4.5	87.6	6.7	5.7	0.5	0.4	1.2	1.2
08MC28	15	199	199	44.8	3.9	51.3	44.8	3.9	51.3	0.0	96.9	3.1	92.1	4.2	3.7	0.5	0.2	0.2	0.2
08MC30	20	242	244	44.5	4.2	51.3	44.8	4.2	51.0	0.8	95.8	3.4	91.4	3.4	5.2	0.4	0.4	0.8	0.8

Sample#	F	L	Lt	QM	F	Lt	Q	F	L	QP	LV	LSM	QM	P	K	P/F	%Mic	%hv	% CO_3
08MC31	10	194	194	46.7	2.6	50.7	46.7	2.6	50.7	0.0	97.3	2.7	94.7	3.2	2.1	0.6	0.4	0.6	0.6
08MC32	17	197	199	43.9	4.4	51.7	44.2	4.4	51.4	1.1	94.2	4.8	90.9	3.8	5.4	0.4	0.8	0.4	0.4
08MC33	35	253	254	39.5	7.3	53.1	39.7	7.3	53.0	0.4	97.6	2.0	84.4	6.7	8.9	0.4	0.2	1.0	1.0
08MC34	12	206	207	42.2	3.2	54.6	42.4	3.2	54.5	0.5	96.9	2.6	93.0	2.3	4.7	0.3	0.2	0.0	0.0
08MC35	14	203	203	43.2	3.7	53.1	43.2	3.7	53.1	0.0	97.4	2.6	92.2	2.8	5.0	0.4	0.4	0.8	0.8
08MC37	12	239	242	46.8	2.5	50.7	47.1	2.5	50.4	1.3	95.3	3.4	94.9	1.7	3.4	0.3	0.2	1.0	1.0
08MC38	71	131	131	57.6	14.9	27.5	57.6	14.9	27.5	0.0	47.5	52.5	79.4	9.6	11.0	0.5	0.4	0.4	0.4
08MC39	74	133	135	55.0	15.9	29.1	55.2	15.9	29.0	1.7	43.6	54.7	77.5	13.4	9.1	0.6	0.8	0.8	0.8
08MC40	57	139	144	57.0	12.2	30.8	57.4	12.1	30.5	3.8	45.1	51.1	82.4	9.3	8.4	0.5	0.6	0.6	0.6
08MC41	66	128	128	59.5	13.8	26.7	59.5	13.8	26.7	0.0	46.7	53.3	81.2	10.0	8.8	0.5	0.4	1.2	1.2
08MC42	54	139	140	58.1	11.7	30.2	58.2	11.6	30.2	0.8	47.2	52.0	83.3	9.0	7.7	0.5	0.6	0.6	0.6
08MC43	45	132	136	60.7	9.8	29.5	61.1	9.7	29.2	3.3	42.6	54.1	86.2	7.7	6.2	0.6	0.6	0.2	0.2
08MC44	48	134	134	60.3	10.5	29.2	60.3	10.5	29.2	0.0	50.4	49.6	85.2	7.1	7.7	0.5	0.6	0.6	0.6

APPENDIX II

DETRITAL ZIRCON ANALYSES DATA

Concordia diagrams, normalized probability plots, isotope ratio tables and apparent age tables for all detrital zircons analyzed in this study are included below. Each sample was plotted on concordia diagrams to determine if each detrital zircon remained part of a closed system or at some point during its history had a lead loss event or a uranium enrichment event. The isotope ratio tables and apparent age tables are the actual data of the detrital zircon analyses and are the data from which all plots were created from.

<u>08MC29</u>

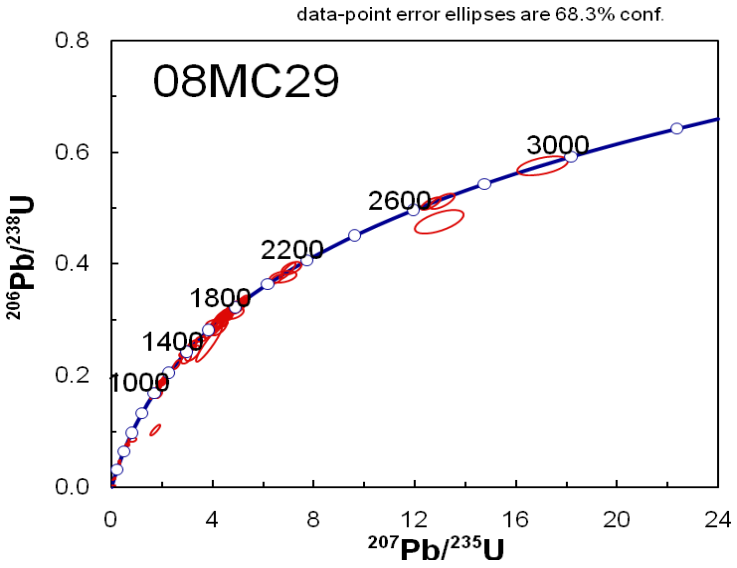

Concordia diagram of detrital zircons from the base of the Muddy Creek Formation from location F (Fig. 2) at Flat Top Mesa. The plot shows that most of the detrital zircons are concordant and are part of a closed system, while a few are discordant. The discordant zircons were excluded from the study.

Table of isotope ratios of detrital zircons from the base of the Muddy Creek Formation from location F at Flat Top Mesa (Fig. 2).

Isotope ratios for sample 08MC29 - Bottom of MCF at Flat Top Mesa										
Analysis	U	^{206}Pb	U/Th	$^{206}Pb^*$	±	$^{207}Pb^*$	±	$^{206}Pb^*$	±	error
	(ppm)	^{204}Pb		$^{207}Pb^*$	(%)	$^{235}U^*$	(%)	^{238}U	(%)	corr.
08MC29-49	124	2384	1.2	20.1629	11.6	0.0188	14.0	0.0028	7.8	0.56
08MC29-21	195	608	1.0	19.9013	431.3	0.0197	431.4	0.0028	5.2	0.01
08MC29-48	280	2770	1.0	19.1930	27.7	0.0221	28.0	0.0031	4.0	0.14
08MC29-32	307	3004	1.3	19.3050	32.1	0.0221	32.5	0.0031	5.1	0.16
08MC29-88	252	4436	2.6	26.3547	23.6	0.0661	23.8	0.0126	3.2	0.13
08MC29-34	146	2164	1.2	18.7926	20.5	0.1104	20.5	0.0151	1.2	0.06
08MC29-5	1088	46584	1.1	19.5594	4.3	0.1088	4.8	0.0154	2.2	0.44
08MC29-75	210	1942	2.5	17.8184	7.4	0.1343	8.3	0.0174	3.9	0.47
08MC29-10	573	11102	1.4	19.5541	6.6	0.1822	6.9	0.0258	1.9	0.28
08MC29-29	60	3646	0.8	20.1333	19.2	0.1955	19.7	0.0285	4.4	0.23
08MC29-78	553	15270	3.2	16.9713	7.3	0.3369	7.7	0.0415	2.5	0.32
08MC29-86	390	22232	2.9	19.4732	5.8	0.3339	6.5	0.0472	3.1	0.47
08MC29-20	331	12918	4.1	17.9813	4.8	0.4406	5.1	0.0575	1.6	0.31
08MC29-90	217	4314	11.7	16.7352	6.4	0.5343	6.4	0.0649	0.6	0.10
08MC29-84	180	3632	7.6	15.9698	5.8	0.5735	6.0	0.0664	1.5	0.25
08MC29-65	552	13000	0.8	17.8884	2.7	0.5518	3.3	0.0716	1.9	0.57
08MC29-80	783	5116	2.5	16.3256	7.7	0.6399	7.9	0.0758	1.7	0.22
08MC29-19	306	20688	1.1	17.6060	3.7	0.5945	4.1	0.0759	1.6	0.39
08MC29-50	248	13654	18.8	16.1821	2.7	0.6863	3.6	0.0805	2.4	0.67
08MC29-7	112	7242	2.0	14.5131	12.4	0.8142	12.7	0.0857	2.9	0.22
08MC29-8	79	7144	1.8	16.7811	9.0	0.8117	9.3	0.0988	2.3	0.24
08MC29-3	493	81656	1.2	16.4800	4.0	0.8334	5.2	0.0996	3.3	0.64
08MC29-77	197	23514	1.7	13.9267	2.1	1.6519	4.0	0.1668	3.4	0.85
08MC29-43	234	24398	3.5	13.4972	4.0	1.7393	4.5	0.1703	2.1	0.47
08MC29-69	276	27370	5.4	13.3834	2.5	1.8398	2.8	0.1786	1.2	0.42
08MC29-39	98	16154	0.7	13.2747	3.3	1.8800	5.5	0.1810	4.5	0.81
08MC29-87	315	53104	3.6	13.0963	4.2	1.9712	4.6	0.1872	2.0	0.42
08MC29-13	173	31614	1.9	13.0897	1.7	1.9609	4.6	0.1862	4.3	0.93
08MC29-68	131	17060	2.2	12.8256	3.5	2.0081	3.8	0.1868	1.4	0.36
08MC29-22	206	11580	2.9	12.7068	2.9	2.0269	3.4	0.1868	1.7	0.50
08MC29-74	342	44538	2.9	12.6468	1.5	2.1849	2.2	0.2004	1.6	0.73
08MC29-58	872	44056	4.3	12.6310	1.8	2.1732	3.2	0.1991	2.7	0.83
08MC29-4	52	47082	1.3	12.5876	3.6	2.2172	3.7	0.2024	0.9	0.25
08MC29-64	51	7512	2.9	12.5577	3.2	2.2065	3.9	0.2010	2.2	0.57
08MC29-27	131	16382	2.6	12.5240	2.8	2.2691	3.5	0.2061	2.0	0.58

Isotope ratios for sample 08MC29 - Bottom of MCF at Flat Top Mesa (Continued)										
Analysis	U	^{206}Pb	U/Th	$^{206}Pb^*$	±	$^{207}Pb^*$	±	$^{206}Pb^*$	±	error
	(ppm)	^{204}Pb		$^{207}Pb^*$	(%)	$^{235}U^*$	(%)	^{238}U	(%)	corr.
08MC29-33	143	5194	3.0	12.3605	3.8	1.8650	4.7	0.1672	2.7	0.58
08MC29-72	495	57000	16.4	12.3479	1.0	2.2904	1.5	0.2051	1.1	0.74
08MC29-85	108	9928	2.4	11.6583	2.4	2.5960	3.4	0.2195	2.4	0.70
08MC29-44	66	9238	2.2	11.4148	4.5	2.8869	4.8	0.2390	1.5	0.32
08MC29-41	73	13390	1.0	11.4130	2.6	2.8822	2.9	0.2386	1.2	0.42
08MC29-16	66	10968	1.9	11.0366	2.7	3.1728	3.4	0.2540	2.1	0.61
08MC29-63	94	12254	2.5	10.9293	2.1	3.0977	2.9	0.2455	2.0	0.68
08MC29-81	110	16990	0.9	10.8645	2.0	3.2835	2.3	0.2587	1.2	0.51
08MC29-60	89	14226	1.6	10.8275	3.1	3.1813	3.5	0.2498	1.7	0.47
08MC29-2	44	21294	1.6	10.7445	3.9	2.9579	4.5	0.2305	2.4	0.52
08MC29-71	152	25550	2.4	10.3698	3.3	3.5355	3.5	0.2659	1.1	0.32
08MC29-37	51	3866	0.7	10.3320	4.7	3.2091	6.0	0.2405	3.8	0.62
08MC29-79	96	14166	2.0	9.8897	2.5	3.8523	3.4	0.2763	2.3	0.67
08MC29-14	35	11172	1.0	9.7613	2.8	4.0603	4.4	0.2874	3.3	0.76
08MC29-6	185	40072	1.6	9.6944	1.1	4.2738	1.6	0.3005	1.1	0.73
08MC29-52	32	7398	0.9	9.6825	6.7	4.1718	6.9	0.2930	1.8	0.26
08MC29-45	90	16914	1.4	9.6806	3.2	4.1176	3.7	0.2891	2.0	0.53
08MC29-12	46	14758	1.0	9.6561	3.0	4.3032	4.4	0.3014	3.1	0.72
08MC29-62	373	10736	1.1	9.6298	3.8	4.1992	6.1	0.2933	4.7	0.78
08MC29-9	35	7932	1.1	9.4703	4.1	4.4720	4.4	0.3072	1.7	0.39
08MC29-67	125	17712	1.7	9.4598	1.9	4.4904	2.6	0.3081	1.8	0.68
08MC29-47	72	18932	2.4	9.4293	1.7	4.2877	2.5	0.2932	1.8	0.74
08MC29-73	128	21742	1.4	9.4258	3.7	4.3211	4.5	0.2954	2.6	0.58
08MC29-40	157	32168	3.2	9.3934	1.9	4.5388	2.1	0.3092	1.1	0.51
08MC29-61	409	62796	2.7	9.3920	3.8	4.5043	4.2	0.3068	1.8	0.42
08MC29-89	251	66252	2.1	9.3718	3.4	4.5028	3.8	0.3061	1.9	0.48
08MC29-18	269	53078	1.9	9.3662	2.4	4.5416	3.2	0.3085	2.1	0.66
08MC29-15	179	47544	3.1	9.3488	2.0	4.6415	2.5	0.3147	1.6	0.64
08MC29-55	232	33564	2.1	9.3407	3.8	4.4797	4.0	0.3035	1.1	0.27
08MC29-59	138	31932	2.2	9.3374	1.2	4.4583	2.2	0.3019	1.8	0.84
08MC29-56	103	16086	1.6	9.3301	2.3	4.6023	2.9	0.3114	1.7	0.60
08MC29-11	108	43316	1.9	9.3066	2.9	4.6322	3.5	0.3127	1.9	0.54
08MC29-82	132	30004	2.0	9.2553	3.9	4.6805	4.1	0.3142	1.3	0.30
08MC29-17	104	28646	4.6	9.2486	2.4	4.6494	3.3	0.3119	2.2	0.67
08MC29-57	36	5644	0.6	9.2286	3.7	4.2653	4.8	0.2855	3.1	0.65
08MC29-26	217	50138	1.9	9.2149	3.2	4.8136	4.1	0.3217	2.6	0.63
08MC29-54	131	26774	3.0	9.2104	1.9	4.7811	2.2	0.3194	1.2	0.54

Isotope ratios for sample 08MC29 - Bottom of MCF at Flat Top Mesa (Continued)										
Analysis	U	^{206}Pb	U/Th	$^{206}Pb^*$	±	$^{207}Pb^*$	±	$^{206}Pb^*$	±	error
	(ppm)	^{204}Pb		$^{207}Pb^*$	(%)	$^{235}U^*$	(%)	^{238}U	(%)	corr.
08MC29-76	235	8156	2.0	9.1849	3.1	3.8570	8.6	0.2569	8.0	0.93
08MC29-30	246	57058	3.1	8.9907	2.7	4.9291	3.2	0.3214	1.8	0.56
08MC29-38	81	30480	1.0	8.9159	2.1	5.0334	3.1	0.3255	2.3	0.73
08MC29-31	169	10438	2.6	8.8867	4.9	4.8396	5.4	0.3119	2.4	0.43
08MC29-24	492	142142	3.0	8.8822	1.9	5.1199	3.4	0.3298	2.7	0.82
08MC29-70	119	11404	2.2	8.8650	2.2	5.2150	2.4	0.3353	0.8	0.32
08MC29-35	281	56492	3.4	8.8447	2.6	5.0568	3.8	0.3244	2.7	0.71
08MC29-23	300	85648	2.2	8.8306	1.8	5.1776	2.6	0.3316	1.8	0.71
08MC29-28	277	56790	3.5	8.7190	1.3	5.1920	2.2	0.3283	1.8	0.81
08MC29-83	715	968	10.6	8.2157	3.6	1.7310	7.2	0.1031	6.3	0.87
08MC29-66	145	33128	1.8	7.8841	1.8	6.5297	2.3	0.3734	1.4	0.61
08MC29-36	142	37972	1.3	7.6802	4.8	6.7716	5.2	0.3772	1.9	0.37
08MC29-25	363	117300	3.1	7.6684	1.5	6.9755	2.9	0.3879	2.5	0.86
08MC29-53	32	8286	1.7	7.5896	3.2	7.1269	3.7	0.3923	1.9	0.52
08MC29-51	38	13782	1.5	5.5567	1.3	12.6243	2.0	0.5088	1.5	0.74
08MC29-46	118	35268	0.8	5.4030	1.8	13.0799	2.5	0.5126	1.8	0.70
08MC29-1	73	4414	0.7	5.0585	3.9	12.9671	4.9	0.4757	3.0	0.60
08MC29-42	33	13496	1.6	4.6563	3.4	17.0441	3.9	0.5756	2.0	0.50

Table of apparent ages (Ma) of detrital zircons from the base of the Muddy Creek Formation from location F at Flat Top Mesa (Fig. 2).

Apparent ages (Ma) for sample 08MC29 - Bottom of MCF at Flat Top Mesa								
Analysis	$^{206}Pb^*$	±	$^{207}Pb^*$	±	$^{206}Pb^*$	±	Best age	±
	$^{238}U^*$	(Ma)	^{235}U	(Ma)	$^{207}Pb^*$	(Ma)	(Ma)	(Ma)
08MC29-49	17.7	1.4	19.0	2.6	176.1	271.4	17.7	1.4
08MC29-21	18.3	0.9	19.8	84.9	206.5	0.0	18.3	0.9
08MC29-48	19.8	0.8	22.1	6.1	289.9	643.0	19.8	0.8
08MC29-32	19.9	1.0	22.2	7.1	276.6	751.5	19.9	1.0
08MC29-88	80.9	2.6	65.0	15.0	489.1	634.0	80.9	2.6
08MC29-34	96.3	1.1	106.4	20.7	337.8	468.2	96.3	1.1
08MC29-5	98.7	2.1	104.9	4.8	246.5	99.7	98.7	2.1
08MC29-75	110.9	4.3	127.9	10.0	457.2	163.4	110.9	4.3
08MC29-10	164.5	3.1	170.0	10.8	247.1	152.0	164.5	3.1
08MC29-29	181.4	7.9	181.3	32.7	179.5	450.0	181.4	7.9
08MC29-78	261.9	6.3	294.8	19.7	564.2	159.3	261.9	6.3

Apparent ages (Ma) for sample 08MC29 - Bottom of MCF at Flat Top Mesa (Continued)								
Analysis	$^{206}Pb^*$	±	$^{207}Pb^*$	±	$^{206}Pb^*$	±	Best age	±
	$^{238}U^*$	(Ma)	^{235}U	(Ma)	$^{207}Pb^*$	(Ma)	(Ma)	(Ma)
08MC29-86	297.0	8.9	292.5	16.6	256.7	132.6	297.0	8.9
08MC29-20	360.2	5.5	370.7	15.7	436.9	107.2	360.2	5.5
08MC29-90	405.1	2.5	434.7	22.7	594.7	138.4	405.1	2.5
08MC29-84	414.6	5.9	460.2	22.2	695.3	124.0	414.6	5.9
08MC29-65	445.7	8.2	446.2	12.1	448.5	61.0	445.7	8.2
08MC29-80	470.8	7.9	502.2	31.3	648.1	165.6	470.8	7.9
08MC29-19	471.6	7.1	473.7	15.3	483.7	82.5	471.6	7.1
08MC29-50	499.4	11.6	530.5	14.8	667.1	56.9	499.4	11.6
08MC29-7	530.0	14.6	604.8	58.1	895.8	257.2	530.0	14.6
08MC29-8	607.3	13.2	603.4	42.4	588.7	196.2	607.3	13.2
08MC29-3	612.1	19.2	615.5	23.8	627.9	85.6	612.1	19.2
08MC29-77	994.7	31.6	990.3	25.5	980.4	43.0	980.4	43.0
08MC29-43	1013.6	20.0	1023.2	29.1	1043.9	80.2	1043.9	80.2
08MC29-69	1059.2	11.4	1059.8	18.3	1060.9	51.0	1060.9	51.0
08MC29-39	1072.5	44.1	1074.1	36.7	1077.3	65.6	1077.3	65.6
08MC29-87	1106.3	19.8	1105.7	31.1	1104.4	83.6	1104.4	83.6
08MC29-13	1100.5	43.4	1102.2	31.0	1105.4	33.9	1105.4	33.9
08MC29-68	1104.0	13.9	1118.3	25.6	1146.1	69.8	1146.1	69.8
08MC29-22	1104.0	17.1	1124.6	22.9	1164.5	57.9	1164.5	57.9
08MC29-74	1177.5	17.4	1176.2	15.5	1173.9	30.1	1173.9	30.1
08MC29-58	1170.4	28.4	1172.5	22.2	1176.4	35.0	1176.4	35.0
08MC29-4	1188.3	9.9	1186.5	25.9	1183.2	70.8	1183.2	70.8
08MC29-64	1180.5	24.2	1183.1	27.5	1187.9	63.9	1187.9	63.9
08MC29-27	1208.0	22.0	1202.7	24.4	1193.2	55.7	1193.2	55.7
08MC29-33	996.6	25.0	1068.8	31.1	1219.1	75.5	1219.1	75.5
08MC29-72	1202.8	12.5	1209.3	10.9	1221.1	20.3	1221.1	20.3
08MC29-85	1279.2	27.5	1299.5	24.8	1333.1	46.6	1333.1	46.6
08MC29-44	1381.5	19.0	1378.5	36.2	1373.8	87.5	1373.8	87.5
08MC29-41	1379.3	15.0	1377.3	21.9	1374.1	50.8	1374.1	50.8
08MC29-16	1458.9	27.4	1450.6	26.5	1438.3	51.7	1438.3	51.7
08MC29-63	1415.4	25.3	1432.1	22.3	1457.0	40.3	1457.0	40.3
08MC29-81	1483.3	15.8	1477.1	18.1	1468.3	38.0	1468.3	38.0
08MC29-60	1437.5	21.4	1452.6	27.0	1474.7	58.5	1474.7	58.5
08MC29-2	1337.1	28.5	1396.9	34.3	1489.3	73.1	1489.3	73.1
08MC29-71	1520.0	15.3	1535.2	27.9	1556.2	62.7	1556.2	62.7
08MC29-37	1389.2	46.9	1459.4	46.8	1563.1	88.8	1563.1	88.8

Apparent ages (Ma) for sample 08MC29 - Bottom of MCF at Flat Top Mesa (Continued)								
Analysis	$^{206}Pb^*$	±	$^{207}Pb^*$	±	$^{206}Pb^*$	±	Best age	±
	$^{238}U^*$	(Ma)	^{235}U	(Ma)	$^{207}Pb^*$	(Ma)	(Ma)	(Ma)
08MC29-79	1572.8	32.0	1603.8	27.5	1644.7	47.0	1644.7	47.0
08MC29-14	1628.8	47.9	1646.4	35.7	1668.9	52.7	1668.9	52.7
08MC29-6	1693.8	17.0	1688.3	12.9	1681.6	20.0	1681.6	20.0
08MC29-52	1656.3	26.1	1668.5	56.6	1683.9	123.1	1683.9	123.1
08MC29-45	1637.0	28.8	1657.8	30.5	1684.2	58.4	1684.2	58.4
08MC29-12	1698.1	46.7	1694.0	35.9	1688.9	55.9	1688.9	55.9
08MC29-62	1657.9	69.0	1673.9	49.9	1693.9	70.8	1693.9	70.8
08MC29-9	1726.7	25.8	1725.8	36.5	1724.7	74.5	1724.7	74.5
08MC29-67	1731.3	26.6	1729.2	21.2	1726.7	34.2	1726.7	34.2
08MC29-47	1657.6	26.7	1691.0	20.3	1732.6	30.4	1732.6	30.4
08MC29-73	1668.5	38.7	1697.4	37.5	1733.3	68.1	1733.3	68.1
08MC29-40	1736.8	16.6	1738.1	17.9	1739.6	33.9	1739.6	33.9
08MC29-61	1725.1	26.8	1731.8	34.8	1739.9	69.7	1739.9	69.7
08MC29-89	1721.3	28.1	1731.5	32.0	1743.8	61.8	1743.8	61.8
08MC29-18	1733.4	31.5	1738.6	26.3	1744.9	43.6	1744.9	43.6
08MC29-15	1763.9	25.0	1756.8	21.2	1748.3	35.7	1748.3	35.7
08MC29-55	1708.5	16.4	1727.2	33.1	1749.9	70.3	1749.9	70.3
08MC29-59	1700.8	27.4	1723.2	18.1	1750.6	21.7	1750.6	21.7
08MC29-56	1747.7	26.5	1749.7	24.0	1752.0	42.0	1752.0	42.0
08MC29-11	1753.8	29.2	1755.1	29.2	1756.6	53.8	1756.6	53.8
08MC29-82	1761.2	19.3	1763.8	34.6	1766.7	72.0	1766.7	72.0
08MC29-17	1749.9	33.6	1758.2	27.4	1768.0	44.6	1768.0	44.6
08MC29-57	1618.9	44.4	1686.7	39.4	1772.0	66.7	1772.0	66.7
08MC29-26	1798.1	40.3	1787.3	34.5	1774.7	58.4	1774.7	58.4
08MC29-54	1786.7	18.7	1781.6	18.8	1775.6	34.5	1775.6	34.5
08MC29-76	1474.2	105.8	1604.7	69.6	1780.6	56.8	1780.6	56.8
08MC29-30	1796.6	28.4	1807.3	27.3	1819.5	48.7	1819.5	48.7
08MC29-38	1816.4	36.1	1825.0	26.5	1834.7	38.8	1834.7	38.8
08MC29-31	1750.2	36.0	1791.8	45.5	1840.6	88.1	1840.6	88.1
08MC29-24	1837.5	43.8	1839.4	28.5	1841.5	35.1	1841.5	35.1
08MC29-70	1864.0	12.3	1855.1	20.2	1845.0	40.7	1845.0	40.7
08MC29-35	1811.1	42.6	1828.9	32.0	1849.2	47.8	1849.2	47.8
08MC29-23	1846.1	29.2	1848.9	21.9	1852.1	32.9	1852.1	32.9
08MC29-28	1830.2	28.8	1851.3	19.0	1875.0	23.6	1875.0	23.6
08MC29-83	632.8	38.0	1020.1	46.6	1981.5	63.2	1981.5	63.2
08MC29-66	2045.2	24.5	2049.9	20.3	2054.6	32.3	2054.6	32.3

Apparent ages (Ma) for sample 08MC29 - Bottom of MCF at Flat Top Mesa (Continued)								
Analysis	$^{206}Pb^*$	±	$^{207}Pb^*$	±	$^{206}Pb^*$	±	Best age	±
	$^{238}U^*$	(Ma)	^{235}U	(Ma)	$^{207}Pb^*$	(Ma)	(Ma)	(Ma)
08MC29-36	2063.1	33.9	2082.0	45.8	2100.7	84.4	2100.7	84.4
08MC29-25	2113.3	45.0	2108.3	25.7	2103.4	25.6	2103.4	25.6
08MC29-53	2133.5	35.2	2127.4	33.2	2121.5	55.8	2121.5	55.8
08MC29-51	2651.4	31.7	2652.0	18.7	2652.5	22.2	2652.5	22.2
08MC29-46	2667.5	38.7	2685.4	23.9	2698.9	29.9	2698.9	29.9
08MC29-1	2508.6	61.9	2677.3	46.6	2807.2	64.5	2807.2	64.5
08MC29-42	2930.7	45.9	2937.3	37.4	2941.8	54.6	2941.8	54.6

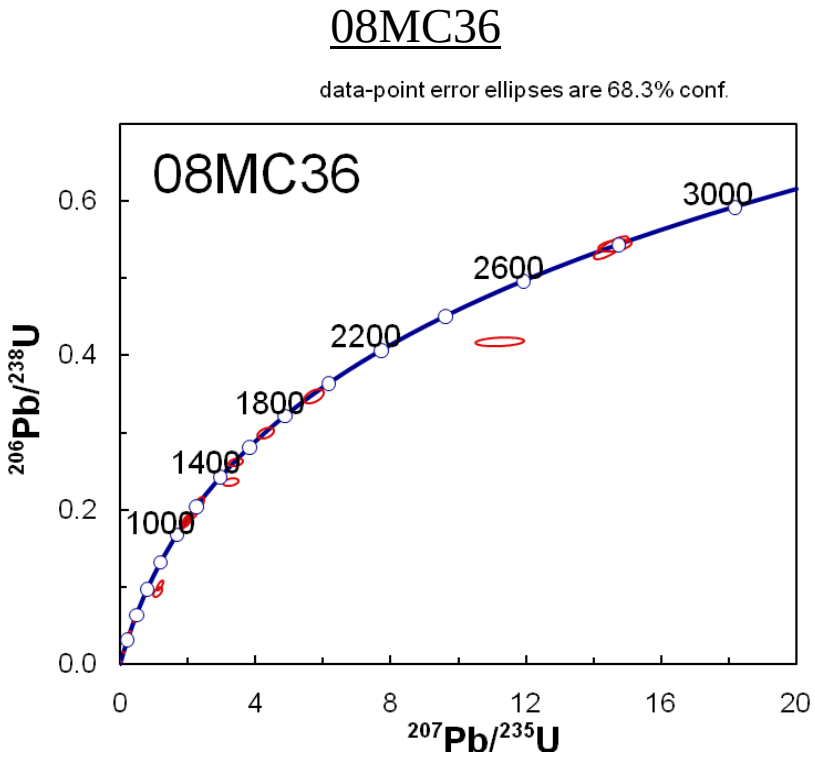

Concordia diagram of detrital zircons from the top of the Muddy Creek Formation from location F at Flat Top Mesa (Fig. 2). The plot shows that most of the detrital zircons are concordant and are part of a closed system.

Table of isotope ratios of detrital zircons from the top of the Muddy Creek Formation at location F at Flat Top Mesa (Fig. 2).

Isotope ratios for sample 08MC36 - Top of MCF at Flat Top Mesa										
Analysis	U (ppm)	^{206}Pb ^{204}Pb	U/Th	$^{206}Pb^*$ $^{207}Pb^*$	± (%)	$^{207}Pb^*$ $^{235}U^*$	± (%)	$^{206}Pb^*$ ^{238}U	± (%)	error corr.
08MC36-9	169	2458	1.3	20.8593	22.9	0.0192	24.3	0.0029	7.9	0.33
08MC36-18	123	2316	1.1	21.3992	15.8	0.0231	17.8	0.0036	8.2	0.46
08MC36-2	96	3154	1.3	19.7955	11.0	0.1073	11.3	0.0154	2.8	0.25
08MC36-21	1062	13872	1.7	20.9552	2.8	0.1290	2.8	0.0196	0.5	0.18
08MC36-17	146	2286	1.1	20.9132	13.8	0.1682	13.9	0.0255	1.6	0.11
08MC36-1	105	2972	1.2	21.1861	13.7	0.2515	13.8	0.0386	1.3	0.09
08MC36-19	147	4296	1.2	20.4061	11.6	0.2630	11.8	0.0389	1.9	0.16
08MC36-3	291	8406	9.1	20.4589	6.8	0.2809	6.9	0.0417	1.1	0.16
08MC36-12	457	23696	1.4	18.8290	4.0	0.4085	4.2	0.0558	1.3	0.30
08MC36-22L	548	184046	3.6	17.0988	2.3	0.7230	2.6	0.0897	1.3	0.49
08MC36-23L	552	48184	3.7	17.3005	1.8	0.7243	2.4	0.0909	1.7	0.69
08MC36-25	273	23680	2.3	11.6588	6.3	1.1033	7.6	0.0933	4.2	0.55
08MC36-23	115	7302	1.0	17.3754	5.3	0.7871	5.5	0.0992	1.4	0.25
08MC36-5	502	40428	3.0	12.0864	3.6	1.1686	5.4	0.1024	4.1	0.75
08MC36-26	132	14556	4.5	13.7598	2.1	1.7073	2.5	0.1704	1.4	0.55
08MC36-4	234	20122	5.7	13.3048	2.3	1.8847	3.2	0.1819	2.3	0.71
08MC36-24	64	8800	4.6	13.0063	3.2	1.9772	4.4	0.1865	2.9	0.67
08MC36-14	51	6442	2.6	12.9813	3.3	1.9838	3.7	0.1868	1.8	0.48
08MC36-11	197	23318	2.7	12.6788	1.6	2.1224	2.9	0.1952	2.4	0.82
08MC36-7	128	22410	2.8	12.4403	2.8	2.1734	3.9	0.1961	2.8	0.71
08MC36-6	154	25144	2.6	12.3742	3.5	2.3104	4.7	0.2074	3.1	0.67
08MC36-16	36	7080	3.1	10.6081	3.8	3.4032	4.0	0.2618	1.3	0.32
08MC36-8	258	3542	1.3	9.9641	4.2	3.2669	4.5	0.2361	1.4	0.32
08MC36-20	77	12248	0.9	9.6062	3.3	4.3010	3.6	0.2997	1.6	0.43
08MC36-10	81	24120	2.0	8.3673	3.0	5.7184	3.5	0.3470	1.8	0.51
08MC36-22	346	2296	5.6	5.1251	4.1	11.2269	4.2	0.4173	0.9	0.22
08MC36-13	67	25970	1.2	5.1245	1.3	14.5195	2.3	0.5396	1.8	0.81
08MC36-15	50	17122	0.9	5.1098	2.0	14.6401	2.2	0.5426	0.9	0.41

Table of apparent ages (Ma) of detrital zircons from the top of the Muddy Creek Formation at location F at Flat Top Mesa (Fig. 2).

Apparent ages (Ma) for sample 08MC36 - Top of MCF at Flat Top Mesa								
Analysis	$^{206}Pb^*$ $^{238}U^*$	± (Ma)	$^{207}Pb^*$ ^{235}U	± (Ma)	$^{206}Pb^*$ $^{207}Pb^*$	± (Ma)	Best age (Ma)	± (Ma)
08MC36-9	18.7	1.5	19.3	4.6	96.3	549.0	18.7	1.5
08MC36-18	23.1	1.9	23.2	4.1	35.5	380.4	23.1	1.9
08MC36-2	98.5	2.7	103.5	11.2	218.8	255.0	98.5	2.7

Apparent ages (Ma) for sample 08MC36 - Top of MCF at Flat Top Mesa								
Analysis	$^{206}Pb^*$	±	$^{207}Pb^*$	±	$^{206}Pb^*$	±	Best age	±
	$^{238}U^*$	(Ma)	^{235}U	(Ma)	$^{207}Pb^*$	(Ma)	(Ma)	(Ma)
08MC36-21	125.1	0.6	123.2	3.3	85.4	65.5	125.1	0.6
08MC36-17	162.4	2.5	157.8	20.3	90.2	328.0	162.4	2.5
08MC36-1	244.4	3.1	227.8	28.2	59.4	328.8	244.4	3.1
08MC36-19	246.2	4.5	237.1	24.9	148.0	273.8	246.2	4.5
08MC36-3	263.3	2.8	251.4	15.3	142.0	159.3	263.3	2.8
08MC36-12	350.0	4.3	347.8	12.4	333.5	90.8	350.0	4.3
08MC36-22L	553.5	6.9	552.4	11.2	547.9	50.0	553.5	6.9
08MC36-23L	560.7	9.0	553.2	10.4	522.2	38.6	560.7	9.0
08MC36-25	575.0	22.9	754.9	40.4	1333.0	122.4	575.0	22.9
08MC36-23	609.7	8.0	589.5	24.7	512.7	117.4	609.7	8.0
08MC36-5	628.7	24.5	786.0	29.8	1263.0	70.2	628.7	24.5
08MC36-26	1014.2	13.1	1011.3	16.2	1004.9	42.7	1004.9	42.7
08MC36-4	1077.1	22.8	1075.7	21.4	1072.8	45.6	1072.8	45.6
08MC36-24	1102.5	29.7	1107.8	29.4	1118.2	64.6	1118.2	64.6
08MC36-14	1103.9	18.2	1110.0	25.3	1122.0	65.6	1122.0	65.6
08MC36-11	1149.3	24.8	1156.1	19.8	1168.9	32.1	1168.9	32.1
08MC36-7	1154.3	29.1	1172.6	27.1	1206.4	54.3	1206.4	54.3
08MC36-6	1214.7	34.7	1215.5	33.2	1216.9	68.5	1216.9	68.5
08MC36-16	1499.2	17.0	1505.1	31.4	1513.5	71.7	1513.5	71.7
08MC36-8	1366.3	17.4	1473.2	34.7	1630.7	78.6	1630.7	78.6
08MC36-20	1689.6	23.2	1693.6	29.7	1698.4	59.9	1698.4	59.9
08MC36-10	1920.4	29.2	1934.2	30.1	1948.9	53.6	1948.9	53.6
08MC36-22	2248.3	17.8	2542.1	39.1	2785.8	66.9	2785.8	66.9
08MC36-13	2781.9	41.6	2784.3	21.5	2786.0	21.6	2786.0	21.6
08MC36-15	2794.2	20.6	2792.1	21.1	2790.7	33.1	2790.7	33.1

08MC11

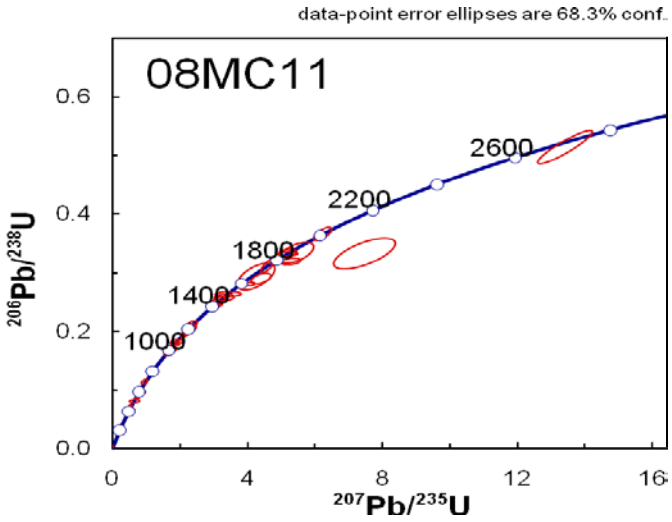

Concordia diagram of detrital zircons from the base of the Muddy Creek Formation from location H in the Beaver Dam Wash (Fig. 2). It shows that most of the detrital zircons are concordant and are part of a closed system. There are a few detrital zircons that are discordant.

Table of isotope ratios of detrital zircons from the base of the Muddy Creek Formation in the Beaver Dam Wash.

Isotope ratios for sample 08MC11 - Bottom of MCF at in Beaver Dam Wash										
Analysis	U	^{206}Pb	U/Th	^{206}Pb*	±	^{207}Pb*	±	^{206}Pb*	±	error
	(ppm)	^{204}Pb		^{207}Pb*	(%)	^{235}U*	(%)	^{238}U	(%)	corr.
08MC11-30	216	3024	1.4	18.6504	15.0	0.0127	27.9	0.0017	23.5	0.84
08MC11-35	117	2234	1.4	19.2376	13.7	0.0236	14.6	0.0033	4.9	0.34
08MC11-15	505	3090	1.3	20.2259	9.2	0.0257	9.7	0.0038	3.3	0.33
08MC11-39	141	3074	1.1	18.2187	10.1	0.2790	11.5	0.0369	5.7	0.49
08MC11-10	597	15998	3.0	18.5017	3.8	0.4211	3.9	0.0565	0.9	0.22
08MC11-26	159	24376	2.5	19.2121	6.7	0.4653	7.3	0.0648	3.1	0.42
08MC11-1	215	8696	2.0	17.5625	14.2	0.5281	14.2	0.0673	1.3	0.09
08MC11-9	473	13760	1.4	18.3512	4.2	0.5209	4.4	0.0693	1.4	0.31
08MC11-12	780	3950	9.9	18.7164	6.5	0.5328	6.6	0.0723	1.2	0.19
08MC11-38	139	4800	0.9	17.2060	14.9	0.6548	15.1	0.0817	2.4	0.16
08MC11-34	98	3136	1.9	15.9666	5.0	0.7509	5.2	0.0870	1.2	0.24
08MC11-20	198	19694	4.6	15.2862	8.8	0.8724	9.0	0.0967	1.5	0.17
08MC11-4	123	19686	1.3	16.4150	5.6	0.9578	6.3	0.1140	2.8	0.44
08MC11-25	283	30432	2.7	13.8359	1.8	1.6780	2.3	0.1684	1.5	0.63
08MC11-5	251	28106	86.8	13.7050	4.3	1.6644	5.0	0.1654	2.7	0.53
08MC11-6	172	30952	2.8	13.5499	4.3	1.8509	4.6	0.1819	1.7	0.36

Isotope ratios for sample 08MC11 - Bottom of MCF at in Beaver Dam Wash (Continued)										
Analysis	^{238}U (ppm)	^{206}Pb ^{204}Pb	U/Th	$^{206}Pb^*$ $^{207}Pb^*$	± (%)	$^{207}Pb^*$ $^{235}U^*$	± (%)	$^{206}Pb^*$ ^{238}U	± (%)	error corr.
08MC11-14	280	32186	2.9	13.5479	2.7	1.7451	3.1	0.1715	1.5	0.49
08MC11-7	333	40510	1.9	13.4663	2.6	1.8469	2.7	0.1804	0.6	0.22
08MC11-16	277	26298	3.0	13.1570	4.6	1.7728	4.9	0.1692	1.8	0.37
08MC11-31	57	7098	1.0	12.6238	2.6	1.9807	3.2	0.1813	1.8	0.56
08MC11-28	115	32562	3.2	12.5784	2.5	2.1929	4.7	0.2001	3.9	0.84
08MC11-24	89	12352	1.3	12.4155	3.5	2.3686	3.8	0.2133	1.6	0.41
08MC11-19	235	36496	9.4	12.2005	4.2	2.2941	5.2	0.2030	3.1	0.59
08MC11-36	236	36906	3.9	11.2057	3.8	2.9903	4.0	0.2430	1.3	0.32
08MC11-29	77	46256	2.6	11.0576	3.4	3.1508	3.9	0.2527	1.9	0.48
08MC11-32	322	25784	1.6	10.9742	3.8	3.0799	3.9	0.2451	0.6	0.15
08MC11-23	181	30802	1.6	10.7751	5.9	3.3011	6.0	0.2580	1.3	0.21
08MC11-3	89	28568	1.4	10.5909	7.3	3.4324	7.3	0.2637	1.0	0.13
08MC11-40	479	6388	2.0	9.5306	7.2	4.2524	8.9	0.2939	5.2	0.58
08MC11-11	247	38018	5.8	9.5210	2.2	4.0707	2.2	0.2811	0.6	0.28
08MC11-27	129	77282	5.5	9.3448	1.9	4.6154	3.1	0.3128	2.5	0.79
08MC11-17	224	21880	1.2	9.1021	3.7	4.4002	4.2	0.2905	2.1	0.49
08MC11-2	207	79454	2.8	8.8731	3.3	5.1894	3.5	0.3340	1.3	0.36
08MC11-18	611	94128	1.7	8.7926	3.7	5.2081	3.8	0.3321	0.9	0.23
08MC11-8	91	18846	1.5	8.4425	5.1	5.4543	6.2	0.3340	3.5	0.56
08MC11-37	58	9698	2.5	8.3198	3.5	5.2936	3.7	0.3194	1.2	0.33
08MC11-13	136	34360	3.2	8.1242	2.0	6.2228	2.9	0.3667	2.1	0.71
08MC11-33	402	64078	2.7	6.1490	6.1	7.4658	8.1	0.3330	5.3	0.66
08MC11-21	125	35476	1.6	5.2914	1.6	13.4027	4.0	0.5144	3.7	0.91

Table of apparent ages (Ma) of detrital zircons from the base of the Muddy Creek Formation from location H in the Beaver Dam Wash (Fig. 2).

Apparent ages (Ma) for sample 08MC11 Bottom of MCF in Beaver Dam Wash								
Analysis	$^{206}Pb^*$ $^{238}U^*$	± (Ma)	$^{207}Pb^*$ ^{235}U	± (Ma)	$^{206}Pb^*$ $^{207}Pb^*$	± (Ma)	Best age (Ma)	± (Ma)
08MC11-30	11.0	2.6	12.8	3.5	355.0	340.7	11.0	2.6
08MC11-35	21.1	1.0	23.6	3.4	284.6	315.7	21.1	1.0
08MC11-15	24.3	0.8	25.8	2.5	168.8	214.5	24.3	0.8
08MC11-39	233.4	13.0	249.9	25.6	407.7	225.6	233.4	13.0
08MC11-10	354.3	2.9	356.8	11.7	373.1	85.3	354.3	2.9
08MC11-26	405.0	12.0	387.9	23.7	287.6	152.7	405.0	12.0

Apparent ages (Ma) for sample 08MC11 Bottom of MCF in Beaver Dam Wash (Continued)								
Analysis	$^{206}Pb^*$	±	$^{207}Pb^*$	±	$^{206}Pb^*$	±	Best age	±
	$^{238}U^*$	(Ma)	^{235}U	(Ma)	$^{207}Pb^*$	(Ma)	(Ma)	(Ma)
08MC11-1	419.7	5.1	430.6	50.0	489.2	314.4	419.7	5.1
08MC11-9	432.1	5.6	425.7	15.3	391.4	93.9	432.1	5.6
08MC11-12	450.1	5.4	433.7	23.4	347.0	147.5	450.1	5.4
08MC11-38	506.3	11.4	511.4	60.7	534.2	327.8	506.3	11.4
08MC11-34	537.5	6.4	568.7	22.6	695.7	107.6	537.5	6.4
08MC11-20	595.2	8.5	636.9	42.4	787.8	185.9	595.2	8.5
08MC11-4	696.1	18.3	682.1	31.2	636.4	121.5	696.1	18.3
08MC11-25	1003.2	13.5	1000.2	14.7	993.7	36.6	993.7	36.6
08MC11-5	986.9	24.4	995.1	31.9	1013.0	86.2	1013.0	86.2
08MC11-6	1077.3	16.7	1063.8	30.5	1036.0	87.1	1036.0	87.1
08MC11-14	1020.2	14.3	1025.4	20.2	1036.3	55.2	1036.3	55.2
08MC11-7	1069.0	5.7	1062.3	17.5	1048.5	52.2	1048.5	52.2
08MC11-16	1007.5	16.8	1035.6	32.0	1095.2	92.0	1095.2	92.0
08MC11-31	1074.3	17.8	1108.9	21.5	1177.5	52.1	1177.5	52.1
08MC11-28	1175.6	42.2	1178.8	32.6	1184.6	50.0	1184.6	50.0
08MC11-24	1246.3	17.8	1233.2	27.2	1210.3	68.2	1210.3	68.2
08MC11-19	1191.4	33.5	1210.5	36.8	1244.6	82.1	1244.6	82.1
08MC11-36	1402.4	16.1	1405.2	30.5	1409.3	72.8	1409.3	72.8
08MC11-29	1452.3	24.2	1445.2	29.8	1434.7	64.5	1434.7	64.5
08MC11-32	1413.4	7.5	1427.7	29.7	1449.2	72.9	1449.2	72.9
08MC11-23	1479.5	17.1	1481.3	47.2	1483.9	112.1	1483.9	112.1
08MC11-3	1508.5	13.0	1511.9	57.6	1516.5	137.0	1516.5	137.0
08MC11-40	1661.2	76.0	1684.2	73.2	1713.0	132.8	1713.0	132.8
08MC11-11	1596.9	8.8	1648.5	18.3	1714.8	39.7	1714.8	39.7
08MC11-27	1754.5	37.9	1752.1	26.0	1749.1	34.8	1749.1	34.8
08MC11-17	1643.9	30.5	1712.4	35.2	1797.1	67.2	1797.1	67.2
08MC11-2	1857.5	20.5	1850.9	30.1	1843.4	59.7	1843.4	59.7
08MC11-18	1848.7	13.8	1853.9	32.0	1859.9	65.9	1859.9	65.9
08MC11-8	1857.6	55.8	1893.4	53.0	1932.9	91.6	1932.9	91.6
08MC11-37	1786.9	19.2	1867.8	31.8	1959.1	62.6	1959.1	62.6
08MC11-13	2013.7	35.6	2007.7	25.3	2001.5	36.1	2001.5	36.1
08MC11-33	1852.7	85.7	2168.9	72.4	2483.2	102.4	2483.2	102.4
08MC11-21	2675.2	79.9	2708.4	37.7	2733.3	26.5	2733.3	26.5

08MC18

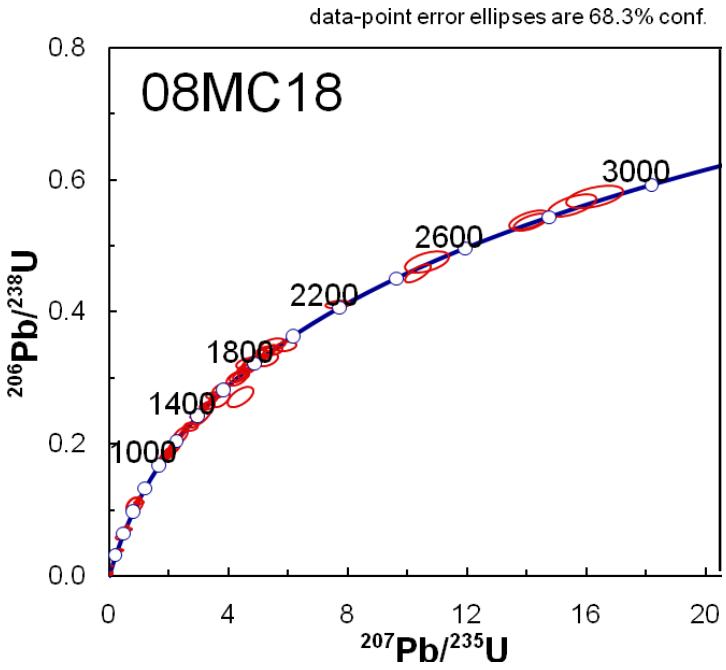

Concordia diagram of detrital zircons from the top of the Muddy Creek Formation at location H in the Beaver Dam Wash (Fig. 2). This plot shows that almost all the detrital zircons are concordant, while a few detrital zircons may be discordant.

Table of isotope ratios of detrital zircons from the top of the Muddy Creek Formation at location H in the Beaver Dam Wash (Fig. 2).

Isotope ratios for sample 08MC18 - Top of MCF in Beaver Dam Wash										
Analysis	U (ppm)	^{206}Pb / ^{204}Pb	U/Th	$^{206}Pb^*$ / $^{207}Pb^*$	± (%)	$^{207}Pb^*$ / $^{235}U^*$	± (%)	$^{206}Pb^*$ / ^{238}U	± (%)	error corr.
08MC18-36	92	312	1.6	8.0745	81.0	0.0289	83.2	0.0017	18.8	0.23
08MC18-78	102	2212	1.5	18.9399	38.9	0.0135	48.9	0.0019	29.7	0.61
08MC18-19	553	708	2.1	7.8151	62.8	0.0352	63.2	0.0020	6.5	0.10
08MC18-94	125	2336	1.9	23.2307	28.6	0.0124	30.8	0.0021	11.4	0.37
08MC18-52	1113	1770	1.8	19.2630	12.0	0.0154	12.3	0.0022	2.8	0.23
08MC18-31	1831	2278	1.5	18.4994	11.4	0.0167	11.6	0.0022	1.8	0.16
08MC18-68	1142	1392	1.7	18.2363	17.9	0.0172	18.5	0.0023	4.6	0.25
08MC18-53	516	2592	2.6	20.4845	37.7	0.0160	38.7	0.0024	8.8	0.23
08MC18-54	1394	830	1.5	15.5297	18.6	0.0212	18.6	0.0024	1.5	0.08
08MC18-66	1288	1314	1.6	21.4319	19.9	0.0156	19.9	0.0024	1.0	0.05
08MC18-64	271	454	1.3	13.4178	58.7	0.0257	59.6	0.0025	10.3	0.17
08MC18-89	1749	8448	1.2	25.4187	22.9	0.0143	22.9	0.0026	1.8	0.08
08MC18-91	2199	2388	1.0	18.0735	17.0	0.0206	17.1	0.0027	1.8	0.11

Isotope ratios for sample 08MC18 - Top of MCF in Beaver Dam Wash (Continued)										
Analysis	U	^{206}Pb	U/Th	$^{206}Pb^*$	±	$^{207}Pb^*$	±	$^{206}Pb^*$	±	error
	(ppm)	^{204}Pb		$^{207}Pb^*$	(%)	$^{235}U^*$	(%)	^{238}U	(%)	corr.
08MC18-56	151	510	3.2	15.2136	116.4	0.0256	117.5	0.0028	16.0	0.14
08MC18-34	548	1084	1.3	18.8028	22.9	0.0217	23.4	0.0030	4.8	0.20
08MC18-8	742	6254	0.7	20.6937	17.8	0.0200	19.5	0.0030	7.9	0.41
08MC18-47	383	926	1.7	20.8435	48.7	0.0212	49.5	0.0032	9.0	0.18
08MC18-100	600	1630	1.0	18.9046	34.8	0.0234	34.9	0.0032	2.3	0.07
08MC18-48	180	2506	0.9	17.7434	16.6	0.0250	21.6	0.0032	13.9	0.64
08MC18-14	117	2600	1.9	15.5892	28.0	0.0286	30.2	0.0032	11.4	0.38
08MC18-69	716	1558	2.3	17.0455	23.7	0.0274	23.7	0.0034	0.6	0.03
08MC18-59	161	2916	1.3	20.7020	45.9	0.0226	46.3	0.0034	6.1	0.13
08MC18-7	267	2756	0.9	14.1496	17.7	0.0337	22.1	0.0035	13.3	0.60
08MC18-16	108	274	1.2	8.3151	58.0	0.0606	58.1	0.0037	3.6	0.06
08MC18-70	293	2726	0.9	18.3844	30.2	0.0277	32.7	0.0037	12.5	0.38
08MC18-63	115	560	1.0	8.6819	46.3	0.0660	52.8	0.0042	25.4	0.48
08MC18-61	382	1100	1.2	25.0791	35.6	0.0236	35.6	0.0043	1.3	0.04
08MC18-3	556	7010	2.2	21.9535	6.1	0.0975	6.6	0.0155	2.4	0.37
08MC18-95	458	10746	2.1	20.4338	6.7	0.1978	6.9	0.0293	1.8	0.27
08MC18-93	177	6272	2.8	15.3441	21.6	0.3485	21.7	0.0388	2.0	0.09
08MC18-84	117	5130	2.7	16.9091	6.1	0.3167	6.8	0.0388	3.0	0.45
08MC18-23	217	63450	3.1	23.9764	25.2	0.3332	25.5	0.0579	3.9	0.15
08MC18-74	110	8604	3.6	17.1752	24.2	0.5666	24.3	0.0706	2.1	0.09
08MC18-2	158	4924	1.5	17.8734	6.6	0.5495	6.9	0.0712	1.9	0.28
08MC18-45	508	27950	1.5	18.4031	4.0	0.5435	4.9	0.0725	2.8	0.57
08MC18-96	275	15938	1.4	16.8878	4.4	0.6183	4.5	0.0757	1.1	0.25
08MC18-25	240	59312	2.8	17.2420	4.2	0.7715	4.3	0.0965	0.9	0.22
08MC18-11	105	5512	2.2	18.3269	10.7	0.7562	10.9	0.1005	2.1	0.20
08MC18-22	120	46308	3.8	18.3004	17.5	0.8000	19.1	0.1062	7.7	0.40
08MC18-71	40	5194	1.9	17.4490	19.4	0.8488	20.5	0.1074	6.5	0.32
08MC18-44	92	6694	2.5	15.3390	9.9	0.9976	10.0	0.1110	1.6	0.16
08MC18-21	276	23794	2.7	16.1151	3.2	0.9819	3.2	0.1148	0.5	0.16
08MC18-24	164	57248	7.1	16.3572	4.2	0.9788	5.0	0.1161	2.7	0.54
08MC18-20	192	18130	3.4	13.5957	3.8	1.8109	4.0	0.1786	1.4	0.33
08MC18-41	133	17440	1.8	13.5103	3.4	1.8857	4.0	0.1848	2.1	0.52
08MC18-58	38	5072	1.1	13.4978	3.1	1.8097	3.8	0.1772	2.2	0.58
08MC18-88	200	45036	12.6	13.3656	5.1	1.8508	6.7	0.1794	4.3	0.64
08MC18-30	346	84630	3.4	13.3582	3.7	1.8713	4.4	0.1813	2.3	0.53
08MC18-4	173	21312	1.4	13.3099	2.9	1.8831	3.1	0.1818	1.2	0.37
08MC18-40	133	20234	4.1	13.2211	4.3	1.9243	4.7	0.1845	1.8	0.39

Isotope ratios for sample 08MC18 - Top of MCF in Beaver Dam Wash (Continued)										
Analysis	U	^{206}Pb	U/Th	$^{206}Pb^*$	±	$^{207}Pb^*$	±	$^{206}Pb^*$	±	error
	(ppm)	^{204}Pb		$^{207}Pb^*$	(%)	$^{235}U^*$	(%)	^{238}U	(%)	corr.
08MC18-27	35	5242	2.2	13.1942	3.7	1.8638	4.0	0.1784	1.4	0.36
08MC18-10	95	61370	2.4	13.1819	4.6	1.8882	4.9	0.1805	1.6	0.33
08MC18-57	362	49102	4.3	13.0625	3.9	2.0255	4.0	0.1919	0.9	0.23
08MC18-99	50	9700	2.2	12.8898	3.6	1.9981	4.4	0.1868	2.6	0.59
08MC18-77	39	6838	2.1	12.6750	3.4	2.1139	3.9	0.1943	1.9	0.50
08MC18-39	75	7964	1.1	12.6512	3.5	2.1648	4.3	0.1986	2.6	0.59
08MC18-85	302	40974	4.6	12.5725	3.9	1.9958	4.1	0.1820	1.1	0.26
08MC18-42	287	49150	4.4	12.5417	2.1	2.2721	3.2	0.2067	2.4	0.74
08MC18-1	37	4534	3.0	12.3912	3.3	2.2043	4.8	0.1981	3.4	0.71
08MC18-26	143	30356	4.4	12.3474	4.9	2.1801	5.8	0.1952	3.2	0.55
08MC18-76	57	11712	3.7	12.2200	5.6	2.3932	6.8	0.2121	3.8	0.56
08MC18-18	1111	116950	21.9	12.1814	1.7	2.4211	2.8	0.2139	2.3	0.81
08MC18-97	165	24360	1.6	11.5126	3.6	2.8800	3.6	0.2405	0.5	0.14
08MC18-51	66	15744	3.1	11.4761	5.5	2.7485	5.6	0.2288	1.3	0.23
08MC18-65	68	11364	0.9	11.4637	5.7	2.7048	5.9	0.2249	1.4	0.23
08MC18-72	276	42020	2.6	10.9842	2.1	3.1972	2.2	0.2547	0.9	0.40
08MC18-83	142	34634	3.4	10.8985	2.3	3.2789	2.7	0.2592	1.4	0.51
08MC18-9	58	81418	0.7	10.8087	5.0	3.2882	5.1	0.2578	1.3	0.24
08MC18-87	250	76580	3.6	10.7224	5.0	3.5216	5.1	0.2739	1.2	0.24
08MC18-98	48	9788	0.5	10.6603	4.0	3.2154	6.4	0.2486	5.0	0.79
08MC18-81	214	33946	2.4	10.5941	2.4	3.4942	2.8	0.2685	1.5	0.53
08MC18-49	110	13720	0.8	10.3873	4.4	3.7525	4.9	0.2827	2.2	0.46
08MC18-60	176	2816	3.7	9.7998	4.1	3.7606	5.0	0.2673	2.9	0.57
08MC18-35	149	23306	0.6	9.6634	3.5	4.3093	3.9	0.3020	1.9	0.48
08MC18-5	63	11642	1.3	9.6169	4.7	4.2877	5.3	0.2991	2.4	0.44
08MC18-37	161	42976	4.8	9.5394	3.1	4.5120	3.4	0.3122	1.4	0.42
08MC18-32	95	25772	1.4	9.5029	5.5	4.6618	5.9	0.3213	1.9	0.32
08MC18-12	83	113354	0.7	9.4699	3.8	4.4052	4.1	0.3026	1.5	0.36
08MC18-6	94	288776	2.5	9.3791	2.3	4.5740	3.3	0.3111	2.4	0.72
08MC18-15	177	97180	1.7	9.2917	3.8	4.7572	4.8	0.3206	2.9	0.61
08MC18-17	210	38114	3.1	9.2357	3.7	4.8003	3.9	0.3215	1.5	0.37
08MC18-82	185	37886	4.6	8.9169	1.6	5.0779	2.5	0.3284	1.8	0.74
08MC18-38	194	43190	1.5	8.9066	3.2	5.2285	3.5	0.3377	1.3	0.39
08MC18-80	89	24504	1.2	8.7707	4.6	5.5093	5.0	0.3505	1.9	0.39
08MC18-13	306	305146	1.3	8.7638	5.1	5.3781	5.3	0.3418	1.4	0.27
08MC18-50	276	52642	2.8	8.7518	2.1	5.3459	2.9	0.3393	2.0	0.69
08MC18-90	209	130622	6.1	8.5125	5.1	4.3977	6.4	0.2715	3.8	0.59

Isotope ratios for sample 08MC18 - Top of MCF in Beaver Dam Wash (Continued)										
Analysis	U	^{206}Pb	U/Th	$^{206}Pb^*$	±	$^{207}Pb^*$	±	$^{206}Pb^*$	±	error
	(ppm)	^{204}Pb		$^{207}Pb^*$	(%)	$^{235}U^*$	(%)	^{238}U	(%)	corr.
08MC18-73	301	59862	4.2	8.4942	3.6	5.3187	4.1	0.3277	1.9	0.47
08MC18-92	126	21724	0.6	8.1003	3.9	5.9185	4.1	0.3477	1.3	0.31
08MC18-86	79	37566	1.9	7.4007	3.4	7.6701	3.5	0.4117	1.0	0.28
08MC18-28	57	50038	1.4	6.1581	4.0	10.6588	4.5	0.4761	2.2	0.49
08MC18-79	228	74728	6.5	6.1099	1.9	10.3637	2.7	0.4592	2.0	0.73
08MC18-29	26	21756	1.0	5.2755	2.5	14.0891	3.1	0.5391	1.8	0.57
08MC18-43	82	30426	2.9	5.2297	2.1	14.1418	2.7	0.5364	1.7	0.62
08MC18-75	68	20636	2.4	4.9893	2.8	15.5145	3.5	0.5614	2.1	0.60
08MC18-33	82	37782	1.5	4.8598	3.4	16.2825	3.9	0.5739	1.9	0.49

Table of apparent ages (Ma) of detrital zircons from the top of the Muddy Creek Formation from location H in the Beaver Dam Wash (Fig. 2).

Apparent ages (Ma) for sample 08MC18 - Top of MCF in Beaver Dam Wash								
Analysis	$^{206}Pb^*$	±	$^{207}Pb^*$	±	$^{206}Pb^*$	±	Best age	±
	$^{238}U^*$	(Ma)	^{235}U	(Ma)	$^{207}Pb^*$	(Ma)	(Ma)	(Ma)
08MC18-36	10.9	2.0	28.9	23.7	2012.3	440.4	10.9	2.0
08MC18-78	11.9	3.5	13.6	6.6	320.1	916.1	11.9	3.5
08MC18-19	12.8	0.8	35.1	21.8	2070.1	1259.7	12.8	0.8
08MC18-94	13.5	1.5	12.5	3.8	-164.9	723.7	13.5	1.5
08MC18-52	13.8	0.4	15.5	1.9	281.6	275.4	13.8	0.4
08MC18-31	14.4	0.3	16.8	1.9	373.4	258.0	14.4	0.3
08MC18-68	14.7	0.7	17.4	3.2	405.5	403.9	14.7	0.7
08MC18-53	15.4	1.3	16.2	6.2	139.0	914.7	15.4	1.3
08MC18-54	15.4	0.2	21.3	3.9	754.5	395.2	15.4	0.2
08MC18-66	15.6	0.2	15.7	3.1	31.8	481.3	15.6	0.2
08MC18-64	16.1	1.7	25.7	15.1	1055.8	1305.3	16.1	1.7
08MC18-89	17.0	0.3	14.4	3.3	-394.1	601.6	17.0	0.3
08MC18-91	17.4	0.3	20.7	3.5	425.5	381.1	17.4	0.3
08MC18-56	18.2	2.9	25.7	29.8	797.8	560.5	18.2	2.9
08MC18-34	19.0	0.9	21.8	5.0	336.6	525.8	19.0	0.9
08MC18-8	19.3	1.5	20.1	3.9	115.1	423.4	19.3	1.5
08MC18-47	20.7	1.8	21.3	10.5	98.1	1219.8	20.7	1.8
08MC18-100	20.7	0.5	23.5	8.1	324.4	813.4	20.7	0.5
08MC18-48	20.7	2.9	25.0	5.3	466.5	369.4	20.7	2.9
08MC18-14	20.8	2.4	28.6	8.5	746.5	602.9	20.8	2.4

Apparent ages (Ma) for sample 08MC18 - Top of MCF in Beaver Dam Wash (Continued)								
Analysis	$^{206}Pb^*$	±	$^{207}Pb^*$	±	$^{206}Pb^*$	±	Best age	±
	$^{238}U^*$	(Ma)	^{235}U	(Ma)	$^{207}Pb^*$	(Ma)	(Ma)	(Ma)
08MC18-69	21.8	0.1	27.4	6.4	554.7	523.7	21.8	0.1
08MC18-59	21.8	1.3	22.7	10.4	114.2	1138.8	21.8	1.3
08MC18-7	22.3	2.9	33.7	7.3	948.0	364.5	22.3	2.9
08MC18-16	23.5	0.8	59.8	33.8	1960.1	1150.4	23.5	0.8
08MC18-70	23.7	3.0	27.7	8.9	387.4	692.8	23.7	3.0
08MC18-63	26.7	6.8	64.9	33.2	1882.7	887.0	26.7	6.8
08MC18-61	27.6	0.4	23.7	8.3	-359.1	946.0	27.6	0.4
08MC18-3	99.3	2.4	94.5	6.0	-26.1	149.0	99.3	2.4
08MC18-95	186.2	3.4	183.3	11.6	144.9	156.8	186.2	3.4
08MC18-93	245.3	4.9	303.6	56.9	779.9	458.7	245.3	4.9
08MC18-84	245.6	7.3	279.4	16.6	572.2	132.0	245.6	7.3
08MC18-23	363.1	13.9	292.0	64.9	-244.2	646.5	363.1	13.9
08MC18-74	439.6	8.8	455.8	89.5	538.2	537.1	439.6	8.8
08MC18-2	443.5	8.3	444.6	24.9	450.3	147.7	443.5	8.3
08MC18-45	451.5	12.1	440.7	17.5	385.1	90.7	451.5	12.1
08MC18-96	470.6	5.2	488.8	17.6	575.0	95.6	470.6	5.2
08MC18-25	593.7	5.3	580.6	19.0	529.7	92.1	593.7	5.3
08MC18-11	617.4	12.6	571.8	47.8	394.4	240.7	617.4	12.6
08MC18-22	650.5	47.6	596.8	86.4	397.7	394.7	650.5	47.6
08MC18-71	657.8	40.7	624.0	95.8	503.5	431.5	657.8	40.7
08MC18-44	678.4	10.6	702.6	50.8	780.6	208.0	678.4	10.6
08MC18-21	700.3	3.3	694.6	16.1	675.9	67.4	700.3	3.3
08MC18-24	708.2	18.2	693.0	25.3	644.0	91.0	708.2	18.2
08MC18-20	1059.1	13.2	1049.4	26.4	1029.2	77.0	1029.2	77.0
08MC18-41	1093.0	21.1	1076.1	26.6	1041.9	68.9	1041.9	68.9
08MC18-58	1051.4	21.7	1049.0	25.1	1043.8	62.7	1043.8	62.7
08MC18-88	1063.8	42.2	1063.7	44.2	1063.6	103.3	1063.6	103.3
08MC18-30	1074.0	23.1	1071.0	29.1	1064.7	74.8	1064.7	74.8
08MC18-4	1076.7	11.5	1075.1	20.9	1072.0	58.8	1072.0	58.8
08MC18-40	1091.6	18.2	1089.6	31.1	1085.5	86.1	1085.5	86.1
08MC18-27	1058.0	13.8	1068.3	26.1	1089.5	74.0	1089.5	74.0
08MC18-10	1069.8	15.8	1077.0	32.3	1091.4	92.0	1091.4	92.0
08MC18-57	1131.6	9.5	1124.1	27.0	1109.6	77.1	1109.6	77.1
08MC18-99	1104.0	26.2	1114.9	29.8	1136.1	71.0	1136.1	71.0
08MC18-77	1144.8	20.3	1153.3	26.8	1169.5	66.8	1169.5	66.8
08MC18-39	1168.0	27.2	1169.8	29.9	1173.2	68.7	1173.2	68.7

Apparent ages (Ma) for sample 08MC18 - Top of MCF in Beaver Dam Wash (Continued)								
Analysis	$^{206}Pb^*$	±	$^{207}Pb^*$	±	$^{206}Pb^*$	±	Best age	±
	$^{238}U^*$	(Ma)	^{235}U	(Ma)	$^{207}Pb^*$	(Ma)	(Ma)	(Ma)
08MC18-85	1077.8	10.4	1114.1	27.6	1185.6	77.9	1185.6	77.9
08MC18-42	1211.1	26.3	1203.7	22.6	1190.4	42.3	1190.4	42.3
08MC18-1	1165.1	36.0	1182.4	33.2	1214.2	65.8	1214.2	65.8
08MC18-26	1149.6	33.6	1174.7	40.7	1221.2	96.2	1221.2	96.2
08MC18-76	1240.0	42.4	1240.6	48.5	1241.5	110.4	1241.5	110.4
08MC18-18	1249.5	25.7	1248.9	20.1	1247.7	32.3	1247.7	32.3
08MC18-97	1389.2	6.2	1376.7	27.0	1357.4	68.5	1357.4	68.5
08MC18-51	1328.0	15.2	1341.7	41.9	1363.5	105.7	1363.5	105.7
08MC18-65	1307.6	16.1	1329.8	43.6	1365.6	110.2	1365.6	110.2
08MC18-72	1462.7	11.6	1456.5	17.4	1447.4	39.2	1447.4	39.2
08MC18-83	1485.6	18.2	1476.0	20.8	1462.3	43.7	1462.3	43.7
08MC18-9	1478.4	16.5	1478.3	40.1	1478.0	94.7	1478.0	94.7
08MC18-87	1560.4	16.8	1532.1	40.3	1493.2	93.7	1493.2	93.7
08MC18-98	1431.3	64.7	1460.9	49.7	1504.2	75.0	1504.2	75.0
08MC18-81	1533.1	20.1	1525.9	22.0	1515.9	44.7	1515.9	44.7
08MC18-49	1604.9	31.8	1582.6	39.5	1553.1	82.3	1553.1	82.3
08MC18-60	1527.0	38.9	1584.4	40.2	1661.6	76.1	1661.6	76.1
08MC18-35	1701.3	28.4	1695.1	32.5	1687.5	63.7	1687.5	63.7
08MC18-5	1686.6	34.9	1691.0	43.6	1696.4	87.4	1696.4	87.4
08MC18-37	1751.4	21.6	1733.2	28.2	1711.3	56.9	1711.3	56.9
08MC18-32	1796.1	29.8	1760.4	49.0	1718.3	101.9	1718.3	101.9
08MC18-12	1704.0	22.2	1713.3	33.7	1724.7	69.6	1724.7	69.6
08MC18-6	1746.3	36.9	1744.5	27.8	1742.4	42.3	1742.4	42.3
08MC18-15	1792.6	45.5	1777.4	40.0	1759.5	69.1	1759.5	69.1
08MC18-17	1797.3	22.9	1785.0	33.1	1770.6	66.9	1770.6	66.9
08MC18-82	1830.6	29.2	1832.4	20.9	1834.5	29.7	1834.5	29.7
08MC18-38	1875.8	21.8	1857.3	29.7	1836.6	58.2	1836.6	58.2
08MC18-80	1936.8	32.5	1902.0	43.3	1864.4	83.8	1864.4	83.8
08MC18-13	1895.5	23.5	1881.4	45.5	1865.8	92.5	1865.8	92.5
08MC18-50	1883.4	33.3	1876.2	25.2	1868.3	38.3	1868.3	38.3
08MC18-90	1548.5	51.9	1711.9	52.6	1918.1	91.9	1918.1	91.9
08MC18-73	1827.1	30.7	1871.9	35.0	1922.0	64.7	1922.0	64.7
08MC18-92	1923.6	21.5	1964.0	35.9	2006.7	69.8	2006.7	69.8
08MC18-86	2222.7	18.2	2193.1	31.4	2165.6	58.6	2165.6	58.6
08MC18-28	2510.0	45.7	2493.8	42.0	2480.7	66.7	2480.7	66.7
08MC18-79	2436.2	40.2	2467.8	25.2	2493.9	31.5	2493.9	31.5

Apparent ages (Ma) for sample 08MC18 - Top of MCF in Beaver Dam Wash (Continued)								
Analysis	$^{206}Pb^*$	±	$^{207}Pb^*$	±	$^{206}Pb^*$	±	Best age	±
	$^{238}U^*$	(Ma)	^{235}U	(Ma)	$^{207}Pb^*$	(Ma)	(Ma)	(Ma)
08MC18-29	2779.6	40.0	2755.7	29.2	2738.3	41.5	2738.3	41.5
08MC18-43	2768.3	37.4	2759.3	25.5	2752.6	34.8	2752.6	34.8
08MC18-75	2872.4	48.4	2847.4	33.3	2829.7	45.5	2829.7	45.5
08MC18-33	2923.8	45.4	2893.5	37.4	2872.5	55.3	2872.5	55.3

08MC09

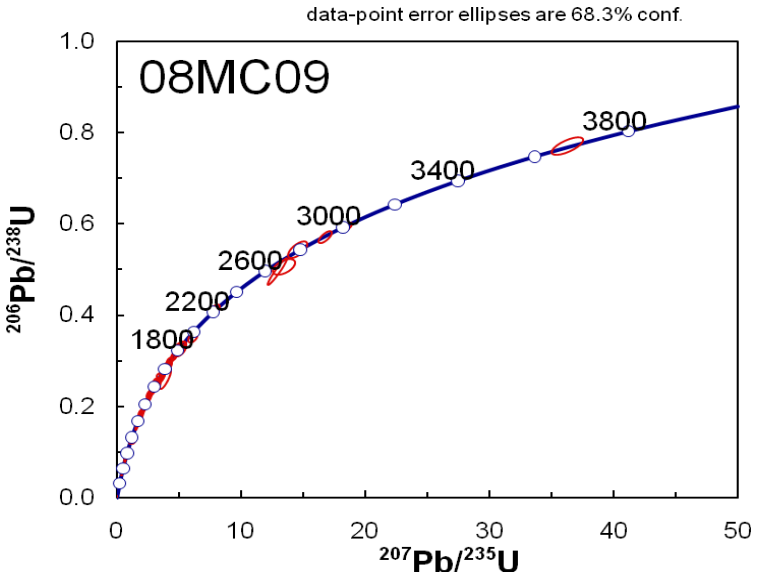

Concordia diagram of detrital zircons from the base of the inset Pliocene unit at location G at Littlefield, Arizona (Fig. 2). It shows that all of the detrital zircons are concordant.

Table of isotope ratios of detrital zircons from the base of the inset Pliocene unit from location G at Littlefield, Arizona (Fig. 2).

Isotope ratios for sample 08MC09 - Inset Pliocene unit at Littlefield, Arizona										
Analysis	U	^{206}Pb	U/Th	$^{206}Pb^*$	±	$^{207}Pb^*$	±	$^{206}Pb^*$	±	error
	(ppm)	^{204}Pb		$^{207}Pb^*$	(%)	$^{235}U^*$	(%)	^{238}U	(%)	corr.
08MC09-88	264	2502	1.0	17.8515	17.1	0.0210	17.4	0.0027	3.3	0.19
08MC09-78	144	2544	1.1	21.2255	8.2	0.0185	8.8	0.0028	3.2	0.36
08MC09-71	153	4266	1.3	19.4765	16.9	0.0255	19.5	0.0036	9.7	0.50
08MC09-3	467	8128	1.3	20.5142	7.5	0.1081	8.2	0.0161	3.5	0.42
08MC09-99	569	13008	1.1	21.0672	4.4	0.1753	5.1	0.0268	2.6	0.52
08MC09-18	456	9464	15.6	20.7487	5.9	0.1876	6.3	0.0282	2.3	0.36
08MC09-31	173	4146	1.3	21.0688	7.9	0.1877	8.3	0.0287	2.6	0.31

Isotope ratios for sample 08MC09 - Inset Pliocene unit at Littlefield, Arizona (Continued)										
Analysis	U	^{206}Pb	U/Th	$^{206}Pb^*$	±	$^{207}Pb^*$	±	$^{206}Pb^*$	±	error
	(ppm)	^{204}Pb		$^{207}Pb^*$	(%)	$^{235}U^*$	(%)	^{238}U	(%)	corr.
08MC09-58	445	14120	1.7	18.9408	6.6	0.3577	6.9	0.0491	2.0	0.29
08MC09-44	309	13378	3.9	18.4311	5.2	0.4241	5.9	0.0567	2.9	0.49
08MC09-63	43	3260	0.7	18.1955	3.5	0.4433	4.0	0.0585	2.0	0.49
08MC09-9	51	2948	1.7	17.4073	6.2	0.4767	6.3	0.0602	1.0	0.16
08MC09-92	553	2384	3.5	15.3763	9.6	0.5560	9.9	0.0620	2.4	0.24
08MC09-36	131	6230	1.2	18.2449	4.9	0.5070	5.2	0.0671	1.5	0.29
08MC09-26	149	8044	1.8	19.0229	5.1	0.4926	6.5	0.0680	3.9	0.61
08MC09-50	314	13146	2.6	17.6878	5.0	0.5321	5.4	0.0683	2.0	0.37
08MC09-94	115	4676	2.2	18.4442	12.0	0.5182	12.1	0.0693	1.5	0.12
08MC09-30	335	4426	1.9	16.8171	3.5	0.5720	5.2	0.0698	3.9	0.74
08MC09-79	396	44510	2.6	17.5139	3.2	0.5516	4.8	0.0701	3.5	0.73
08MC09-96	832	11890	9.6	16.8585	4.4	0.6352	5.4	0.0777	3.1	0.57
08MC09-46	101	4696	2.2	16.8340	8.6	0.6824	8.8	0.0833	2.0	0.22
08MC09-2	118	10026	1.0	17.1844	3.0	0.6986	3.6	0.0871	2.1	0.57
08MC09-6	108	10710	2.1	17.0024	3.3	0.7780	4.3	0.0959	2.8	0.64
08MC09-22	154	11952	1.5	16.6014	5.5	0.7995	5.8	0.0963	2.0	0.34
08MC09-76	207	33996	1.8	16.4561	3.7	0.8179	4.2	0.0976	2.0	0.48
08MC09-39	118	7364	1.3	16.7471	5.5	0.8066	5.7	0.0980	1.5	0.26
08MC09-42	235	19914	2.4	16.5356	3.2	0.8416	3.8	0.1009	2.1	0.55
08MC09-80	337	32128	1.6	16.5576	6.8	0.8458	7.1	0.1016	1.8	0.26
08MC09-93	195	9882	3.0	16.6284	6.6	0.8648	6.8	0.1043	1.7	0.24
08MC09-89	162	10202	1.8	15.8699	6.9	0.9170	7.4	0.1055	2.7	0.36
08MC09-95	188	15806	2.0	15.1294	5.6	1.1263	6.2	0.1236	2.6	0.41
08MC09-27	1052	5862	18.3	12.9839	6.8	1.3128	7.6	0.1236	3.5	0.46
08MC09-11	72	14252	1.9	13.8121	3.2	1.6876	3.8	0.1691	2.2	0.57
08MC09-45	29	3526	3.9	13.7087	2.6	1.6530	4.4	0.1643	3.5	0.81
08MC09-68	157	20382	2.8	13.6779	2.0	1.6480	3.9	0.1635	3.3	0.85
08MC09-20	137	18820	3.4	13.5244	1.1	1.8109	2.1	0.1776	1.8	0.84
08MC09-47	589	48002	2.0	13.4753	2.2	1.6926	2.8	0.1654	1.7	0.62
08MC09-66	208	35314	1.0	13.4529	2.7	1.5752	3.7	0.1537	2.4	0.66
08MC09-23	362	54348	3.9	13.3357	1.5	1.8180	2.8	0.1758	2.4	0.84
08MC09-67	73	9858	1.4	13.3289	2.8	1.8304	3.6	0.1769	2.2	0.62
08MC09-91	371	27480	1.7	13.2978	3.0	1.8966	3.4	0.1829	1.6	0.46
08MC09-65	266	28100	3.3	13.2822	2.0	1.8125	2.6	0.1746	1.6	0.63
08MC09-38	60	6852	1.2	13.2624	2.7	1.8796	3.5	0.1808	2.3	0.64
08MC09-60	261	28986	9.0	13.2530	2.9	1.9180	4.6	0.1844	3.5	0.78
08MC09-57	215	28712	3.7	13.2498	4.6	1.8641	5.7	0.1791	3.4	0.60
08MC09-75	35	5986	1.8	13.2402	3.4	1.8919	3.7	0.1817	1.5	0.40
08MC09-34	80	12666	3.8	13.2120	2.7	1.8950	2.8	0.1816	0.9	0.32
08MC09-14	21	4422	1.8	13.2114	1.9	1.9299	3.0	0.1849	2.3	0.77
08MC09-21	368	66622	5.1	13.1982	2.6	1.8632	3.2	0.1784	1.9	0.60
08MC09-64	213	10042	2.9	13.1905	3.9	1.6458	4.2	0.1574	1.5	0.37
08MC09-35	124	21012	137.9	13.1771	4.7	1.9221	5.3	0.1837	2.4	0.46
08MC09-28	72	10358	2.6	13.1666	3.7	1.8906	5.4	0.1805	4.0	0.73

Isotope ratios for sample 08MC09 - Inset Pliocene unit at Littlefield, Arizona (Continued)										
Analysis	U	^{206}Pb	U/Th	$^{206}Pb^*$	±	$^{207}Pb^*$	±	$^{206}Pb^*$	±	error
	(ppm)	^{204}Pb		$^{207}Pb^*$	(%)	$^{235}U^*$	(%)	^{238}U	(%)	corr.
08MC09-53	144	28260	3.2	13.1340	2.8	1.9135	3.4	0.1823	1.8	0.54
08MC09-4	33	5840	0.9	13.0320	3.2	1.8746	3.5	0.1772	1.4	0.39
08MC09-73	200	21894	2.4	13.0181	4.1	1.9919	4.6	0.1881	2.1	0.45
08MC09-97	374	49988	3.2	12.8642	1.7	2.0713	4.3	0.1932	4.0	0.92
08MC09-40	159	13544	2.7	12.4821	4.0	2.1983	5.1	0.1990	3.1	0.61
08MC09-41	132	16322	4.0	12.3940	2.4	2.1058	8.8	0.1893	8.4	0.96
08MC09-5	219	32294	5.2	11.9394	4.2	2.6006	4.9	0.2252	2.5	0.50
08MC09-8	134	23030	2.7	11.7865	1.5	2.6503	1.7	0.2266	1.0	0.56
08MC09-7	10	2684	0.5	11.7021	4.2	2.6754	5.9	0.2271	4.2	0.71
08MC09-17	14	2334	2.6	11.6466	3.8	2.7450	4.6	0.2319	2.6	0.57
08MC09-85	125	18334	2.3	11.4445	2.6	2.8785	3.9	0.2389	2.9	0.75
08MC09-70	93	13708	1.1	11.4324	1.0	2.9018	1.7	0.2406	1.3	0.79
08MC09-16	136	30540	2.9	11.0919	5.2	3.1476	5.8	0.2532	2.5	0.43
08MC09-62	322	53994	2.9	11.0875	2.7	2.9065	3.1	0.2337	1.5	0.49
08MC09-43	83	14462	2.2	11.0824	2.7	2.9865	3.6	0.2400	2.4	0.67
08MC09-56	170	29448	2.8	10.9423	2.3	3.1855	3.2	0.2528	2.2	0.68
08MC09-51	310	57764	2.8	10.9399	1.9	3.1770	2.7	0.2521	1.9	0.69
08MC09-83	30	6524	1.2	10.9079	3.9	3.1604	4.3	0.2500	1.9	0.44
08MC09-10	62	15870	1.7	10.9051	3.5	3.0928	4.1	0.2446	2.1	0.51
08MC09-98	394	63752	2.5	10.8199	4.1	3.4168	4.2	0.2681	1.3	0.30
08MC09-72	186	25068	1.5	10.7698	2.5	3.1339	3.4	0.2448	2.2	0.66
08MC09-87	195	29216	2.3	10.3980	2.6	3.6353	3.6	0.2741	2.5	0.69
08MC09-49	265	38886	3.7	10.0618	2.6	3.6275	3.7	0.2647	2.7	0.73
08MC09-1	60	13730	0.9	9.9983	4.1	3.9330	4.4	0.2852	1.7	0.39
08MC09-19	169	36704	2.4	9.9455	2.3	3.7602	3.5	0.2712	2.7	0.76
08MC09-24	80	18538	0.9	9.9441	2.3	3.7281	3.9	0.2689	3.2	0.82
08MC09-100	118	29274	1.9	9.7582	3.8	4.1221	4.1	0.2917	1.7	0.42
08MC09-32	283	51542	2.2	9.7239	3.3	4.2528	3.7	0.2999	1.6	0.44
08MC09-48	94	16940	1.2	9.5317	2.4	4.2057	3.2	0.2907	2.1	0.66
08MC09-77	110	24790	0.9	9.4373	2.2	4.3078	2.6	0.2948	1.3	0.53
08MC09-90	370	54604	7.7	9.3404	2.1	4.6861	3.8	0.3175	3.2	0.84
08MC09-74	188	30480	2.1	9.3352	3.1	4.5872	3.6	0.3106	1.8	0.51
08MC09-81	553	60090	2.9	9.2483	3.3	4.7619	3.4	0.3194	1.1	0.32
08MC09-59	256	6900	4.1	9.1928	4.1	3.9097	7.1	0.2607	5.8	0.82
08MC09-84	363	59416	3.7	9.0631	2.9	4.9826	3.5	0.3275	2.0	0.57
08MC09-86	38	11458	3.9	8.8743	6.1	5.0693	7.0	0.3263	3.3	0.48
08MC09-33	364	20766	4.3	8.8219	3.1	5.2608	3.2	0.3366	0.9	0.28
08MC09-54	157	35360	1.6	8.7162	1.8	5.3286	2.0	0.3369	0.9	0.47
08MC09-25	110	38274	1.7	8.6838	3.1	5.2849	3.5	0.3328	1.7	0.48
08MC09-69	69	20316	3.2	7.9351	3.7	6.1070	4.3	0.3515	2.1	0.50
08MC09-37	141	35322	2.4	7.2008	2.8	7.8741	3.4	0.4112	2.0	0.57
08MC09-12	18	9908	1.3	5.2967	1.2	12.8955	4.1	0.4954	3.9	0.96
08MC09-61	78	29528	2.3	5.1895	3.8	13.4388	4.4	0.5058	2.3	0.53
08MC09-52	238	83770	1.4	5.1434	2.5	14.5611	3.4	0.5432	2.2	0.66

Isotope ratios for sample 08MC09 - Inset Pliocene unit at Littlefield, Arizona (Continued)										
Analysis	U	^{206}Pb	U/Th	$^{206}Pb^*$	±	$^{207}Pb^*$	±	$^{206}Pb^*$	±	error
	(ppm)	^{204}Pb		$^{207}Pb^*$	(%)	$^{235}U^*$	(%)	^{238}U	(%)	corr.
08MC09-29	128	57132	1.7	4.6975	1.5	16.7654	2.2	0.5712	1.6	0.72
08MC09-55	39	24982	1.6	4.4024	0.9	18.5834	1.4	0.5934	1.0	0.75
08MC09-82	49	31534	1.0	2.9316	1.7	36.2881	2.3	0.7716	1.6	0.70

Table of apparent ages (Ma) of detrital zircons from the base of the inset Pliocene unit from location G at Littlefield, Arizona (Fig. 2).

Apparent ages (Ma) for sample 08MC09 - Inset Pliocene unit at Littlefield, Arizona								
Analysis	$^{206}Pb^*$	±	$^{207}Pb^*$	±	$^{206}Pb^*$	±	Best age	±
	$^{238}U^*$	(Ma)	^{235}U	(Ma)	$^{207}Pb^*$	(Ma)	(Ma)	(Ma)
08MC09-88	17.5	0.6	21.1	3.6	453.1	381.9	17.5	0.6
08MC09-78	18.3	0.6	18.6	1.6	54.9	196.5	18.3	0.6
08MC09-71	23.2	2.3	25.6	4.9	256.3	391.9	23.2	2.3
08MC09-3	102.8	3.5	104.2	8.1	135.6	175.4	102.8	3.5
08MC09-99	170.4	4.4	164.0	7.7	72.8	103.8	170.4	4.4
08MC09-18	179.5	4.0	174.6	10.1	108.9	139.1	179.5	4.0
08MC09-31	182.3	4.6	174.7	13.3	72.6	187.7	182.3	4.6
08MC09-58	309.2	6.0	310.5	18.4	320.0	149.5	309.2	6.0
08MC09-44	355.5	10.2	359.0	18.0	381.7	116.1	355.5	10.2
08MC09-63	366.5	7.1	372.6	12.6	410.5	78.5	366.5	7.1
08MC09-9	376.7	3.7	395.8	20.6	508.7	136.7	376.7	3.7
08MC09-92	387.8	9.0	448.9	35.8	775.5	201.9	387.8	9.0
08MC09-36	418.6	6.1	416.5	17.7	404.4	110.8	418.6	6.1
08MC09-26	423.9	16.2	406.7	21.7	310.2	117.2	423.9	16.2
08MC09-50	425.7	8.3	433.2	19.0	473.5	110.3	425.7	8.3
08MC09-94	432.0	6.2	423.9	42.1	380.1	271.6	432.0	6.2
08MC09-30	434.7	16.2	459.3	19.3	584.1	76.4	434.7	16.2
08MC09-79	436.5	14.8	446.0	17.2	495.3	71.2	436.5	14.8
08MC09-96	482.2	14.2	499.3	21.2	578.7	96.0	482.2	14.2
08MC09-46	515.9	9.8	528.2	36.2	581.9	186.3	515.9	9.8
08MC09-2	538.2	10.6	538.0	15.2	537.0	65.7	538.2	10.6
08MC09-6	590.5	15.6	584.3	19.2	560.2	72.7	590.5	15.6
08MC09-22	592.5	11.1	596.6	26.3	612.0	118.6	592.5	11.1
08MC09-76	600.4	11.6	606.9	19.3	631.0	79.8	600.4	11.6
08MC09-39	602.5	8.5	600.5	25.8	593.1	119.2	602.5	8.5
08MC09-42	619.9	12.5	620.1	17.8	620.6	68.9	619.9	12.5
08MC09-80	623.6	10.8	622.3	33.0	617.7	147.8	623.6	10.8
08MC09-93	639.5	10.2	632.7	32.2	608.5	143.6	639.5	10.2
08MC09-89	646.8	16.3	660.8	35.8	708.6	146.3	646.8	16.3
08MC09-95	751.2	18.2	766.0	33.4	809.4	118.3	751.2	18.2
08MC09-27	751.4	24.8	851.4	43.9	1121.6	135.1	751.4	24.8

Apparent ages (Ma) for sample 08MC09 - Inset Pliocene unit at Littlefield, Arizona (Continued)								
Analysis	$^{206}Pb^*$	±	$^{207}Pb^*$	±	$^{206}Pb^*$	±	Best age	±
	$^{238}U^*$	(Ma)	^{235}U	(Ma)	$^{207}Pb^*$	(Ma)	(Ma)	(Ma)
08MC09-11	1006.9	20.3	1003.8	24.5	997.2	64.4	997.2	64.4
08MC09-45	980.9	32.0	990.7	27.6	1012.4	52.3	1012.4	52.3
08MC09-68	976.1	29.9	988.8	24.4	1017.0	40.9	1017.0	40.9
08MC09-20	1054.0	17.2	1049.4	13.7	1039.8	22.8	1039.8	22.8
08MC09-47	986.9	15.8	1005.8	17.7	1047.2	43.8	1047.2	43.8
08MC09-66	921.6	20.9	960.5	22.7	1050.5	55.1	1050.5	55.1
08MC09-23	1044.2	23.1	1052.0	18.6	1068.1	30.6	1068.1	30.6
08MC09-67	1050.3	21.4	1056.4	23.4	1069.2	56.3	1069.2	56.3
08MC09-91	1082.9	15.7	1079.9	22.5	1073.9	60.3	1073.9	60.3
08MC09-65	1037.4	15.6	1050.0	17.0	1076.2	40.5	1076.2	40.5
08MC09-38	1071.3	22.2	1073.9	23.2	1079.2	53.8	1079.2	53.8
08MC09-60	1090.7	35.5	1087.4	30.4	1080.6	57.4	1080.6	57.4
08MC09-57	1062.2	33.7	1068.4	37.7	1081.1	91.3	1081.1	91.3
08MC09-75	1076.1	14.5	1078.2	24.5	1082.6	68.0	1082.6	68.0
08MC09-34	1075.6	9.0	1079.3	18.7	1086.8	53.3	1086.8	53.3
08MC09-14	1093.8	22.9	1091.5	19.9	1086.9	38.1	1086.9	38.1
08MC09-21	1058.0	18.8	1068.1	21.1	1088.9	51.1	1088.9	51.1
08MC09-64	942.6	13.5	987.9	26.3	1090.1	77.5	1090.1	77.5
08MC09-35	1087.1	24.0	1088.8	35.1	1092.1	93.7	1092.1	93.7
08MC09-28	1069.9	39.1	1077.8	36.1	1093.7	74.4	1093.7	74.4
08MC09-53	1079.4	18.2	1085.8	22.5	1098.7	56.8	1098.7	56.8
08MC09-4	1051.6	13.1	1072.2	22.9	1114.3	63.7	1114.3	63.7
08MC09-73	1110.9	21.2	1112.8	31.0	1116.4	81.7	1116.4	81.7
08MC09-97	1139.0	41.4	1139.3	29.6	1140.1	34.0	1140.1	34.0
08MC09-40	1170.0	33.0	1180.5	35.4	1199.8	79.6	1199.8	79.6
08MC09-41	1117.5	86.6	1150.7	60.4	1213.8	46.7	1213.8	46.7
08MC09-5	1309.3	29.1	1300.8	35.8	1286.9	82.2	1286.9	82.2
08MC09-8	1316.4	11.5	1314.7	12.9	1311.9	28.2	1311.9	28.2
08MC09-7	1319.1	49.7	1321.7	43.6	1325.9	80.9	1325.9	80.9
08MC09-17	1344.3	31.9	1340.7	34.5	1335.1	73.9	1335.1	73.9
08MC09-85	1381.1	36.6	1376.3	29.4	1368.8	49.3	1368.8	49.3
08MC09-70	1389.8	16.8	1382.4	12.8	1370.9	20.1	1370.9	20.1
08MC09-16	1455.0	32.6	1444.4	44.7	1428.8	99.9	1428.8	99.9
08MC09-62	1354.0	18.2	1383.6	23.1	1429.6	51.0	1429.6	51.0
08MC09-43	1386.9	30.2	1404.2	27.5	1430.4	51.4	1430.4	51.4
08MC09-56	1452.9	28.2	1453.7	24.6	1454.7	44.3	1454.7	44.3
08MC09-51	1449.2	24.0	1451.6	20.6	1455.1	36.5	1455.1	36.5
08MC09-83	1438.6	24.4	1447.6	33.4	1460.7	74.0	1460.7	74.0
08MC09-10	1410.6	26.4	1430.9	31.1	1461.2	66.2	1461.2	66.2
08MC09-98	1531.3	17.3	1508.3	33.4	1476.1	76.9	1476.1	76.9
08MC09-72	1411.5	28.4	1441.0	26.0	1484.9	47.8	1484.9	47.8
08MC09-87	1561.8	34.5	1557.3	28.9	1551.1	49.6	1551.1	49.6
08MC09-49	1513.9	36.7	1555.6	29.8	1612.6	47.9	1612.6	47.9

Apparent ages (Ma) for sample 08MC09 - Inset Pliocene unit at Littlefield, Arizona (Continued)								
Analysis	$^{206}Pb^*$	±	$^{207}Pb^*$	±	$^{206}Pb^*$	±	Best age	±
	$^{238}U^*$	(Ma)	^{235}U	(Ma)	$^{207}Pb^*$	(Ma)	(Ma)	(Ma)
08MC09-1	1617.5	24.3	1620.5	35.6	1624.4	75.4	1624.4	75.4
08MC09-19	1547.0	36.7	1584.3	28.3	1634.2	42.9	1634.2	42.9
08MC09-24	1535.1	43.8	1577.4	31.4	1634.5	41.9	1634.5	41.9
08MC09-100	1650.2	25.2	1658.7	33.8	1669.5	69.4	1669.5	69.4
08MC09-32	1691.0	24.1	1684.3	30.5	1676.0	61.6	1676.0	61.6
08MC09-48	1645.2	30.8	1675.1	26.3	1712.8	44.2	1712.8	44.2
08MC09-77	1665.7	19.7	1694.8	21.0	1731.1	39.9	1731.1	39.9
08MC09-90	1777.3	50.2	1764.8	32.2	1750.0	38.3	1750.0	38.3
08MC09-74	1743.6	27.7	1746.9	29.7	1751.0	56.0	1751.0	56.0
08MC09-81	1786.8	17.5	1778.2	28.9	1768.1	59.6	1768.1	59.6
08MC09-59	1493.3	77.0	1615.7	57.4	1779.1	74.9	1779.1	74.9
08MC09-84	1826.3	31.6	1816.4	29.6	1805.0	52.4	1805.0	52.4
08MC09-86	1820.3	53.0	1831.0	59.1	1843.2	110.6	1843.2	110.6
08MC09-33	1870.3	14.8	1862.5	27.3	1853.9	55.5	1853.9	55.5
08MC09-54	1871.5	15.1	1873.5	17.1	1875.6	31.9	1875.6	31.9
08MC09-25	1852.2	27.2	1866.4	29.9	1882.3	55.1	1882.3	55.1
08MC09-69	1941.6	35.9	1991.2	37.5	2043.2	65.8	2043.2	65.8
08MC09-37	2220.5	37.0	2216.7	30.9	2213.2	48.7	2213.2	48.7
08MC09-12	2593.9	83.5	2672.0	38.5	2731.7	19.5	2731.7	19.5
08MC09-61	2638.7	50.2	2711.0	41.8	2765.3	61.7	2765.3	61.7
08MC09-52	2796.7	50.6	2787.0	32.1	2779.9	41.5	2779.9	41.5
08MC09-29	2912.7	37.7	2921.5	21.3	2927.6	24.7	2927.6	24.7
08MC09-55	3003.0	25.0	3020.4	13.4	3032.1	14.8	3032.1	14.8
08MC09-82	3686.4	45.5	3674.3	22.9	3667.8	25.2	3667.8	25.2

08MC20

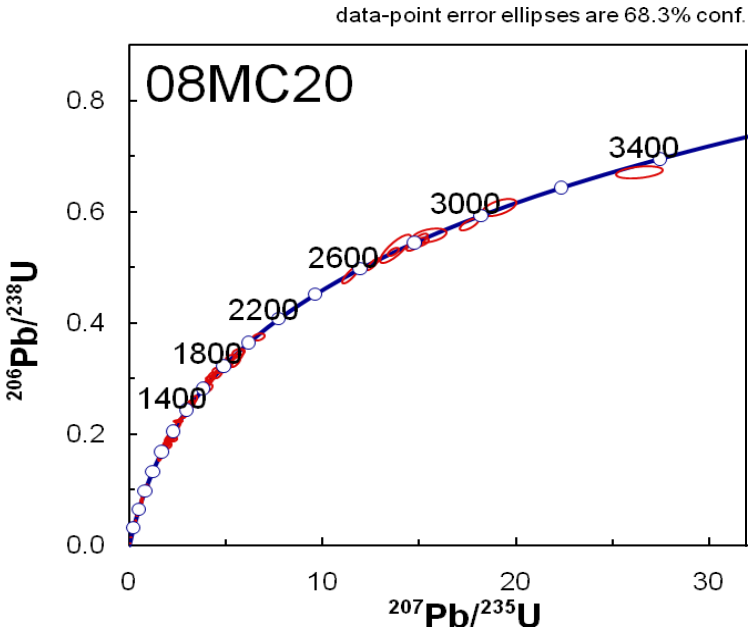

Concordia diagram of detrital zircons from the modern Virgin River at location I in the Virgin River Gorge (Fig. 2). This plot shows that almost all of the detrital zircons analyzed are concordant and are part of a closed system.

Table of isotope ratios of detrital zircons from the modern Virgin River at location I in the Virgin River Gorge (Fig. 2).

Isotope ratios for sample 08MC20 - Modern Virgin River										
Analysis	U	^{206}Pb	U/Th	$^{206}Pb^*$	±	$^{207}Pb^*$	±	$^{206}Pb^*$	±	error
	(ppm)	^{204}Pb		$^{207}Pb^*$	(%)	$^{235}U^*$	(%)	^{238}U	(%)	corr.
08MC20-1	185	424	1.2	20.9	19.4	0.0	19.8	0.0	4.0	0.20
08MC20-32	354	2660	2.2	20.2	35.1	0.0	35.3	0.0	3.2	0.09
08MC20-33	176	2498	1.2	19.3	24.7	0.0	25.8	0.0	7.8	0.30
08MC20-19	116	2450	1.2	18.6	26.3	0.0	27.0	0.0	5.9	0.22
08MC20-72	119	236	1.2	22.1	28.9	0.0	29.9	0.0	7.8	0.26
08MC20-31	571	1572	1.6	18.9	22.5	0.0	23.8	0.0	7.6	0.32
08MC20-49	1274	11854	3.2	19.9	3.9	0.1	4.4	0.0	2.1	0.48
08MC20-88	327	7172	1.2	19.0	5.9	0.2	6.5	0.0	2.6	0.41
08MC20-56	318	8220	1.4	19.7	3.7	0.2	4.3	0.0	2.2	0.50
08MC20-47	182	7732	1.8	18.0	5.9	0.3	6.7	0.0	3.3	0.49
08MC20-89	294	7414	1.6	18.8	6.4	0.3	7.9	0.0	4.6	0.58
08MC20-68	647	26500	3.1	19.2	3.7	0.3	3.8	0.0	0.8	0.21
08MC20-26	172	6364	1.6	18.0	7.9	0.4	8.2	0.1	2.2	0.27
08MC20-14	237	8146	1.5	18.8	6.7	0.4	6.7	0.1	0.7	0.11
08MC20-55	455	6528	1.2	17.6	3.9	0.5	4.4	0.1	2.0	0.45
08MC20-45	172	6960	2.0	18.7	5.2	0.4	6.1	0.1	3.2	0.52
08MC20-95	303	18066	2.4	18.0	3.4	0.5	4.2	0.1	2.5	0.59

Isotope ratios for sample 08MC20 - Modern Virgin River (Continued)										
Analysis	U	^{206}Pb	U/Th	$^{206}Pb^*$	±	$^{207}Pb^*$	±	$^{206}Pb^*$	±	error
	(ppm)	^{204}Pb		$^{207}Pb^*$	(%)	$^{235}U^*$	(%)	^{238}U	(%)	corr.
08MC20-28	414	16286	1.3	17.9	4.5	0.5	5.6	0.1	3.3	0.58
08MC20-30	130	7712	1.9	17.0	3.0	0.6	4.6	0.1	3.5	0.76
08MC20-9	285	4136	1.0	16.9	2.7	0.6	3.5	0.1	2.1	0.61
08MC20-92	426	15894	1.3	17.8	1.4	0.6	2.0	0.1	1.5	0.73
08MC20-22	619	3672	1.6	16.1	4.4	0.7	4.5	0.1	1.2	0.25
08MC20-99	200	11406	2.5	17.9	3.7	0.6	4.5	0.1	2.5	0.56
08MC20-8	220	13402	4.1	17.4	3.2	0.7	3.5	0.1	1.5	0.42
08MC20-39	238	20380	5.3	17.1	2.1	0.7	3.8	0.1	3.1	0.83
08MC20-85	212	14942	1.5	17.3	2.6	0.7	3.1	0.1	1.8	0.57
08MC20-25	189	11986	1.6	17.0	4.1	0.8	4.2	0.1	0.9	0.20
08MC20-40	94	11516	1.1	16.6	3.9	0.8	4.3	0.1	1.7	0.39
08MC20-13	179	14944	1.0	17.2	4.5	0.8	5.6	0.1	3.3	0.59
08MC20-64	55	4410	1.5	16.2	11.4	0.9	11.6	0.1	2.2	0.19
08MC20-98	368	37418	2.4	16.5	2.5	0.9	3.2	0.1	1.9	0.61
08MC20-61	281	33004	8.4	14.1	2.1	1.6	3.2	0.2	2.4	0.75
08MC20-73	68	8762	2.9	13.7	4.1	1.8	4.7	0.2	2.3	0.49
08MC20-21	89	11602	2.4	13.7	3.4	1.8	4.2	0.2	2.4	0.59
08MC20-66	376	54466	14.7	13.7	2.2	1.8	2.8	0.2	1.8	0.64
08MC20-20	920	2918	2.5	13.6	3.6	1.6	4.9	0.2	3.4	0.68
08MC20-36	72	15338	4.7	13.5	3.9	1.8	4.5	0.2	2.4	0.53
08MC20-70	50	7632	1.6	13.5	4.3	1.8	4.6	0.2	1.6	0.35
08MC20-75	228	28152	12.6	13.4	3.3	1.9	4.1	0.2	2.5	0.60
08MC20-65	112	14588	1.7	13.4	2.8	1.8	4.6	0.2	3.7	0.80
08MC20-90	438	60704	3.3	13.3	1.7	1.9	2.0	0.2	1.1	0.55
08MC20-100	129	16278	3.2	13.3	4.0	2.0	4.4	0.2	1.9	0.42
08MC20-54	70	10062	3.0	13.3	3.5	1.8	5.1	0.2	3.6	0.72
08MC20-18	515	52348	4.1	13.2	1.2	1.9	2.6	0.2	2.3	0.88
08MC20-59	131	20508	2.8	13.2	3.9	1.9	4.2	0.2	1.5	0.36
08MC20-50	24	3470	1.6	13.2	3.9	1.9	5.3	0.2	3.6	0.68
08MC20-3	247	31914	4.2	13.1	1.3	1.9	2.6	0.2	2.2	0.86
08MC20-93	124	19784	3.1	13.1	3.7	2.0	4.3	0.2	2.4	0.54
08MC20-83	280	62354	3.9	13.0	1.6	2.0	2.0	0.2	1.3	0.63
08MC20-43	160	17024	2.7	12.9	3.7	2.0	3.8	0.2	0.9	0.24
08MC20-91	164	22850	4.7	12.9	2.3	2.1	3.7	0.2	2.9	0.78
08MC20-94	187	33888	3.6	12.9	2.7	2.1	3.1	0.2	1.5	0.47
08MC20-11	57	7104	2.2	12.9	5.2	2.0	5.8	0.2	2.6	0.44
08MC20-86	57	7152	3.5	12.7	4.0	2.0	4.3	0.2	1.8	0.40
08MC20-57	45	8504	1.3	12.7	3.8	2.1	5.1	0.2	3.3	0.66
08MC20-7	86	14092	2.2	12.6	1.9	2.1	3.1	0.2	2.4	0.79
08MC20-44	196	31346	2.9	12.6	2.6	2.2	3.0	0.2	1.6	0.51
08MC20-29	32	4262	1.4	12.6	3.0	2.1	3.2	0.2	1.1	0.33
08MC20-27	100	12940	3.8	12.5	4.1	2.2	4.3	0.2	1.4	0.31
08MC20-12	310	20536	2.6	12.3	4.5	2.0	4.9	0.2	1.9	0.40
08MC20-42	63	9628	1.9	12.2	5.1	2.2	5.8	0.2	2.7	0.47

Isotope ratios for sample 08MC20 - Modern Virgin River (Continued)										
Analysis	U	^{206}Pb	U/Th	$^{206}Pb^*$	±	$^{207}Pb^*$	±	$^{206}Pb^*$	±	error
	(ppm)	^{204}Pb		$^{207}Pb^*$	(%)	$^{235}U^*$	(%)	^{238}U	(%)	corr.
08MC20-5	60	10938	3.0	12.1	6.1	2.3	6.4	0.2	2.0	0.31
08MC20-74	31	4884	1.0	12.1	5.8	2.6	5.9	0.2	0.8	0.14
08MC20-15	87	18750	2.7	12.0	3.0	2.5	4.5	0.2	3.4	0.74
08MC20-4	233	8134	2.9	11.9	5.9	2.3	6.2	0.2	2.0	0.31
08MC20-69	16	3030	2.1	11.4	4.1	2.3	4.4	0.2	1.5	0.34
08MC20-81	204	42720	3.4	11.4	2.5	2.9	2.9	0.2	1.4	0.50
08MC20-17	141	26484	2.8	11.2	2.6	3.0	3.0	0.2	1.5	0.49
08MC20-62	79	14246	1.8	11.1	2.5	3.0	3.8	0.2	2.9	0.75
08MC20-76	40	7260	0.9	11.0	3.8	3.2	4.2	0.3	1.9	0.44
08MC20-71	162	29880	2.1	10.8	2.7	3.3	3.5	0.3	2.2	0.63
08MC20-67	369	65606	2.4	10.7	1.5	3.3	2.3	0.3	1.8	0.75
08MC20-16	198	28162	0.8	10.1	2.9	3.9	3.4	0.3	1.8	0.53
08MC20-63	180	38716	5.9	10.0	1.9	4.0	2.1	0.3	0.8	0.38
08MC20-41	250	40240	5.2	9.9	2.4	4.2	3.8	0.3	2.9	0.77
08MC20-35	95	10712	1.7	9.9	3.8	4.2	3.9	0.3	0.7	0.19
08MC20-78	45	8350	1.4	9.7	1.6	4.3	2.7	0.3	2.2	0.80
08MC20-77	248	49688	1.7	9.6	1.1	4.4	1.5	0.3	1.1	0.73
08MC20-96	321	60034	3.1	9.5	3.5	4.6	3.7	0.3	1.2	0.32
08MC20-79	228	8284	3.4	9.4	2.1	4.1	2.6	0.3	1.5	0.58
08MC20-80	275	42638	2.1	9.3	1.6	4.7	2.4	0.3	1.9	0.76
08MC20-53	133	23056	2.3	9.3	2.9	4.6	3.5	0.3	1.9	0.55
08MC20-34	209	46212	2.6	9.0	2.2	4.9	2.5	0.3	1.2	0.47
08MC20-51	154	40994	2.9	8.9	2.6	5.2	2.8	0.3	1.0	0.36
08MC20-48	188	43438	2.2	8.6	2.1	5.2	2.5	0.3	1.4	0.54
08MC20-58	136	41462	1.7	8.5	3.6	5.7	3.8	0.3	1.2	0.32
08MC20-24	107	28428	3.3	8.3	2.3	5.6	3.3	0.3	2.4	0.71
08MC20-6	586	58336	1.8	8.3	2.4	5.5	3.1	0.3	2.0	0.65
08MC20-2	79	20312	1.4	7.8	2.9	6.7	3.1	0.4	1.2	0.37
08MC20-60	71	32560	2.3	5.9	1.4	11.4	2.5	0.5	2.2	0.84
08MC20-87	151	69212	1.2	5.5	0.9	12.6	1.7	0.5	1.5	0.86
08MC20-82	43	20240	0.8	5.3	2.2	13.8	3.8	0.5	3.2	0.82
08MC20-84	83	34728	1.1	5.3	1.1	13.7	1.4	0.5	0.9	0.64
08MC20-10	139	36848	0.6	5.1	1.4	14.9	2.4	0.5	1.9	0.80
08MC20-23	165	59310	1.0	5.0	1.7	15.1	2.0	0.5	1.0	0.48
08MC20-46	131	50100	2.6	5.0	3.3	15.5	3.7	0.6	1.6	0.43
08MC20-97	41	19302	1.2	4.5	1.2	17.6	1.8	0.6	1.3	0.72
08MC20-52	80	30216	2.7	4.4	2.5	19.1	3.0	0.6	1.7	0.57
08MC20-37	181	83736	3.8	3.5	2.8	26.4	3.0	0.7	1.1	0.36

Table of apparent ages (Ma) of detrital zircons from the modern Virgin River at location I in the Virgin River Gorge (Fig. 2).

Apparent ages (Ma) for sample 08MC20 - Modern Virgin River								
Analysis	$^{206}Pb^*$	±	$^{207}Pb^*$	±	$^{206}Pb^*$	±	Best age	±
	$^{238}U^*$	(Ma)	^{235}U	(Ma)	$^{207}Pb^*$	(Ma)	(Ma)	(Ma)
08MC20-1	18.6	0.7	19.2	3.8	96.1	462.3	18.6	0.7
08MC20-32	19.3	0.6	20.6	7.2	170.0	842.9	19.3	0.6
08MC20-33	20.0	1.6	22.3	5.7	277.3	572.3	20.0	1.6
08MC20-19	23.6	1.4	27.2	7.2	359.6	602.5	23.6	1.4
08MC20-72	24.0	1.9	23.3	6.9	-45.6	714.5	24.0	1.9
08MC20-31	24.2	1.8	27.4	6.4	320.2	517.8	24.2	1.8
08MC20-49	93.9	2.0	98.2	4.1	203.7	90.0	93.9	2.0
08MC20-88	172.2	4.5	182.2	10.8	313.2	134.4	172.2	4.5
08MC20-56	179.8	3.8	183.7	7.3	234.6	86.5	179.8	3.8
08MC20-47	266.1	8.5	284.1	16.7	434.9	131.3	266.1	8.5
08MC20-89	271.4	12.3	278.8	19.3	340.9	145.7	271.4	12.3
08MC20-68	272.4	2.1	274.4	9.1	291.3	84.2	272.4	2.1
08MC20-26	343.9	7.3	355.9	24.5	434.9	175.7	343.9	7.3
08MC20-14	357.7	2.5	355.7	20.1	342.7	151.2	357.7	2.5
08MC20-55	363.1	7.0	379.6	14.0	481.7	87.0	363.1	7.0
08MC20-45	365.7	11.4	363.7	18.8	351.3	118.4	365.7	11.4
08MC20-95	406.9	9.7	410.5	14.1	431.0	75.2	406.9	9.7
08MC20-28	414.2	13.1	419.5	19.2	448.8	100.5	414.2	13.1
08MC20-30	429.4	14.5	449.8	16.7	555.6	65.0	429.4	14.5
08MC20-9	443.2	9.0	464.4	12.9	570.6	59.6	443.2	9.0
08MC20-92	455.8	6.4	456.5	7.3	459.9	30.3	455.8	6.4
08MC20-22	480.1	5.3	516.8	18.4	682.7	94.0	480.1	5.3
08MC20-99	503.8	12.2	494.3	17.7	451.0	83.1	503.8	12.2
08MC20-8	532.8	7.5	528.6	14.5	510.9	70.2	532.8	7.5
08MC20-39	545.1	16.3	546.7	15.9	553.4	46.1	545.1	16.3
08MC20-85	548.7	9.4	544.1	13.2	525.0	56.7	548.7	9.4
08MC20-25	615.5	5.0	603.5	19.1	558.6	89.6	615.5	5.0
08MC20-40	625.2	9.9	623.5	19.9	617.3	84.7	625.2	9.9
08MC20-13	629.3	19.6	609.4	25.6	536.1	99.1	629.3	19.6
08MC20-64	637.8	13.2	644.3	55.4	667.3	244.7	637.8	13.2
08MC20-98	648.3	11.9	643.6	15.2	627.2	54.7	648.3	11.9
08MC20-61	974.2	21.8	970.2	20.0	961.0	42.9	974.2	21.8
08MC20-73	1041.0	22.2	1032.8	30.7	1015.6	83.7	1015.6	83.7
08MC20-21	1047.4	23.6	1038.0	27.1	1018.1	68.4	1018.1	68.4
08MC20-66	1038.7	17.3	1032.6	18.2	1019.8	43.8	1019.8	43.8

Apparent ages (Ma) for sample 08MC20 - Modern Virgin River (Continued)								
Analysis	$^{206}Pb^*$	±	$^{207}Pb^*$	±	$^{206}Pb^*$	±	Best age	±
	$^{238}U^*$	(Ma)	^{235}U	(Ma)	$^{207}Pb^*$	(Ma)	(Ma)	(Ma)
08MC20-20	958.7	29.8	979.8	30.9	1027.2	72.6	1027.2	72.6
08MC20-36	1034.3	22.9	1036.3	29.5	1040.4	77.9	1040.4	77.9
08MC20-70	1030.5	15.5	1035.3	30.1	1045.6	87.5	1045.6	87.5
08MC20-75	1072.2	24.2	1069.4	27.2	1063.7	66.4	1063.7	66.4
08MC20-65	1052.2	35.9	1056.6	30.5	1065.7	56.4	1065.7	56.4
08MC20-90	1074.7	10.9	1073.8	13.3	1071.8	33.8	1071.8	33.8
08MC20-100	1125.3	19.3	1108.7	29.9	1076.4	80.8	1076.4	80.8
08MC20-54	1047.5	35.2	1057.8	33.4	1079.2	71.1	1079.2	71.1
08MC20-18	1055.5	22.4	1064.3	17.2	1082.2	24.7	1082.2	24.7
08MC20-59	1085.2	15.0	1086.7	27.9	1089.8	78.2	1089.8	78.2
08MC20-50	1077.2	35.5	1081.8	35.1	1090.8	77.6	1090.8	77.6
08MC20-3	1080.5	21.8	1086.6	17.0	1098.7	26.3	1098.7	26.3
08MC20-93	1132.3	24.4	1122.9	29.5	1104.8	73.0	1104.8	73.0
08MC20-83	1130.6	13.3	1126.1	13.8	1117.2	31.5	1117.2	31.5
08MC20-43	1116.4	9.4	1120.5	26.0	1128.4	74.0	1128.4	74.0
08MC20-91	1135.7	30.0	1133.9	25.1	1130.4	45.4	1130.4	45.4
08MC20-94	1166.4	15.8	1154.5	21.5	1132.1	54.6	1132.1	54.6
08MC20-11	1118.2	26.2	1125.1	39.5	1138.4	104.0	1138.4	104.0
08MC20-86	1085.6	17.5	1112.0	29.3	1164.1	78.6	1164.1	78.6
08MC20-57	1147.7	35.0	1156.3	34.9	1172.6	75.2	1172.6	75.2
08MC20-7	1159.7	25.8	1164.8	21.2	1174.3	36.9	1174.3	36.9
08MC20-44	1197.8	16.9	1191.4	21.1	1179.7	51.0	1179.7	51.0
08MC20-29	1146.5	11.0	1161.3	22.0	1189.0	59.4	1189.0	59.4
08MC20-27	1182.6	14.6	1187.2	30.3	1195.6	81.0	1195.6	81.0
08MC20-12	1063.1	19.0	1120.5	33.2	1233.5	88.2	1233.5	88.2
08MC20-42	1138.3	28.5	1173.1	40.2	1237.9	99.9	1237.9	99.9
08MC20-5	1189.9	21.2	1217.0	45.2	1265.3	118.5	1265.3	118.5
08MC20-74	1300.4	9.5	1288.0	42.9	1267.4	113.8	1267.4	113.8
08MC20-15	1274.5	39.1	1273.9	33.0	1272.8	59.2	1272.8	59.2
08MC20-4	1157.8	20.7	1203.3	43.8	1285.9	114.9	1285.9	114.9
08MC20-69	1124.3	15.5	1211.3	31.0	1369.9	79.2	1369.9	79.2
08MC20-81	1384.4	17.8	1382.6	21.6	1379.8	47.5	1379.8	47.5
08MC20-17	1404.4	18.7	1404.5	22.9	1404.6	50.2	1404.6	50.2
08MC20-62	1380.7	35.5	1397.2	29.1	1422.6	48.7	1422.6	48.7
08MC20-76	1467.9	24.3	1458.5	32.6	1444.9	72.1	1444.9	72.1
08MC20-71	1494.6	29.3	1489.7	27.4	1482.6	51.8	1482.6	51.8
08MC20-67	1457.3	22.8	1471.0	18.0	1490.7	28.8	1490.7	28.8

Apparent ages (Ma) for sample 08MC20 - Modern Virgin River (Continued)								
Analysis	$^{206}Pb^*$	±	$^{207}Pb^*$	±	$^{206}Pb^*$	±	Best age	±
	$^{238}U^*$	(Ma)	^{235}U	(Ma)	$^{207}Pb^*$	(Ma)	(Ma)	(Ma)
08MC20-16	1624.8	26.1	1615.5	27.6	1603.3	53.7	1603.3	53.7
08MC20-63	1626.9	11.2	1629.2	16.8	1632.1	35.7	1632.1	35.7
08MC20-41	1681.4	43.1	1665.3	31.1	1645.0	45.3	1645.0	45.3
08MC20-35	1693.2	10.9	1672.1	31.7	1645.8	70.4	1645.8	70.4
08MC20-78	1689.2	32.5	1683.8	22.5	1677.2	30.3	1677.2	30.3
08MC20-77	1720.1	16.9	1712.5	12.8	1703.3	19.5	1703.3	19.5
08MC20-96	1764.2	18.5	1747.5	30.9	1727.6	64.3	1727.6	64.3
08MC20-79	1603.6	21.2	1661.1	21.0	1734.5	38.4	1734.5	38.4
08MC20-80	1780.4	28.9	1770.3	20.4	1758.4	28.7	1758.4	28.7
08MC20-53	1736.8	28.9	1746.8	29.0	1758.7	53.2	1758.7	53.2
08MC20-34	1805.0	18.7	1808.7	21.3	1813.0	40.3	1813.0	40.3
08MC20-51	1872.3	16.7	1859.2	24.1	1844.4	47.6	1844.4	47.6
08MC20-48	1807.5	21.6	1846.2	21.5	1890.1	38.2	1890.1	38.2
08MC20-58	1922.7	20.1	1925.4	33.0	1928.4	65.1	1928.4	65.1
08MC20-24	1888.6	38.6	1921.7	28.5	1957.5	41.3	1957.5	41.3
08MC20-6	1837.9	32.0	1901.3	26.5	1971.2	41.9	1971.2	41.9
08MC20-2	2051.3	20.2	2068.0	27.8	2084.8	51.6	2084.8	51.6
08MC20-60	2558.5	45.4	2560.0	23.8	2561.1	22.9	2561.1	22.9
08MC20-87	2640.9	32.1	2650.2	16.2	2657.3	14.6	2657.3	14.6
08MC20-82	2753.1	70.8	2735.5	36.4	2722.5	36.1	2722.5	36.1
08MC20-84	2730.0	20.5	2727.5	13.6	2725.6	18.1	2725.6	18.1
08MC20-10	2808.9	43.0	2807.7	22.6	2806.9	23.4	2806.9	23.4
08MC20-23	2806.2	21.8	2818.6	18.9	2827.4	28.4	2827.4	28.4
08MC20-46	2855.6	36.5	2847.9	35.3	2842.4	54.5	2842.4	54.5
08MC20-97	2936.9	30.7	2967.0	17.3	2987.5	20.0	2987.5	20.0
08MC20-52	3061.8	41.2	3048.6	28.7	3040.0	39.3	3040.0	39.3
08MC20-37	3309.5	28.0	3361.1	29.5	3392.0	43.8	3392.0	43.8

08MC21

Sample 08MC21 from the modern Beaver Dam Wash was analyzed and yielded only three detrital zircons. Due to the fact that only three detrital zircons were analyzed in this

study, the data are not included in the study. The three detrital zircons produced ages of 14 Ma, 24 Ma, and 174 Ma. The lack of data does not allow for valid interpretations.

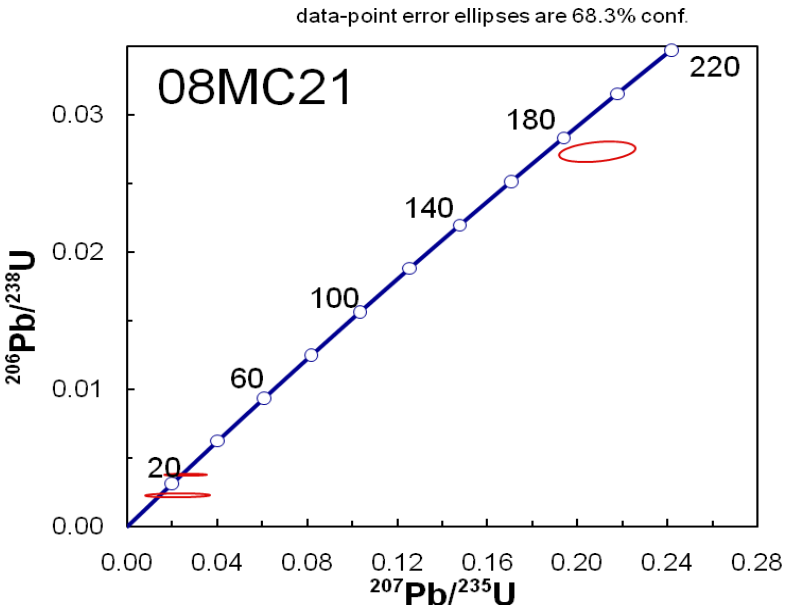

Concordia diagram of detrital zircons from the modern Beaver Dam Wash. While the detrital zircons may appear to be discordant, they would not be discordant if the scale were extended.

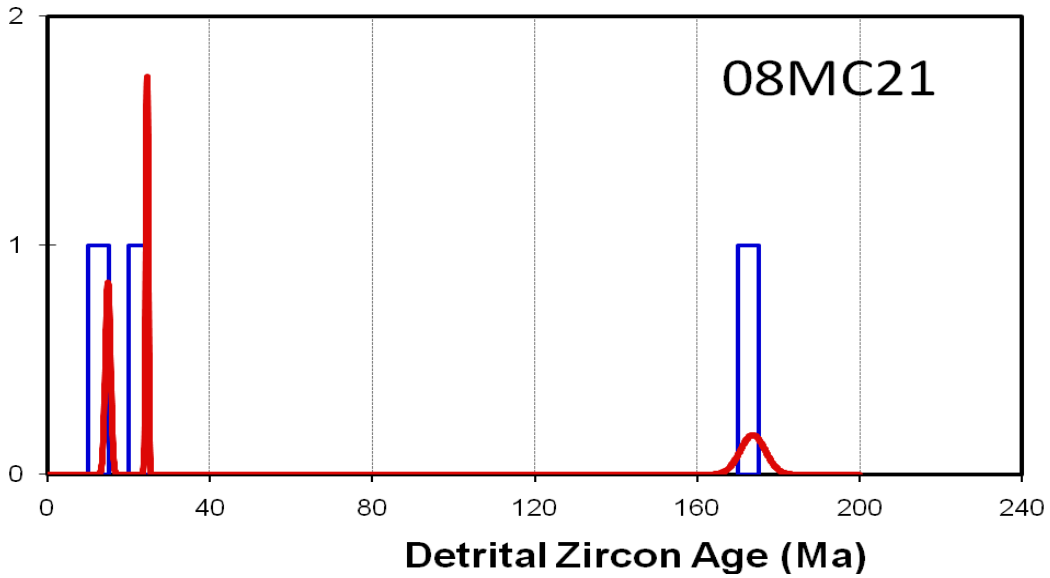

Relative probability plot of detrital zircons from the modern Beaver Dam Wash. No age peaks were identified for this sample.

Table of isotope ratios of detrital zircons from the modern Beaver Dam Wash.

Isotope ratios for sample 08MC21 - Modern Beaver Dam Wash										
Analysis	U	^{206}Pb	U/Th	$^{206}Pb^*$	±	$^{207}Pb^*$	±	$^{206}Pb^*$	±	error
	(ppm)	^{204}Pb		$^{207}Pb^*$	(%)	$^{235}U^*$	(%)	^{238}U	(%)	corr.
08MC21-1	986	2316	1.2	20.2489	24.0	0.0259	24.0	0.0038	1.3	0.05
08MC21-2	206	380	1.3	14.0896	42.1	0.0226	42.3	0.0023	4.3	0.10
08MC21-3	5801	6902	3.1	18.0080	5.1	0.2090	5.4	0.0273	1.8	0.33

Table of apparent ages (Ma) of detrital zircons from the modern Beaver Dam Wash.

Apparent ages (Ma) for sample 08MC21 - Modern Beaver Dam Wash								
Analysis	$^{206}Pb^*$	±	$^{207}Pb^*$	±	$^{206}Pb^*$	±	Best age	±
	$^{238}U^*$	(Ma)	^{235}U	(Ma)	$^{207}Pb^*$	(Ma)	(Ma)	(Ma)
08MC21-1	24.5	0.3	26.0	6.2	166.1	567.7	24.5	0.3
08MC21-2	14.9	0.6	22.7	9.5	956.7	900.5	14.9	0.6
08MC21-3	173.6	3.1	192.7	9.5	433.6	113.5	173.6	3.1

APPENDIX III

CONGLOMERATE CLAST COUNT DATA

Histograms of conglomerate clast counts performed in the Muddy Creek Formation at Flat Top Mesa, Beaver Dam Wash, Mormon Mesa, and the inset Pliocene units at Littlefield, Arizona and in the Beaver Dam Wash. Four additional conglomerate clast counts were performed within the Muddy Creek Formation at Mormon Mesa.

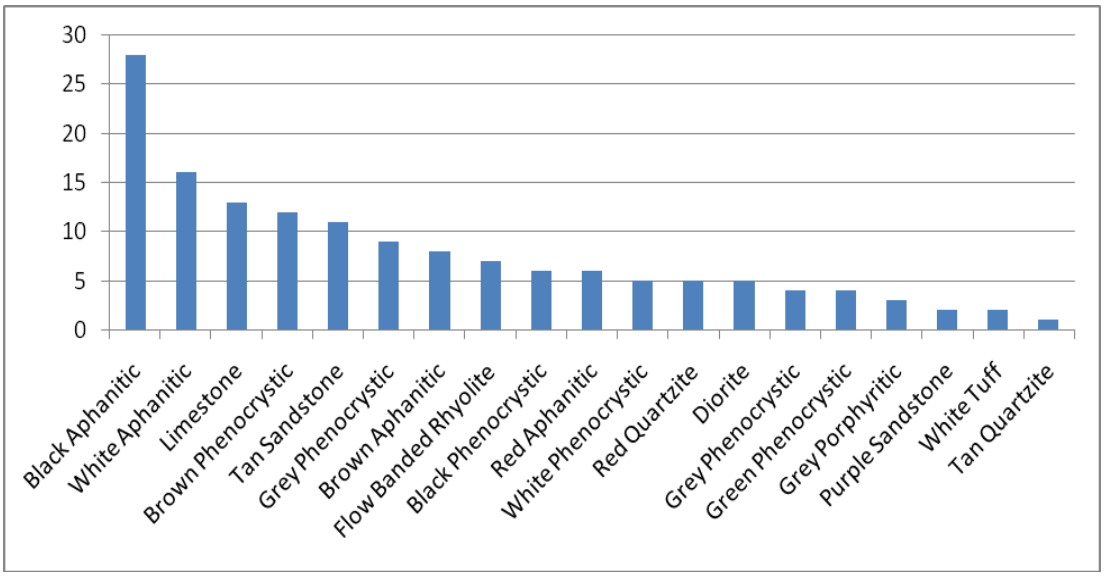

Histogram of an interbedded conglomerate within the Muddy Creek Formation from location F (Fig. 2) from Flat Top Mesa at 86 m showing which clast types were counted. The histogram shows that the majority of clasts were volcanic clasts.

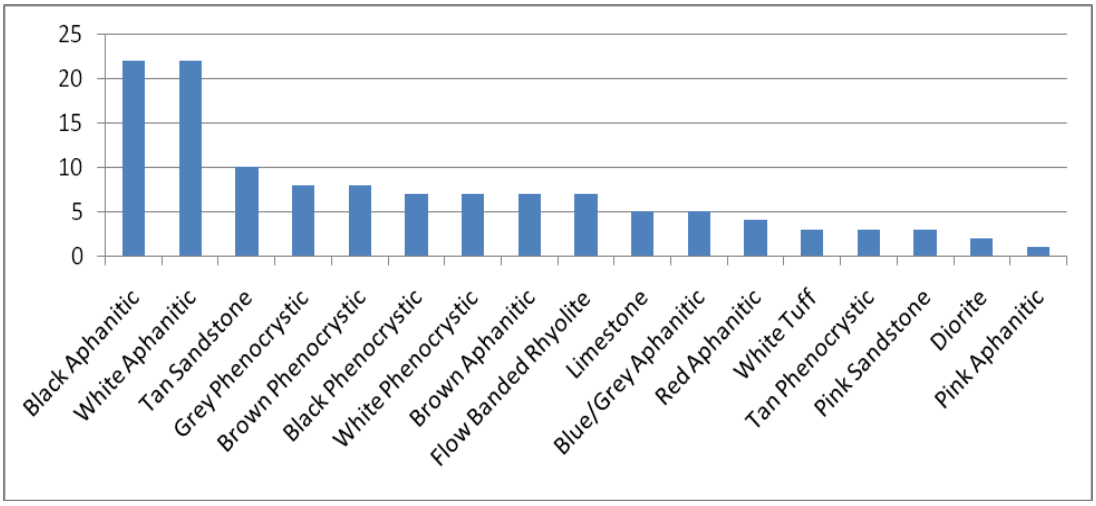

Histogram of an interbedded conglomerate within the Muddy Creek Formation at location F (Fig. 2) from Flat Top Mesa at 110 m showing one conglomerate clast count that details which clasts were counted. The histogram shows that the majority of clasts were volcanic clasts, similar to the other conglomerate clast count at Flat Top Mesa.

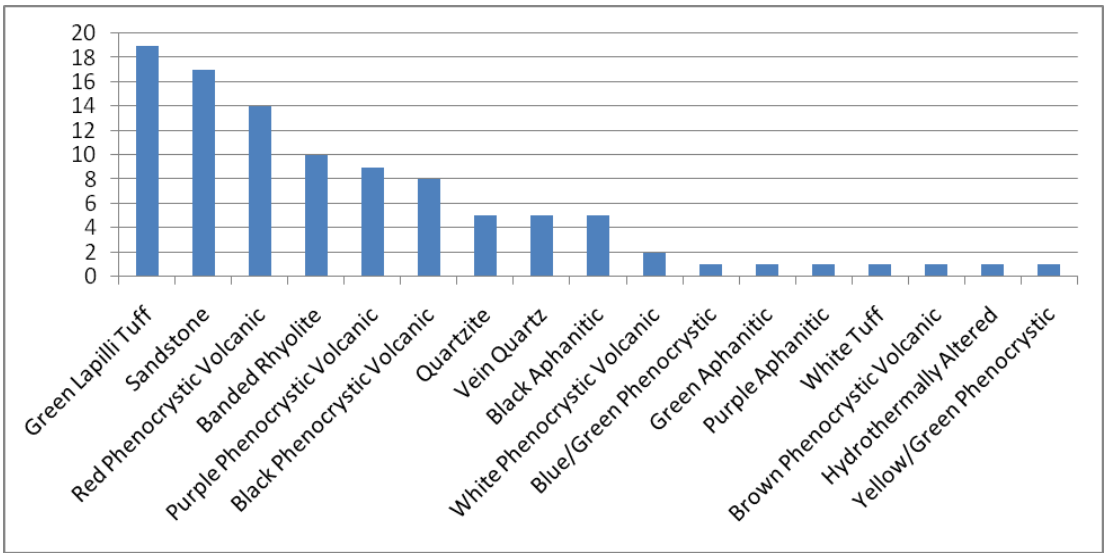

Histogram of a conglomerate clast count from the Muddy Creek Formation from location H (Fig. 2) in the Beaver Dam Wash at 62 m showing the composition of the clasts that were counted. This histogram shows that the conglomerate is made up of predominantly volcanic clasts.

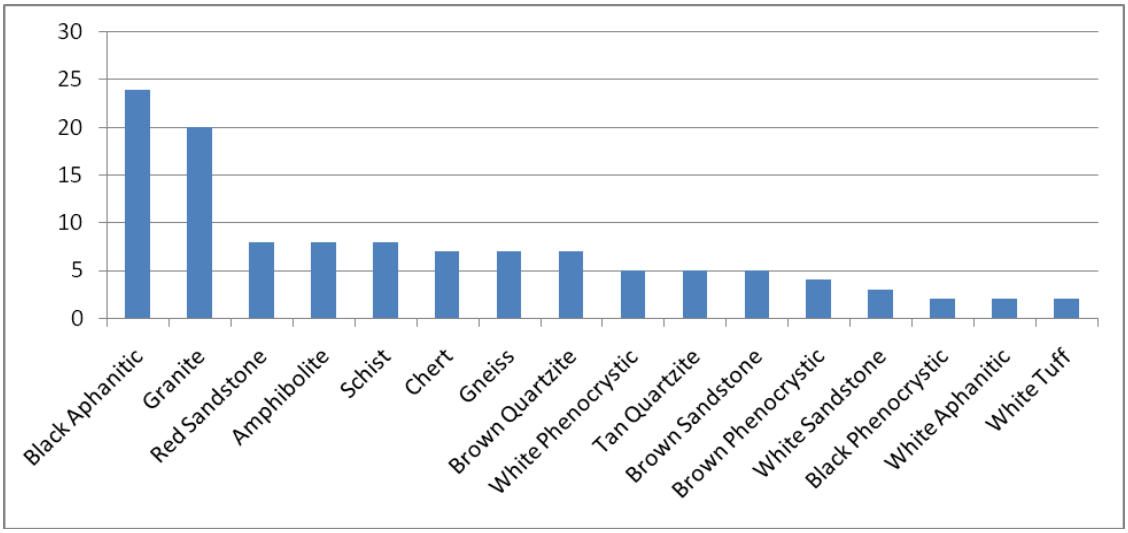

Conglomerate clast count histogram from the Muddy Creek Formation from location A at Mormon Mesa (Fig. 29) at 66 m detailing what clast types were counted. The figure shows that the conglomerate consists of volcanic, plutonic, sedimentary, and metamorphic clasts.

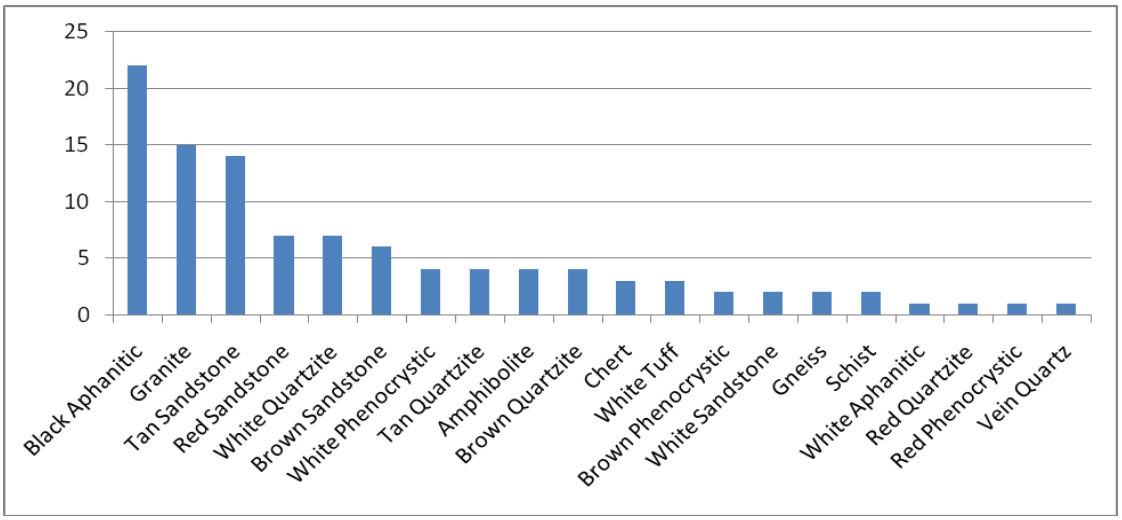

Histogram of a second conglomerate clast count from the Muddy Creek Formation from location A at Mormon Mesa (Fig. 29) at 84 m detailing what clast types were counted. The histogram indicates that the conglomerate is composed of volcanic, plutonic, sedimentary, and metamorphic clasts.

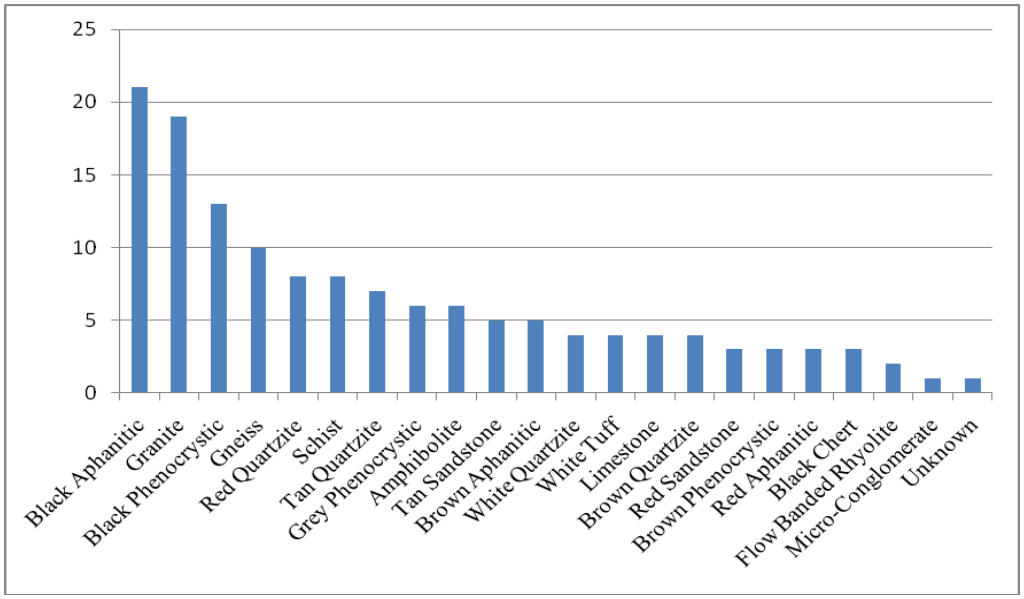

Conglomerate clast count histogram from the Muddy Creek Formation from location B at Mormon Mesa (Fig. 29) detailing what clast types were counted. The figure shows that the conglomerate consists of volcanic, plutonic sedimentary, and metamorphic clasts.

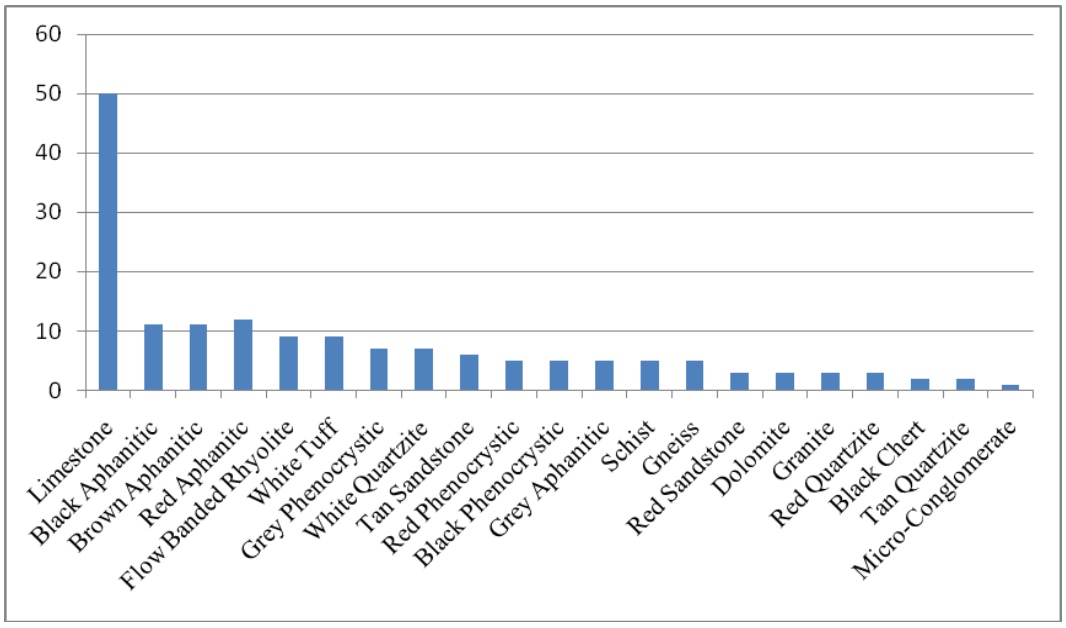

Conglomerate clast count histogram from the Muddy Creek Formation from location C at Mormon Mesa (Fig. 29) detailing what clast types were counted. The figure shows that the conglomerate consists of volcanic, sedimentary, and metamorphic clasts.

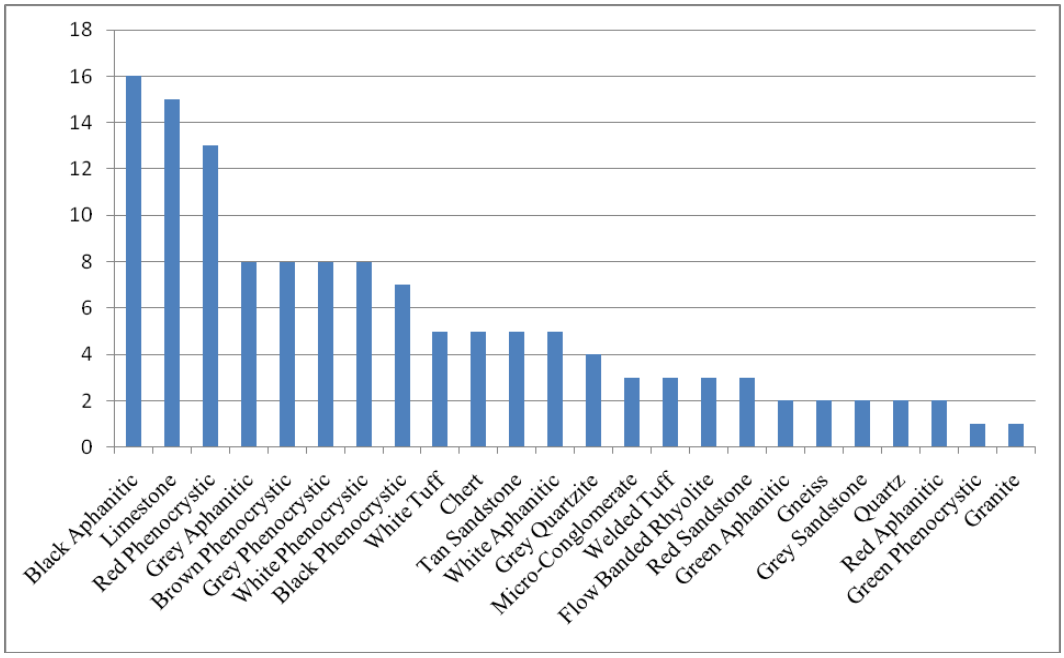

Conglomerate clast count histogram from the Muddy Creek Formation from location D at Mormon Mesa (Fig. 29) detailing what clast types were counted. The figure shows that the conglomerate consists of predominantly volcanic clasts and some sedimentary clasts.

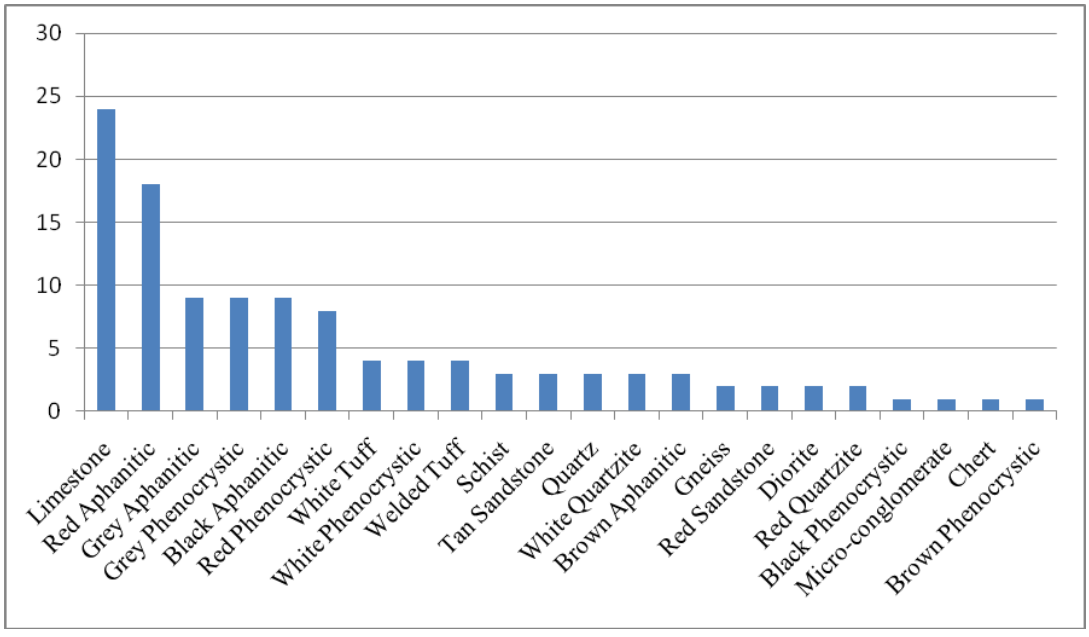

Conglomerate clast count histogram from the Muddy Creek Formation from location E at Mormon (Fig. 29) Mesa detailing what clast types were counted. The figure shows that the conglomerate consists of predominantly volcanic clasts and some sedimentary clasts.

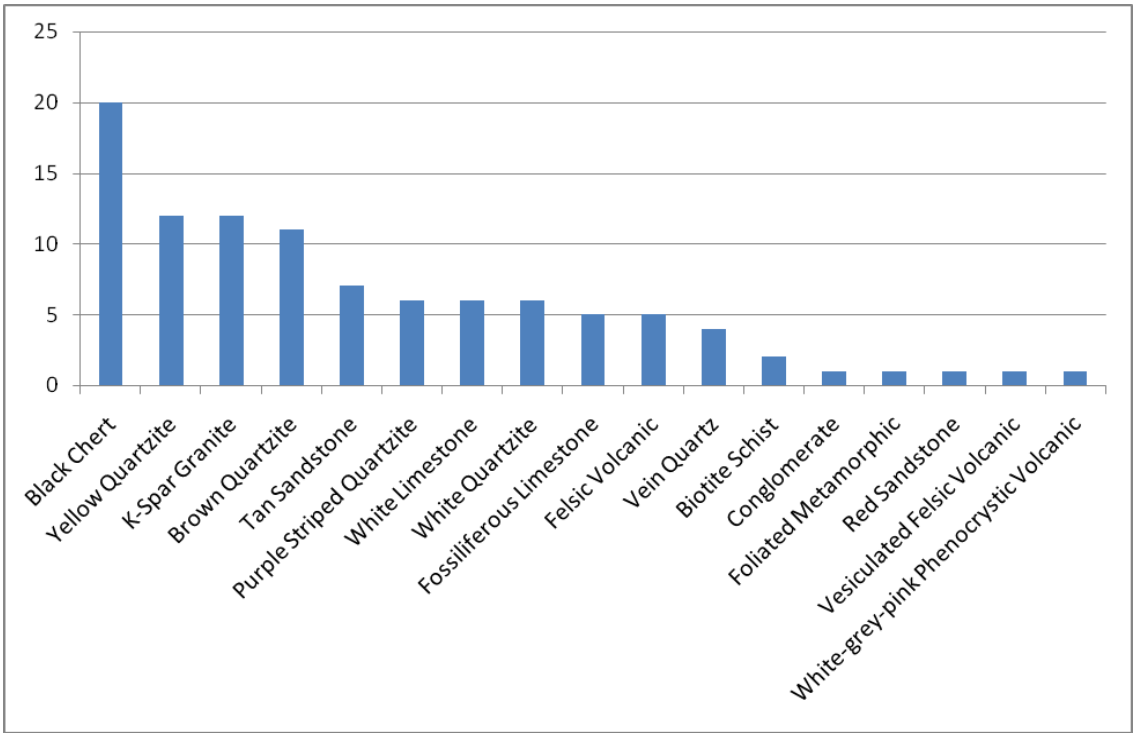

Conglomerate clast count from the inset Pliocene unit from location G in Littlefield, Arizona (Fig. 2) at 2 m showing the composition of clasts that were counted. The conglomerate at this location is predominantly composed of sedimentary and metamorphic clasts.

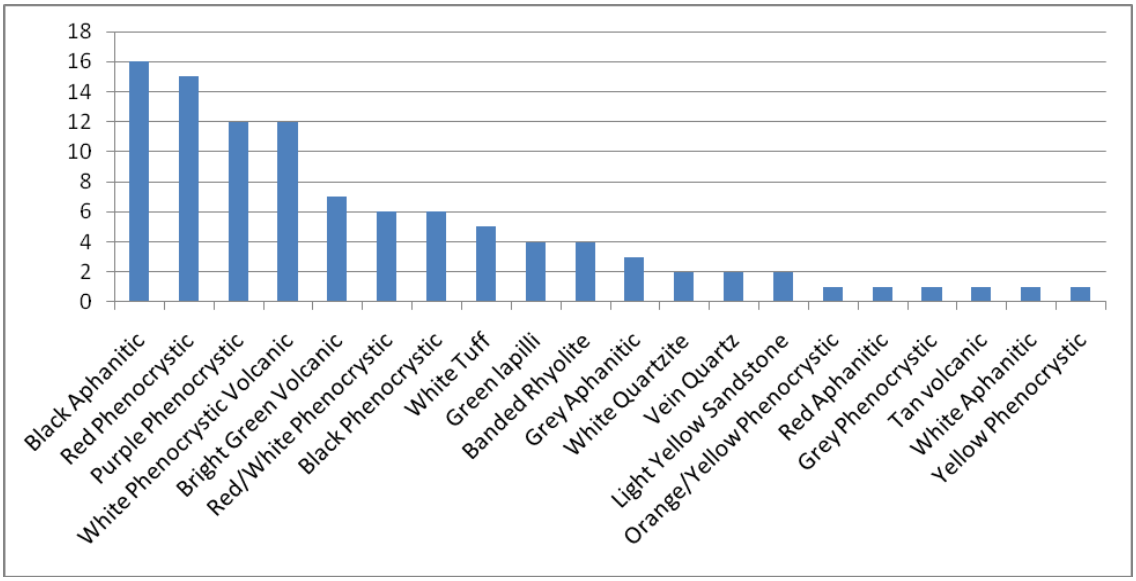

Conglomerate clast count from the inset Pliocene unit from location I (Fig. 2) in the Beaver Dam Wash at 34 m showing what clast types were counted. The conglomerate in this location is composed of mostly volcanic clasts.

REFERENCES

Anderson, R.E., and Barnhard, T.P., 1993, Aspects of three-dimensional strain at the margin of the extensional orogen, Virgin River depression area, Nevada, Utah, and Arizona: Geological Society of America Bulletin, v. 105, p. 1019-1052.

Atwater, T., 1970, Implications of plate tectonics for the Cenozoic tectonic evolution of western North America: Geological Society of America Bulletin, v. 81, p. 3513-3536.

Axen, G.J., Wernicke, B.P., Skelly, M.F., and Taylor, W.J., 1990, Mesozoic and Cenozoic tectonics of the Sevier thrust belt in the Virgin River valley area, southern Nevada, *in* Wernicke, B.P., ed., Basin and Range extensional tectonics near the latitude of Las Vegas, Nevada: Geological Society of America Memoir 176, p. 123-153.

Baars, D.L., 2000, The Colorado Plateau: A geologic history: Albuquerque, New Mexico, University of New Mexico Press, 254 p.

Beard, L.S., Anderson, R.E., Block, D.L., Bohannon, R.G., Brady, R.J., Castor, S.B., Duebendorfer, E.M., Faulds, J.E., Felger, T.J., Howard, K.A., Kuntz, M.A., and Williams, V.S., 2007, Preliminary geologic map of the Lake Mead 30’ X 60’ quadrangle, Clark County, Nevada, and Mohave County, Arizona: United States Geological Survey.

Best, M.G., Scott R.B., Rowley, P.D., Swadley, W.C., Anderson, R.E., Gromme, C.S., Harding, A.E., Deino, A.L., Christiansen, E.H., Tingey, D.G., and Sullivan, K.R., 1993, Oligiocene-Miocene caldera complexes, ash-flow sheets, and tectonism in the central and southeastern Great Basin: *In* Lahren, M.M., Trexler, J.H. Jr., and Spinosa, C., eds., Crustal evolution of the Great Basin and Sierra Nevada: Geological Society

of America field trip guidebook, Cordilleran/Rocky Mountain section meeting, Reno, Nevada, p. 285-311.

Billingsley, G.H., 1995, Geologic map of the Littlefield quadrangle, northern Mohave County, Arizona: United States Geological Survey, Open-file report 95-559.

Bohannon, R.G., 1984, Nonmarine sedimentary rocks of Tertiary age in the Lake Mead region, southeastern Nevada and northwestern Arizona: U.S. Geological Survey Report P-1259, 72 p.

Bohannon, R.G., Grow, J.A., Miller, J.J., and Blank, R.H. Jr., 1993, Seismic stratigraphy and tectonic development of Virgin River depression and associated basins, southeastern Nevada and northwestern Arizona: Geologic Society of America Bulletin, v. 105, p. 501-520.

Brock, A.L., and Buck, B.J., 2009, Polygenetic development of the Mormon Mesa, NV petrocalcic horizons: Geomorphic and paleoenvironmental interpretations: Catena, v. 77, p. 65-75.

Cromme, S., Deino, A.M., Best, M.G., and Hudson, M.G., 1997, Geochronologic and paleomagnetic evidence defining the relationship between the Miocene Hiko and Racer Canyon tuffs, eccentric outflow lobes from the Caliente Caldera complex, southeastern Great Basin, USA: Bulletin of Volcanology, v. 59, p. 21-35.

Dicke, S.M., 1990, Stratigraphy and sedimentology of the Muddy Creek Formation, southeastern Nevada [M.S. Thesis]: University of Kansas, 36 p.

Dickinson, W.R., and Suczek, C.A., 1979, Plate tectonics and sandstone compositions: American Association of Petroleum Geologists Bulletin, v. 63, p. 2164-2182.

Dickinson, W.R., 2004, Evolution of the North American Cordillera: Annual Review of

Earth and Planetary Sciences, v. 32, p. 13-45.

Douglass, J., Meek, N., Dorn, R.I., and Schmeeckle, M.W., 2009, A criteria-based methodology for determining the mechanism of transverse drainage development, with application to the southwestern United States: Geological Society of America Bulletin, v. 121, p. 586-598.

Duebendorfer, E.M. and Simpson, D.A., 1994, Kinematics and timing of Tertiary extension in the western Lake Mead region, Nevada: Geological Society of America Bulletin, v. 106, p. 1057-1073.

Duebendorfer, E.M., Beard, L.S., and Smith, E.I., 1998, Restoration of Tertiary deformation in the Lake Mead region, southern Nevada: The role of strike-slip transfer faults: Geological Society of America Special Paper 323, p. 127-148.

Duebendorfer, E.M., 2006, Geologic map of the Government Wash quadrangle, Nevada: Nevada Bureau of Mines and Geology Map.

Eaton, G.P., 1982, The Basin and Range Province: Origin and tectonic significance: Annual Review of Earth and Planetary Sciences, v. 10, p. 409-440.

Eberly, L.D., and Stanley, T.B., 1978, Cenozoic stratigraphy and geologic history of southwestern Arizona: Geological Society of America Bulletin, v. 89, p. 921-940.

Faulds, J.E., Feuerbach, D.L., Miller, C.F., and Smith, E.I., 2001, Cenozoic evolution of the northern Colorado River extensional corridor, southern Nevada and northwest Arizona: Utah Geological Association Publication, v. 78, p. 239-272.

Fenneman, N.M., 1928, Physiographic divisions of the United States; Annals of the Association of American Geographers, 3rd ed., v. 18, p. 261-353.

Fenneman, N.M., 1931, Physiography of Western United States, New York: McGraw-

Hill, 534 p.

Gardner, L.R., 1972, Origin of the Mormon Mesa Caliche, Clark County, Nevada: Geological Society of America Bulletin, v. 83, p. 143-156.

Gehrels, G.E., Dickinson, W.R., Ross, G.M., Stewart, J.H., and Howell, D.G., 1995, Detrital zircon reference for Cambrian to Triassic miogeoclinal strata of western North America: Geology, v. 23, p. 831-834.

Hanson, A.D., Druschke, P.A., Howley, R.A., Suurmeyer, N.R., Benneman, B., Erwin, M.B., and McLaurin, B.T., 2005, Deformation of the Miocene-Pliocene Muddy Creek Formation, southern Nevada: Lake Mead Fault System, salt tectonics, or both?: Geological Society of America Abstracts with Programs, v. 37, p. 42.

Howard, K.A., and Bohannon, R.G., 2001, Lower Colorado River: Upper Cenozoic deposits, incision, and evolution: *in* Young, R.A., and Spamer, E.E., eds., Colorado River Origin and Evolution, p. 101-105.

House, P.K., Pearthree, P.A., Howard, K.A., Bell, J.W., Perkins, M.E., Faulds, J.E., and Brock, A.L., 2005, Birth of the lower Colorado River-Stratigraphic and geomorphic evidence for its inception near the conjunction of Nevada, Arizona, and California: Geological Society of America Field Guide 6, p. 357-387.

Johnson, M., Dixon, G.L., Rowley, P.D., Katzer, T.C., and Winters, M., 2002, Hydrology and ground-water conditions of the Tertiary Muddy Creek Formation in the lower Virgin River Basin of southeastern Nevada and adjacent Arizona and Utah: Geological Society of America Field Guide, p. 284-315.

Kimbrough, D., Grove, M., Gehrels, G., Dorsey, R., House, P.K., Howard, K., Pearthree,

P.A., Spencer, J.E., and Mahoney, B., 2007, Detrital zircon record of Colorado River incision: Eos Transactions American Geophysical Union, 88(23), Joint Assembly Supplement, Abstract T41C-03.

Kowallis, B.J., and Everett, B.H., 1986, Sedimentary environments of the Muddy Creek Formation near Mesquite, Nevada, in thrusting and extensional structures and mineralization in the Beaver Dam Mountains, southwestern Utah: Salt Lake City, Utah Geological Association Publication 15, p. 69-75.

Lamb, M., Umhoefer, P.J., Anderson, E., Beard, S.L., Hickson, T., and Martin, L.K., 2005, Development of Miocene faults and basins in the Lake Mead region: A tribute to Ernie Anderson and a review of new research on basins: *in* Pederson, J., and Dehler, C.M., eds., Interior Western United States: Geological Society of America Field Guide 6, p. 389-418.

Langenheim, V.E., Glen, J.M., Jachens, R.C., Dixon, D.L., Katzer, T.C., and Morin, R.L., 2000, Geophysical constraints on the Virgin River Depression, Nevada, Utah, and Arizona: United States Geological Survey, Open Report 00-407, 26 p.

Langenheim, V.E., Bohannon, R.G., Glen, J.M., Jachens, R.C., Grow, J.A., Miller, J.J., Dixon, G.L., and Katzer, T.C., 2001, Basin configuration of the Virgin River depression, Nevada, Utah, and Arizona: A geophysical view of the deformation along the Colorado Plateau-Basin and Range transition: Utah Geological Association Publication, v. 78, p. 205-225.

Longwell, C.R., 1946, How old is the Colorado River?: American Journal of Science, v. 244, p. 818-835.

Lucchitta, I., 1990, History of the Grand Canyon and of the Colorado River in Arizona, *in*

Beus, S., and Morales, M., eds., Grand Canyon Geology: New York, Oxford University Press, p. 311-332.

Meek, N., and Douglass, J., 2001, Lake overflow: An alternative hypothesis for Grand Canyon incision and development of the Colorado River: *in* Young, R.A., and Spamer, E.E., eds., Colorado River Origin and Evolution, p. 199-204.

Metcalf, L.A., 1982, Tephrostratigraphy and Potassium Argon determinations of seven volcanic ash layers in the Muddy Creek Formation of southern Nevada: Desert Research Institute and Unversity of Nevada system publication 45023, 187 p.

Noble, D.C., and McKee, E.H., 1972, Description of K-Ar ages of volcanic units of the Caliente volcanic field, Lincoln County, Nevada, and Washington County, Utah: Isochron/West, 5, 17-24.

Page, W.R., Lundstrom, S.C., Harris, A.G., Langenheim, V.E., Workman, J.B., Mahan, S.A., Paces, J.B., Dixon, G.L., Rowley, P.D., Burchfiel, B.C., Bell, J.W., and Smith, E.I., 2005, Geologic and Geophysical Maps of the Las Vegas 30’ x 60’ Quadrangle, Clark and Nye Counties, Nevada, and Inyo Country, California: U. S. Geological Survey Scientific Inquiries Map 2814.

Pederson, J.L., 1998, A long-term record of hillslope sediment delivery to basins in southeastern Nevada: Sediment from the paleo-Colorado River (?): Geological Society of America Abstracts with Programs, v. 30, p. 33.

Pederson, J.L., 2001, Searching for the pre-Grand Canyon Colorado River: The Muddy Creek Formation north of Lake Mead: *in* Young, R.A., and Spamer, E.E., eds., Colorado River Origin and Evolution, p. 71-76.

Pederson, J.L., 2008, The mystery of the pre-Grand Canyon Colorado River-Results

from the Muddy Creek Formation: GSA Today, v.18, p. 4-10.

Peterson, F., and Turner-Peterson, C., 2000, Geology of the Colorado Plateau: International Geological Congress, Field Trip Guidebook T130: Washington, D.C., American Geophysical Union, 65 p.

Popescu, I., Lericolais, G., Panin, N., Normand, A., Dinu, C., and Le Drezen, E., 2004, The Danube submarine canyon (Black Sea): Morphology and sedimentary processes: Marine Geology, v. 206, p. 246-265.

Proffett, J.M., 1977, Cenozoic geology of the Yerington district, Nevada, and implications for the nature and origin of Basin and Range faulting: Geological Society of America Bulletin, v. 112, p. 247-266.

Quigley, M.C., Karlstrom, K.E., Beard, S., and Bohannon, B., 2002, Influence of Proterozoic and Laramide structures on the Miocene extensional strain field, North Muddy Mountains, Nevada/Arizona: Geological Society of America-Rocky Mountain Section Annual Meeting Field Trip Guide, 104 p.

Rahl, J.M., Reiners, P.W., Campbell, I.H., Nicolescu, S., and Allen, C.M., 2003, Combined single-grain (U-Th)/He and U/Pb dating of detrital zircons from the Navajo Sandstone, Utah: Geology, v. 31, p. 761-764.

Riggs, N.R., Ash, S.R., Barth, A.P., Gehrels, G.E., and Wooden, J.L., 2003, Isotopic age of the Black Forest Bed, Petrified Forest Member, Chinle Formation, Arizona: an example of dating a continental sandstone: GSA Bulletin, v. 115, p. 1315-1323.

Scheirer, D.S., and Andreasen, A.D., 2008, Results of gravity fieldwork conducted in March 2008 in the Moapa Valley region of Clark County, Nevada: U.S. Geological Survey Open-File Report 2008-1300, 40 p.

Schmidt, D.L., 2000, Integration of the Colorado River across the western Colorado Plateau in northwestern Arizona between about 10-5 Ma on the basis of the composition of Muddy Creek Formation of southeastern Nevada: *in* Young, R.A., ed., Abstracts for a working conference on the Cenozoic geologic evolution of the Colorado River system and the erosional chronology of the Grand Canyon region: The Colorado River, origin and evolution, p. 80-81.

Schweickert, R.A., Bogen, N.L., Girty, G.H., Hanson, R.E., and Merguerian, C., 1984, Timing and structural expression of the Nevadan orogeny, Sierra Nevada: Geological Society of America Bulletin, v. 95, p. 967-979.

Scott, A.J., 1988, The Muddy Creek Formation: Depositional environment, provenance, and tectonic significance in the western Lake Mead area, Nevada and Arizona [M.S. Thesis]: University of Nevada, Las Vegas, 114 p.

Shurbet, D.H., and Cebull, S.E., 1971, Crustal low-velocity layer and regional extension in Basin and Range province: Geological Society of America Bulletin, v. 82, p. 3241-3244.

Spencer, J.E., and Pearthree, P.A., 2001, Headward erosion vs. closed-basin spillover as alternative causes of capture of the ancestral Colorado River by the Gulf of California: *in* Young, R.A., and Spamer, E.E., eds., The Colorado River: Origin and Evolution: Grand Canyon, Arizona, Grand Canyon Association Monograph 12, p. 215-219.

Spencer, J.E., and Pearthree, P.A., 2005, Abrupt initiation of the Colorado River and initial incision of the Grand Canyon: Arizona Geological Survey, v. 35, 5 p.

Spencer, J.E., Richard, S.M., and Ferguson, C.A., 2001, Cenozoic structure and

evolution of the boundary between the Basin and Range and Transition Zone Provinces in Arizona: Utah Geological Association Publication, v. 78, p. 273-289.

Stewart, J.H., 1978, Basin-Range structure in Western North America-a review: Cenozoic tectonics and regional geophysics of the Western Cordillera: Geological Society of America Memoir 152, p. 1-31.

Stock, C., 1921, Later Cenozoic mammalian remains from the Meadow Valley region, southeastern Nevada: American Journal of Science, 5th series, v. 2, p. 250-264.

Trapp, H. Jr., and Horn, M.A., 1997, Groundwater atlas of the United States: Delaware, Maryland, New Jersey, North Carolina, Pennsylvania, Virginia, and West Virginia: United States Geological Society Report HA 730-L, 105 p.

Van Der Plos, L., and Tobi, A.C., 1965, A chart for judging the reliability of point counting results: American Journal of Science, v. 263, p. 87-90.

Wernicke, B., 1981, Low-angle normal faults in the Basin and Range province: nappe tectonics in an extending orogen: Nature, v. 291, p. 645-648.

Wernicke, B., Walker, J.D., and Beaufait, M.S., 1985, Structural discordance between Neogene detachments and frontal Sevier thrusts, central Mormon Mountains, southern Nevada: Tectonics, v. 4, p. 213-246.

Wernicke, B., 1992, Cenozoic extensional tectonics of the U.S. Cordillera: *in* Burchfiel, B.C., Lipman, P.W., and Zoback, M.L., eds., The Cordilleran Orogen: Conterminous U.S., The Geology of North America, G-3: Geological Society of America, Boulder, Colorado, p. 553-582.

Williams, V.S., 1996, Preliminary geologic map of the Mesquite quadrangle, Clark

and Lincoln Counties, Nevada and Mohave County, Arizona: U.S. Geological Survey Open-File Report 96-676,.

Young, R.A., and Spamer, E.E., 2001, Colorado River Origin and Evolution: Proceedings of a symposium held at Grand Canyon National Park in June 2000, Grand Canyon Association, Grand Canyon, AZ, 275 p.

VITA

Graduate College
University of Nevada, Las Vegas

Steven Wayne Forrester

Degrees:

Bachelor of Science, Geology, 2007
Washington State University

Awards

2008	Society for Sedimentary Geology Rocky Mountain Section Edwin D. McKee Grant
2008	UNLV Geoscience Scholarship
2008	Geological Society of America Research Grant
2008	Nevada Petroleum Society Research Grant

Publications:

Wellman, D. M., K. M. Gunderson, J. P. Icenhower, and S. W. Forrester (2007), Dissolution kinetics of synthetic and natural meta-autunite minerals, $X_{3-n}^{(n)+}[(UO_2)(PO_4)]_2 \cdot xH_2O$, under acidic conditions, Geochemistry, Geophysics Geosystems, 8, Q11001, doi:10.1029/2007GC001695.

Wellman, D.M., S. V. Mattigod, B. W. Arey and S.W. Forrester. Immobilization of Uranium in Cement – Based Matrices: *In-Situ* Identification of Solubility Limiting Uranium-Bearing Minerals.

Thesis Title: Provenance of the Miocene-Pliocene Muddy Creek Formation near Mesquite, Nevada

Thesis Examination Committee:

Chairperson, Dr. Andrew Hanson, Ph. D.
Committee Member, Dr. Stephen Rowland, Ph. D.
Committee Member, Dr. Wanda Taylor, Ph. D.
Graduate Faulty Representative, Dr. Vernon Hodge, Ph. D.